# UNIVERSITÉ DE STRASBOURG

*ÉCOLE DOCTORALE DE SCIENCES CHIMIQUES*

**L'Institut de chimie et procédés pour l'énergie, l'environnement et la santé**

# THÈSE présentée par :

**Dmitry KOMISSARENKO**

soutenue le : **24 septembre 2015**

pour obtenir le grade de : **Docteur de l'université de Strasbourg**

Discipline/ Spécialité : chimie

# OXYDATION CATALYTIQUE SELECTIVE DU METHANE EN GAZ DE SYNTHESE AVEC DES OXYDES MIXTES DE COBALT ET DES ELEMENTS DES TERRES RARES

**THÈSE dirigée par :**

| | |
|---|---|
| **Mme ROGER Anne-Cécile** | Professeur, Université de Strasbourg |
| **M DEDOV Alexey** | Professeur, Université d'État Gubkin du Pétrole et du Gaz |

**RAPPORTEURS :**

| | |
|---|---|
| **M ANISIMOV Alexander** | Professeur, Université d'État Lomonossov de Moscou |
| **Mme BATIOT-DUPEYRAT Catherine** | Professeur, Université de Poitiers |

---

**AUTRES MEMBRES DU JURY :**

| | |
|---|---|
| **M LOUIS Benoit** | Chargé de recherche CNRS, Université de Strasbourg |
| **Mme PARKHOMENKO Ksenia** | Chargé de recherche CNRS, Université de Strasbourg |
| **M LOKTEV Alexey** | Professeur, Université d'État Gubkin du Pétrole et du Gaz |

**Pertinence du sujet.**

Utilisation rationnelle des matières premières telle comme gaz naturel (GN) - une tâche actuelle et urgente pour la Fédération de Russie. Les réserves prouvées de GN dans le monde sont à environ 187 trln $m^3$, tandis que la Fédération de Russie est à la première place avec les réserves prouvées du gaz naturel ayant 30% (55 trln $m^3$) des réserves mondiales. En 2014, le volume de gaz extrait s'est élevé à 640 bln $m^3$. Toutefois, l'ampleur de la production d'hydrocarbures gazeux dépasse largement leur part de l'utilisation qualifié. Dans le même temps le méthane est le composant principal des NG est non seulement l'un des sources de carbone les plus respectueux de l'environnement, mais il sert aussi de brick de base pour toute une gamme de produits pétrochimiques. La Russie, étant l'un des leaders dans la production de NG, par son traitement en retard sur les États-Unis de 5 fois. A cet égard, impliquant le traitement chimique du méthane est une tâche urgente.

L'un des domaines clés de la transformation chimique est la conversion du méthane en gaz de synthèse. La production de gaz de synthèse - un processus industriel à grande échelle. A la base de gaz de synthèse des produits pétrochimiques importants sont synthétisés, tels que le méthanol, les carburants de synthèse de Fischer-Tropsch. Par exemple, la capacité de production de méthanol en 2014 a dépassé 60 mln t. Toutefois, environ 60% du coût de production de méthanol tombe sur le stade de la production de gaz de synthèse. Par conséquent, toute amélioration technologique de la production de gaz de synthèse est une tâche extrêmement importante.

À ce jour, la principale méthode de production de gaz de synthèse est un processus endothermique de reformage à la vapeur de méthane (RVM). Les inconvénients du RVM sont les Capex très élevés et la composition du gaz de synthèse résultant nécessitant un conditionnement supplémentaire pour la pétrochimie. Un autre procédé mis en œuvre industriellement est oxydation partielle du méthane avec l'oxygène. Ce procédé est non catalytique, et se déroule à des températures élevées - jusqu'à 1500 °C. Un autre procédé prometteur pour la production de gaz de synthèse est l'oxydation partielle catalytique de méthane (OPM) avec de l'oxygène. Avantages de l'OPM sont les demandes relativement faible d'énergie (exothermique), et la composition du gaz de synthèse résultant convient pour la synthèse du méthanol et de Fischer-Tropsch sans préconditionnement. Un autre procédé prometteur de produire du gaz de synthèse – reformage du méthane à sec avec le dioxyde de carbone (RMS) permet d'engager dans le recyclage chimique de dioxyde de carbone dans la pétrochimie et permet d'obtenir le gaz de synthèse, qui ne nécessite pas de conditionnement avant les synthèses de diméthyle éther ou des hydrocarbures à longue chaîne. Les principaux problèmes de l'OPM et le RMS sont liés à la sélectivité basse tout en maintenant un fonctionnement stable des catalyseurs.

Par conséquent, il est important et urgente d'améliorer ces procédés (l'OPM et le RMS) par le développement de nouveaux systèmes catalytique qui, d'une part, sont capables de fournir un rendement élevé du produit souhaité, réduire la température pour convertir le méthane en gaz de synthèse, et d'autre part - sont capables maintenir l'activité et la sélectivité stables dans le fonctionnement à long terme. La résolution de ce problème nécessite l'étude approfondie de la nature des sites actifs des catalyseurs et leurs effets sur la formation et le fonctionnement des réactifs et des produits de réaction de tous les composants du système catalytique.

**Objectifs de thèse.**

L'objet d'études est l'amélioration des processus d'oxydation partielle du méthane avec de l'oxygène dans le gaz de synthèse et de reformage de méthane à sec par la création de nouveaux catalyseurs sélectifs et stables à base d'oxydes mixtes à base de perovskites, et par l'identification des corrélations entre la structure cristalline et des propriétés à haute température de catalyseurs avec les résultats de tests catalytiques.

Pour atteindre ces objectifs, les problèmes suivants ont été résolus :

1. le choix de la composition et la structure des catalyseurs;
2. variation de la méthode pour la synthèse de catalyseurs;
3. étude d'OPM en présence de catalyseurs synthétisés et choisir des conditions optimales du procédé;
4. étude de RMS en présence de catalyseurs synthétisés et choisir des conditions optimales du procédé;
5. étude des propriétés physiques et chimiques des catalyseurs synthétisés, l'effet de la nature des composants actifs de catalyseurs sur l'efficacité des réactions.

**Nouveauté scientifique du travail** est déterminée par les résultats suivants:

1. Pour la première fois l'oxydation partielle du méthane avec de l'oxygène a été étudié en présence de nouveaux catalyseurs: $LaSrCoO_4$, $La_{1.25}Sr_{0.75}CoO_4$, $NdCaCoO_4$ et $Nd_{1.25}Ca_{0.75}CoO_4$

2. Un nouveau catalyseur d'oxydation partielle du méthane en gaz de synthèse sélective et stable à base d'oxyde complexe $NdCaCoO_4$ a été créé.

3. Pour la première fois la forte activité, la sélectivité et la stabilité du catalyseur $NdCaCoO_4$ en l'oxydation partielle du méthane ont été démontrées, due à la formation de clusters de Co métallique de taille nano dans la structure finement disperse de $Nd_2O_3$ et CaO, qui sont formés au cours de la transformation de la structure perovskite d'origine lors de la catalyse.

4. Un nouveau catalyseur pour le reformage du méthane à sec à base de $NdCaCoO_4$ a été développé. Le catalyseur fournit le rendement stable de CO et de $H_2$ à 80% pendant la réaction de longue durée.

5. Il a été démontré qu'un mélange de CO et $H_2$ peut être préparée avec 100% de sélectivité à 90% de conversion du méthane en présence d'un nouveau catalyseur de l'oxydation partielle du méthane - $NdCaCoO_4$. 100% de sélectivité en gaz de synthèse est maintenu pendant 140 heures sans tendance à désactiver le catalyseur.

6. Un nouveau catalyseur de reformage du méthane à sec à base de $NdCaCoO_4$ produit le gaz de synthèse avec le rendement avoisinant 90% pendant 50 heures de la réaction sans une tendance à la désactivation du catalyseur.

**Contribution personnelle de l'auteur**.

L'auteur a participé à la formulation des problèmes de recherche, conception des expériences, la sélection et l'analyse de la littérature scientifique sur le sujet de l'œuvre, la synthèse de catalyseurs et l'étude des processus de conversion du méthane en leur présence, l'étude des propriétés physiques et chimiques des catalyseurs, le traitement, l'interprétation et la présentation des résultats.

**Description de résultats de travail de thèse**

Le traitement chimique des matières premières gazeuses, en premier lieu, le gaz naturel est le problème extrêmement aigu. La direction clé du traitement chimique du méthane à présent est sa conversion en gaz de synthèse. La production du gaz de synthèse est le procès industriel de grande échelle, est le gaz de synthèse est le base pour les synthèse des importants produits de l'industrie chimique, tels comme l'hydrogène, méthanol, fuel synthétique etc. Selon les données des experts en chimie de gaz naturel, près de 70% des tous les dépenses de la production des produits de la

pétrochimie à partir du méthane sont consommés par le stade de la production du gaz de synthèse. Aujourd'hui on produit le gaz de synthèse dans l'industrie, essentiellement, par les procédés énergivores de la conversion à vapeur et l'oxydation non catalytique partielle du méthane, demandant des températures élevées. Perfectionnement de ces procédés de la production du gaz de synthèse est une importante tâche. Les collectifs mondiaux et russes travaillent sur ses problèmes. La plupart des études sont orientés vers l'élaboration de l'oxydation catalytique partielle du méthane par l'oxygène (OPM) et reformage du méthane à sec (RMS). Les tâches principales scientifiques sont la création des catalyseurs sélectifs et stables, et la réduction de la température de la conversion du méthane en gaz de synthèse. La résolution de ce problème nécessite l'étude approfondie de la nature des sites actifs des catalyseurs et leurs effets sur la formation et le fonctionnement des réactifs et des produits de réaction de tous les composants du système catalytique.

L'objet d'études est l'amélioration des processus d'oxydation partielle du méthane avec de l'oxygène dans le gaz de synthèse et de reformage de méthane à sec par la création de nouveaux catalyseurs sélectifs et stables à base d'oxydes mixtes à base de perovskites, et par l'identification des corrélations entre la structure cristalline et des propriétés à haute température de catalyseurs avec les résultats de tests catalytiques.

La synthèse des catalyseurs a été réalisée par la méthode « solide-state ». Quantités stœchiométriques des $La_2O_3$, $Nd_2O_3$, $SrCO_3$, $CaCO_3$ et $Co_3O_4$, préalablement calciné pour évacuer des vapeurs d'eau et des traces de dioxyde de carbone ont été utilisé comme des précurseurs initiaux. Les quantités stœchiométriques de réactifs ont été moulées dans le moulin planétaire avec l'ajout de l'heptane pendant 30 minutes. Après l'évaporation de l'heptane le mélange a été placé au creuset et calciné dans le four à moufle à 1100°C pendant 24 heures. Puis la poudre a été moulée encore une fois dans le moulin planétaire, pressée et calciné à 1200°C pendant 10 heures et refroidie jusqu'à la température ambiante.

Les expériences catalytiques de l'oxydation partielle du méthane ont été faits sur l'installation pilote de laboratoire avec le réacteur en quartz à la pression atmosphérique, à 800-950 °C, mélange utilisés sont $CH_4$:$O_2$ = (1,8÷4,6) :1 à la vitesse (W) = 10÷75 $L \cdot g_{cat}^{-1} h^{-1}$ et $CH_4$:$CO_2$ = (1÷1,5) :1 avec W = 14÷19 $L \cdot g_{cat}^{-1} h^{-1}$. Les produits gazeux ont été analysés par la chromatographie en phase gazeuse sur les colonnes de remplissage et capillaires.

Pour l'étude des caractéristiques physico-chimiques des catalyseurs on a utilisé les méthodes suivantes: DRX (Bruker AXSD8 Advanced Powder Diffraction System et Huber IMAGE FOIL G670); XPS (Thermo Multilab 2000 XPS); TPR-$H_2$ (Micromeritics Autochem II Chemisorption Analyzer RS232 Status); MEB (LEO-SUPRA 50 VP); MET (JEOL JEM 2010 UHR).

Dans le premier temps l'activité des oxydes mixtes avec la structure de pérovskite lamellaire de composition $NdCaCoO_{3.96}$, $Nd_{1.25}Ca_{0.75}CoO_{4.04}$, $LaSrCoO_{4.00}$ et $La_{1.25}Sr0._{75}CoO_{4.03}$ a été étudiée dans l'oxydation partielle du méthane et dans le reformage de méthane à sec. Les résultats des tests catalytiques sont montrés figures 1 - 4.

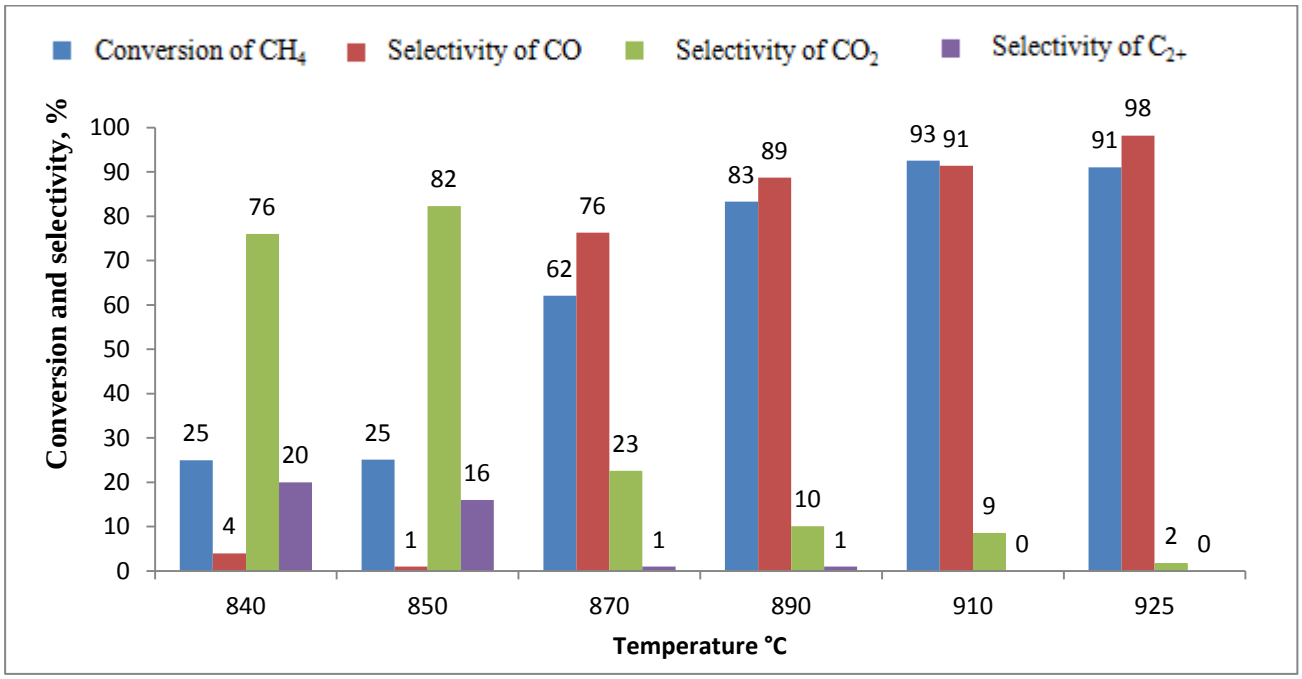


Figure 1 – Conversion du méthane et sélectivités de formation de produits en fonction de température ($NdCaCoO_{3.96}$; $CH_4/O_2 = 2$; $W = 22\ L*g^{-1}*h^{-1}$).

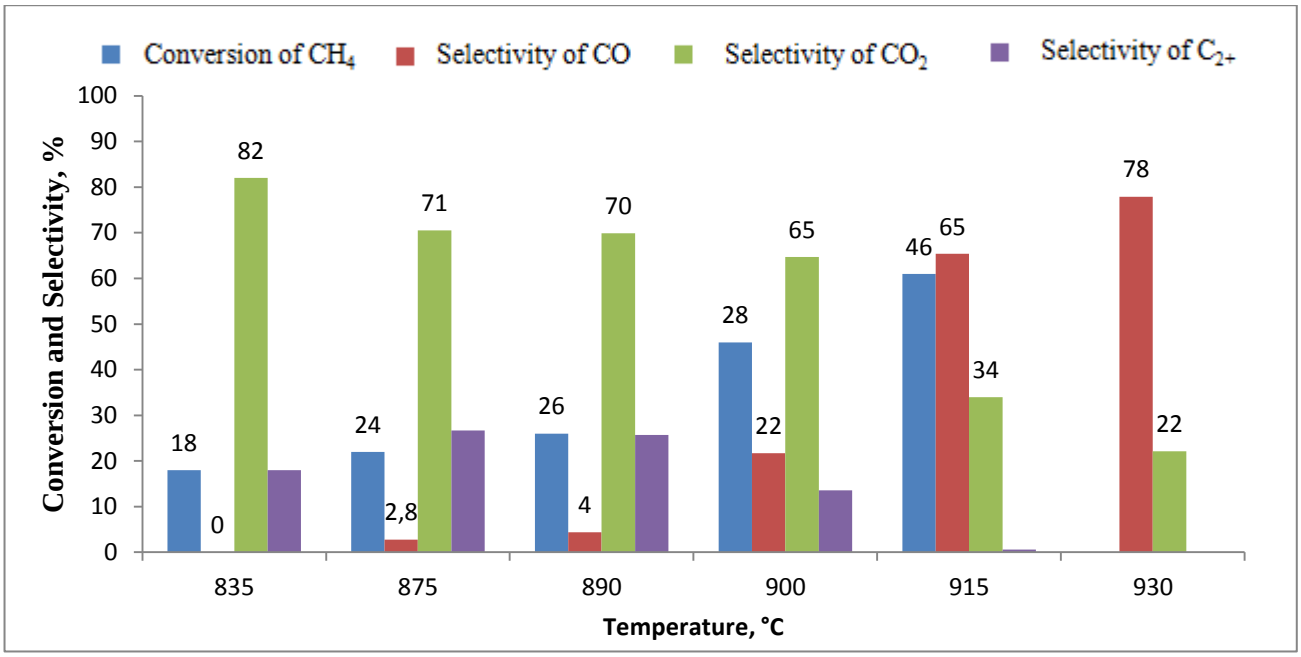

Figure 2 – Conversion du méthane et sélectivités de formation de produits en fonction de température ($Nd_{1.25}Ca_{0.75}CoO_{4.04}$; $CH_4/O_2$ = 2; W = 22 $L*g^{-1}*h^{-1}$).

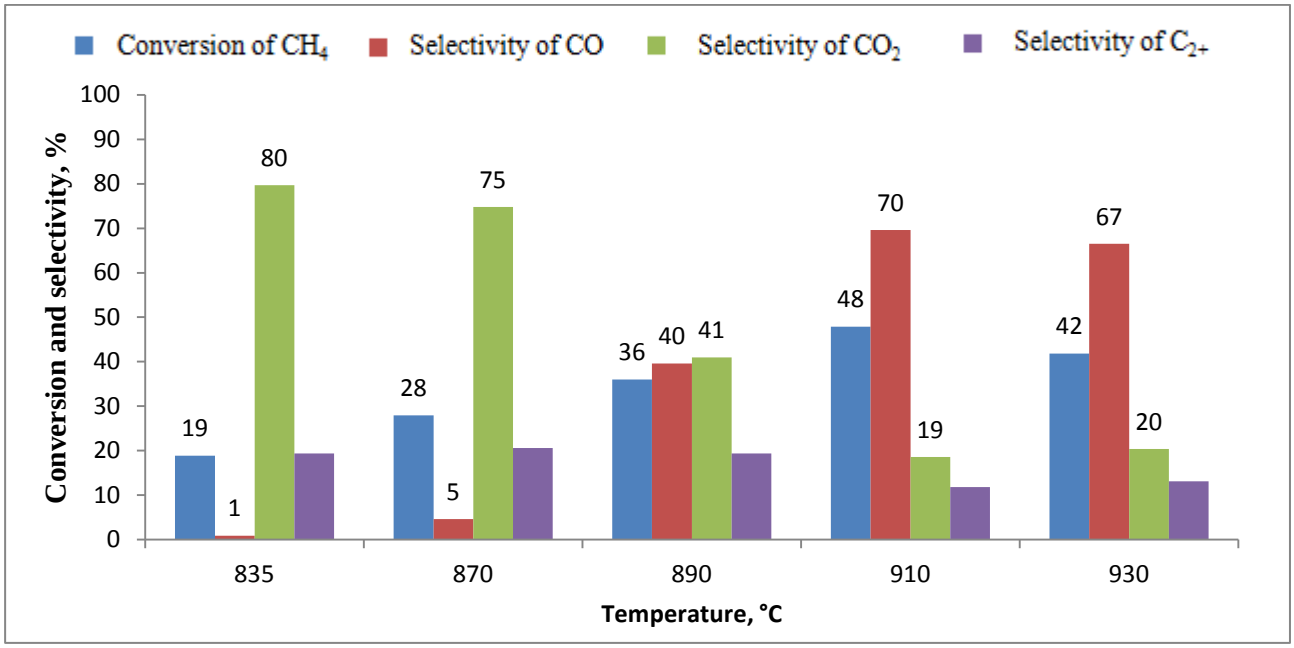


Figure 3 – $CH_4$ Conversion du méthane et sélectivités de formation de produits en fonction de température ($LaSrCoO_{4.00}$; $CH_4/O_2$ = 2; W = 22 $L*g^{-1}*h^{-1}$).

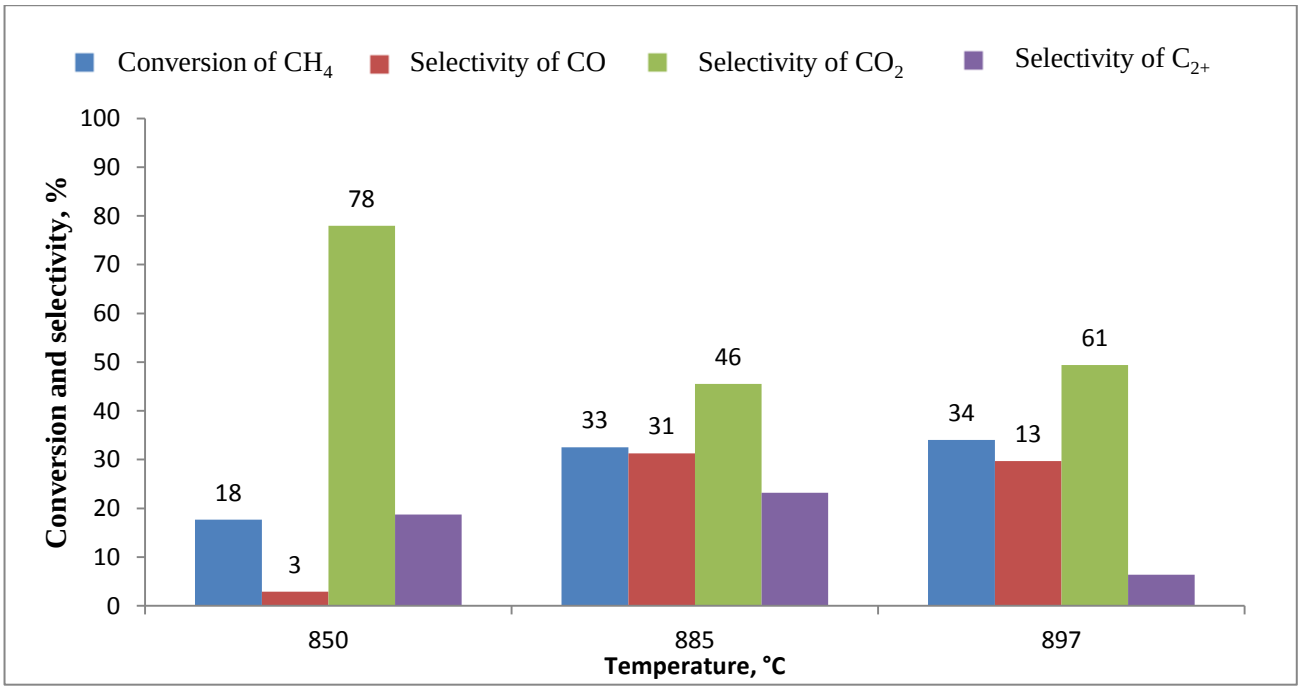


Figure 4 – Conversion du méthane et sélectivités de formation de produits en fonction de température ($La_{1.25}Sr_{0.75}CoO_{4.03}$; $CH_4/O_2$ = 2; W = 22 $L*g^{-1}*h^{-1}$).

Les résultats de la conversion du $CH_4$ et de la sélectivité de formation des produits de la

réaction sont donnés pour le rapport $CH_4/O_2$ = 2:1 et W = 22 $L \cdot g_{cat}^{-1} h^{-1}$. Comme on voit des figures, à la température plus basse que 850 °C on observe la conversion basse de $CH_4$ pour tous quatre catalyseurs, n'excédant pas 25%. De plus la sélectivité de la formation du monoxyde de carbone était proche au zéro, mais l'oxydation passait principalement avec la formation des produits de l'oxydation profonde du méthane - $CO_2$ et $H_2O$.

Comme on voit de Fig. 1-4, la matière de la composition $NdCaCoO_{3.96}$ s'est trouvé le plus effectif. L'augmentation de température de 850 à 870 ºC à l'essai $NdCaCoO_{3.96}$ (fig. 1) amenait à l'augmentation de la sélectivité de la formation du CO de 1 à 76% et les conversions de $CH_4$ de 25 à 62%. À 910°C le degré de la conversion de $CH_4$ atteignait 90% et ne variait pas à l'augmentation de température ultérieure. La sélectivité de CO et $H_2$ s'approchait vers 100%.

À l'utilisation du catalyseur $Nd_{1.25}Ca_{0.75}CoO_{4.04}$ (fig. 2) la conversion et la sélectivité étaient considérablement moins, qu'en cas de $NdCaCoO_{3.96}$. Ainsi, à l'augmentation de température de 835 à 900 $^oC$ la conversion du méthane sur $Nd_{1.25}Ca_{0.75}CoO_{4.04}$ s'est agrandie de 18% à 28 %, mais à l'augmentation de température ultérieure jusqu'à 930°C la conversion de $CH_4$ atteignait seulement 61%. Bien que l'augmentation de température soit accompagnée par l'augmentation de la sélectivité de la formation du gaz de synthèse et la réduction de la sélectivité des produits $CO_2$ et $C_{2+}$, mais la sélectivité maxima de la formation de CO et $H_2$ à 930 $^oC$ n'excédait pas 78%, sans atteindre 100%, comme en cas de $NdCaCoO_{3.96}$.

Les matériaux à base de La et Sr, se sont trouvés aussi moins actifs et sélectifs dans l'oxydation partielle du méthane. La conversion $CH_4$ atteignait les maxima sur le catalyseur $LaSrCoO_{4.00}$ à 910°C et n'excédait pas 50 %, et la sélectivité de la formation du gaz de la synthèse n'excédait pas 70% (fig. 3). L'augmentation de température ultérieure n'amenait pas aux changements considérables ni la conversion du méthane, ni la sélectivité de la formation du gaz de synthèse. La sélectivité de la formation $CO_2$ à 930°C faisait 20 %, la sélectivité sur produits $C_{2+}$ fasait 13%. Le catalyseur de la composition $La_{1.25}Sr_{0.75}CoO_{4.03}$ (fig. 4) s'est trouvé le moins actif et sélectif - l'augmentation de température de 850 à 897°C amenait à l'augmentation de la conversion de 18 à 34 %. La sélectivité de la formation du gaz de synthèse à 897°C n'excédait pas 13%.

Un des critères principaux de l'efficacité du catalyseur est la stabilité de son fonctionnement dans le temps. Le catalyseur $NdCaCoO_{3.96}$ le plus actif et sélectif a été étudié pour l'estimation de la stabilité de son fonctionnement. De fig. 5 on voit que la sélectivité de la formation du gaz de synthèse, proche de 100 %, était gardée à la longueur de 140 h à la conversion du méthane proche à 90%, sans tendance à la désactivation.

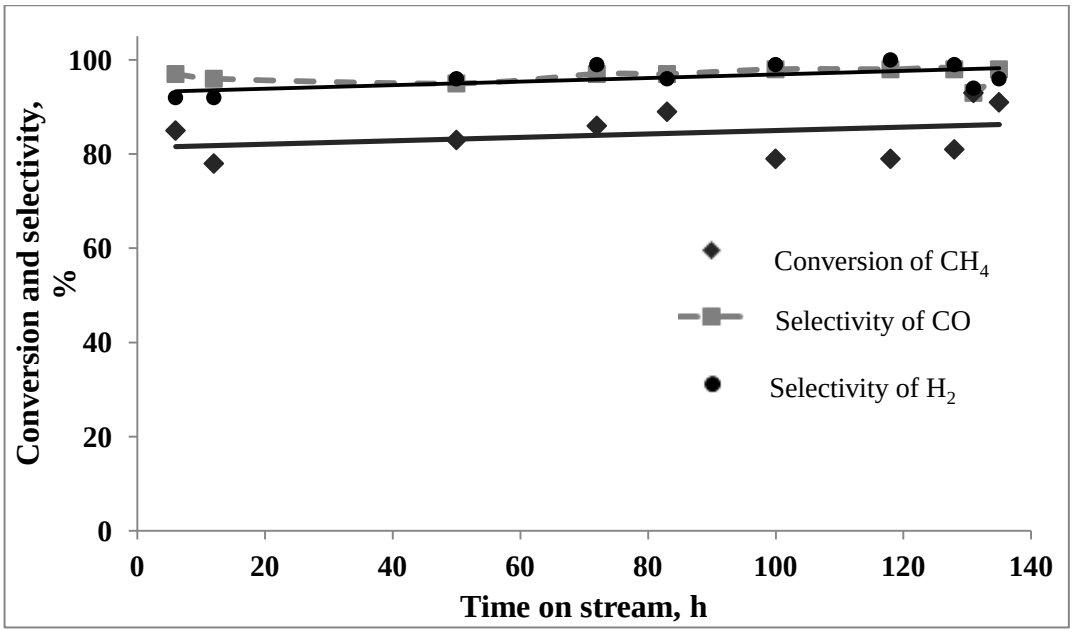


Figure 5 – Conversion de $CH_4$ et sélectivité en CO et $H_2$ en fonction de température en présence de $NdCaCoO_{3.96}$ (T = 915 - 925°C; $CH_4/O_2$ = 2-2.7; W = 20-22 $L*g^{-1}*h^{-1}$).

Les résultats obtenus permettent de supposer que les catalyseurs $LaSrCoO_{4.00}$, $La_{1.25}Sr_{0.75}CoO_{4.03}$ et $Nd_{1.25}Ca_{0.75}CoO_{4.04}$, moins sélectifs et actifs dans l'oxydation partielle du méthane se distinguent beaucoup de $NdCaCoO_{3.96}$ qui est capable de forme les centres actifs de taille nano. En raison de cela il était nécessaire d'étudier en détail les caractéristiques physico-chimiques des catalyseurs et estimer l'influence de ces caractéristiques sur les résultats des réactions.

Selon les données de l'analyse DRX, tous les matériaux ont une phase et ont la structure de pérovskite lamellaire comme le $K_2NiF_4$. Des raies correspondantes aux substances initiales ou d'autres phases, n'ont pas été découvert sur les difractogrammes. L'étude du plus actif cobaltate $NdCaCoO_{3.96}$ par la méthode de l'analyse roentgen diffraction après les expériences catalytiques a montré qu'au cours de la réaction il y a une transformation de sa structure initiale (Fig. 6).

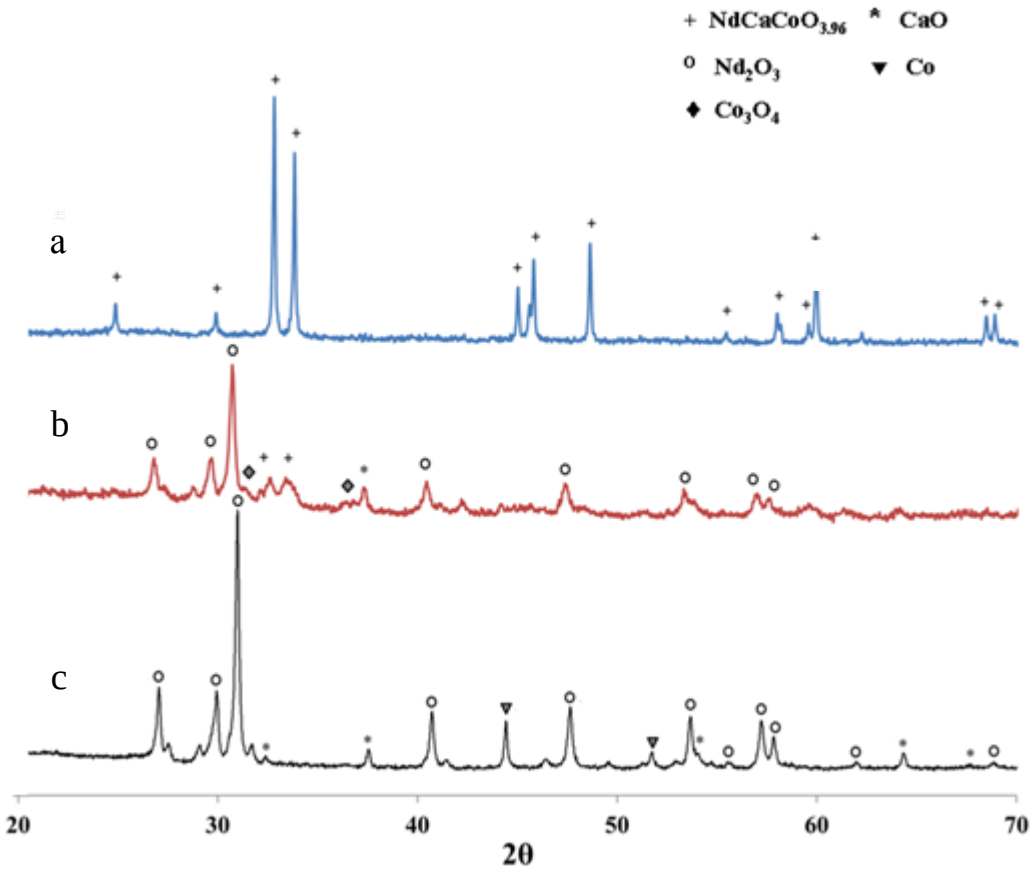


Figure 6 – Profils DRX de $NdCaCoO_{3.96}$ : a – avant OPM; b – après 12 h d'OPM; c – après 140 h d'OPM.

On voit que le catalyseur frais avait la structure de la pérovskite lamellaire et ne contenait pas dans son composition d'autres phases. Mais déjà après 12 h du fonctionnement dans la réaction d'oxydation partielle du méthane la quantité de phase initiale était beaucoup réduite, et on formait les phases suivantes $Nd_2O_3$, CaO et $Co_3O_4$. L'interaction ultérieure du catalyseur avec le milieu réactionnaire amenait à l'achèvement de la désagrégation de la phase de la pérovskite $NdCaCoO_{3.96}$ et à l'apparition de raies correspondantes à $Co^0$. De plus le catalyseur gardait une haute activité et la sélectivité en CO et $H_2$, proche à 100% (voir Fig. 5). Les résultats acquis montrent que $NdCaCoO_{3.96}$ est un precursor, qui forme pendans OPM les particules actives du cobalt métallique, dispersés dans la matrice oxyde $Nd_2O_3$-CaO.

L'étude de $NdCaCoO_{3.96}$ par la méthode de la microscopie électronique à balayage (Fig. 7) indique aussi la transformation de la microstructure initiale de la matière au contact avec le milieu réactionnaire. On observe l'apparition des particules plus fines, selon les données de l'analyse DRX contenant $Nd_2O_3$, CaO et CO.

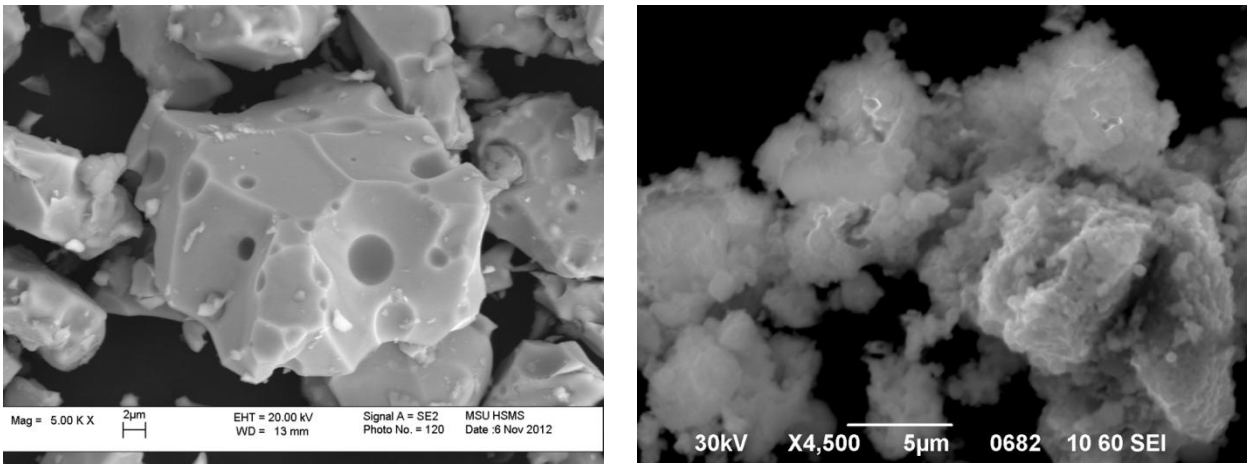


a b

Figure 7 –Images MEB of $NdCaCoO_{3.96}$: a - avant OPM; b – après 12 h d'OPM

Les résultats de l'étude des catalyseurs synthétisés par la méthode de la réduction thermo programmé par l'hydrogène ($H_2$-TPR) sont présentés Fig. 8. On voit qu'à la réduction de tous les catalyseurs des séries $La_{2-x}Sr_xCoO_{4\pm\delta}$ et $Nd_{2-x}Ca_xCoO_{4\pm\delta}$ deux pics principale de l'absorption de l'hydrogène sont obtenus.

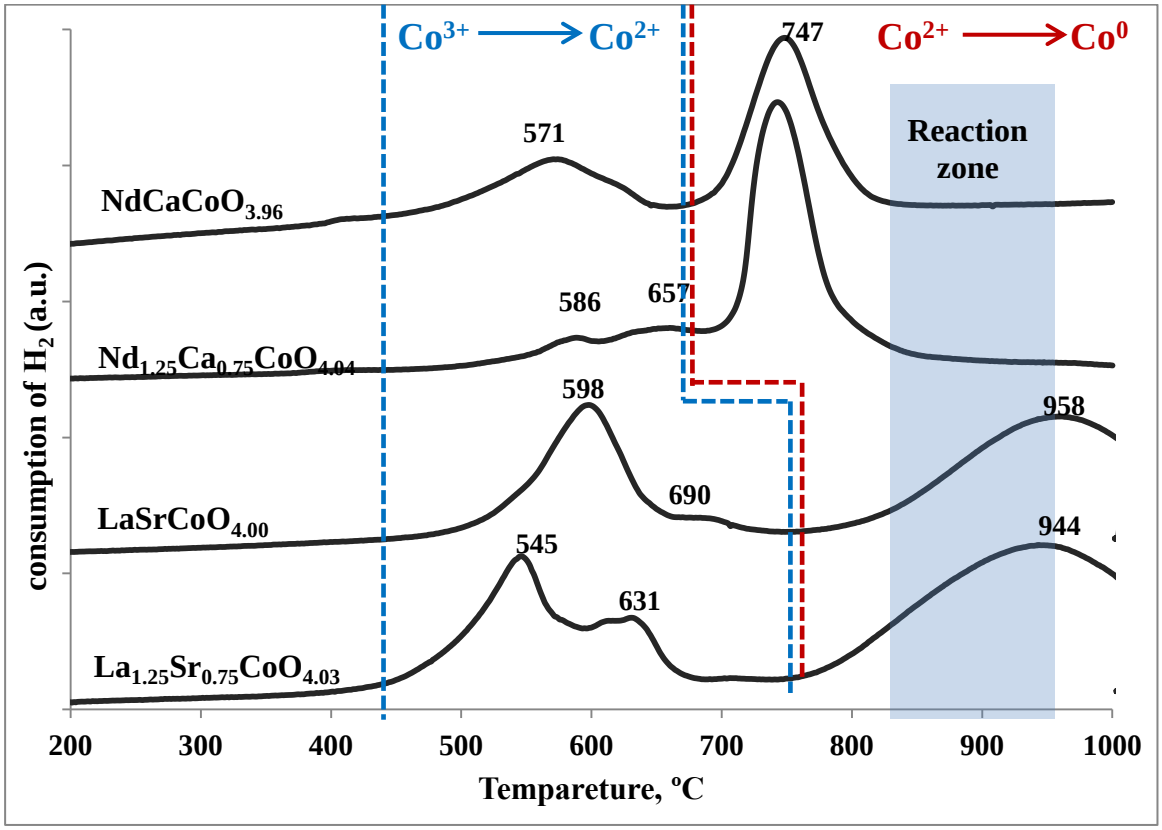


Figure 8 – $H_2$-temperature programmed reduction curves of synthesized catalysts.

Selon les données littéraires, le pic à basse température à 550-650°C peut être attribué à la réduction des ions $Co^{3+}$ jusqu'à $Co^{2+}$. Le pic de la réduction aux températures plus élevées correspond

d'habitude à la réduction $Co^{+3}$ et $Co^{2+}$ jusqu'à $Co^0$.

Au contraire des catalyseurs de la série $Nd_{2-x}Ca_xCoO4_{\pm\,\delta}$, en cas des cobaltates du lanthane le deuxième pic de l'absorption de l'hydrogène, témoignant la formation de la phase $Co^0$, est déplacé à des températures plus élevées avec le maximum ~ 950ºC. La température donnée est plus haute que la température de l'OPM dans les expériences faites par nous. Donc, on peut supposer que la formation de la phase active de Co métallique dans ces systèmes est difficile: la température initiale de la deuxième pic de l'absorption $H_2$ est de 800ºC, tandis que les matériaux contenant Nd et Ca à cette température sont déjà réduits entièrement. On peut expliquer par cela l'activité et la sélectivité basses des cobaltates de lantana-strontium par rapport aux cobaltates du néodyme-calcium.

Ainsi, les études des catalyseurs par la méthode $H_2$-TPR permettent de supposer que l'activité catalytique des cobaltates synthétisés dépend de leur capacité de la réduction et de la température à laquelle on forme la phase active métallique du cobalt. En raison de cela il présentait un intérêt d'étudier des propriétés catalytiques de $La_{2-x}Sr_xCoO_{4\pm\,\delta}$ et $Nd_{2-x}Ca_xCoO_{4\pm\,\delta}$ préalablement réduits dans l'hydrogène, i.e. avec la phase $Co^0$ déjà formée. Les températures de la réduction des catalyseurs étaient choisies en vertu des données de $H_2$-TPR. Après l'acquisition de la température nécessaire, le flux de gaz était changé de l'hydrogène pour le mélange $CH_4/O_2$ (2/1). Les résultats sont présentés Fig. 9 et 10.

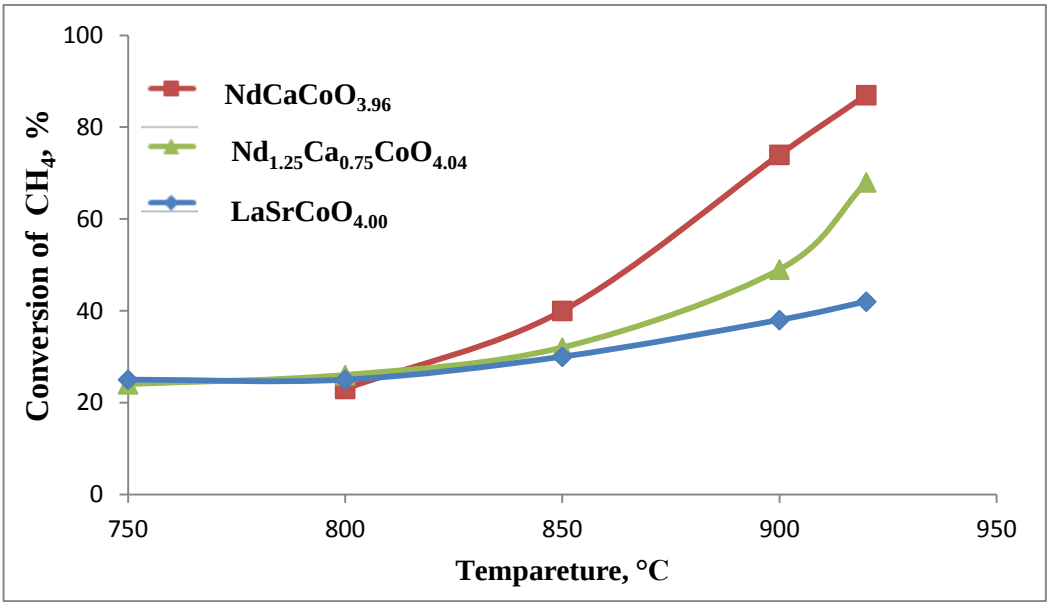


Figure 9 – Conversion du méthane en fonction de la température en présence des catalyseurs réduits préalablement en flux d'hydrogène ($CH_4/O_2$ = 2; W = 22 $L*g^{-1}*h^{-1}$)

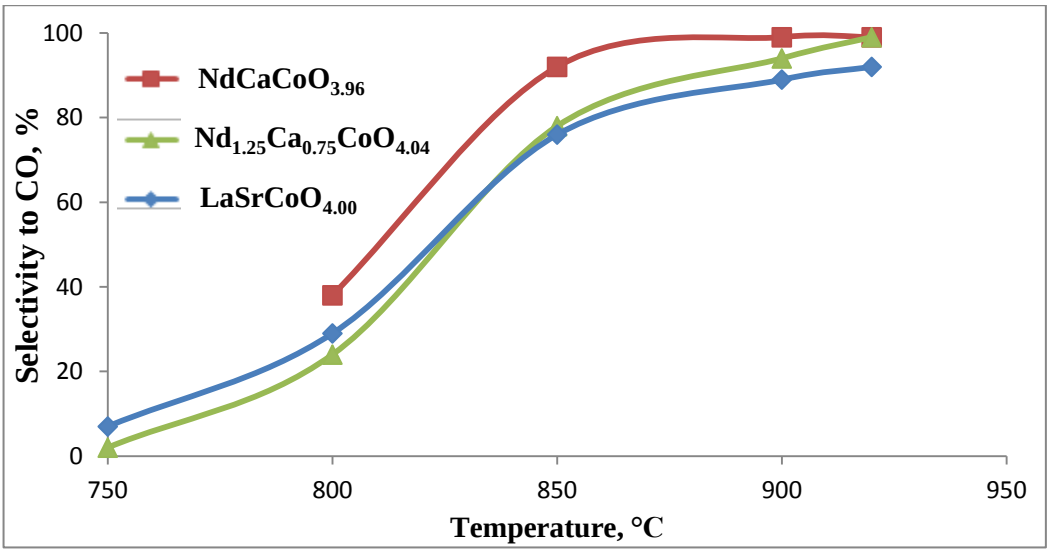


Figure 10 – Sélectivité de formation de CO en fonction de la température en présence des catalyseurs réduits préalablement en flux d'hydrogène ($CH_4/O_2$ = 2; W = 22 $L*g^{-1}*h^{-1}$).

On voit que la formation de CO commençait déjà à 800 °C (la comparaison avec les données de Fig. 1-3). Le catalyseur le plus actif est de nouveau $NdCaCoO_{3.96}$ - la conversion du méthane sur le catalyseur atteignait 87%. L'activité des cobaltates, toujours, diminuait dans une série: $NdCaCoO_{3.96}$ < $Nd_{1.25}Ca_{0.75}CoO_{4.04}$ < $LaSrCoO_{4.00}$ ce que correspond aux résultats de OPM sur les catalyseurs sans stade préliminaire de la réduction. En même temps, la réduction préliminaire augmentait beaucoup la sélectivité, qui déjà à 850°C atteignait 80-95%, tandis que les catalyseurs non réduits à la température donnée conduisaient seulement les réactions de l'oxydation profonde. Les catalyseurs moins actifs $Nd_{1.25}Ca_{0.75}CoO_{4.04}$ et $LaSrCoO_{4.00}$ sans réduction montraient la sélectivité maxima au niveau de 80 et 70%, en conséquence, mais étant préalablement réduits, l'ont augmenté jusqu'à 99 et 92%.

Les résultats de l'étude $NdCaCoO_{3.96}$, $Nd_{1.25}Ca_{0.75}CoO_{4.04}$ et $LaSrCoO_{4.00}$ par la méthode de l'analyse DRX après la réduction et la réaction d'OPM sont présentés Fig. 11. On voit de diffractogrammes que les cobaltates $NdCaCoO_{3.96}$ et $Nd_{1.25}Ca_{0.75}CoO_{4.04}$ préalablement réduits formaient le système $Co^0/Nd_2O_3$-CaO, qui était gardé entièrement pendant la catalyse, tandis que le système $Co/La_2O_3$-SrO formé de $LaSrCoO_{4.00}$, partiellement se reoxydait pendant la réaction et la structure initiale de pérovskite lamellaire a été formée.

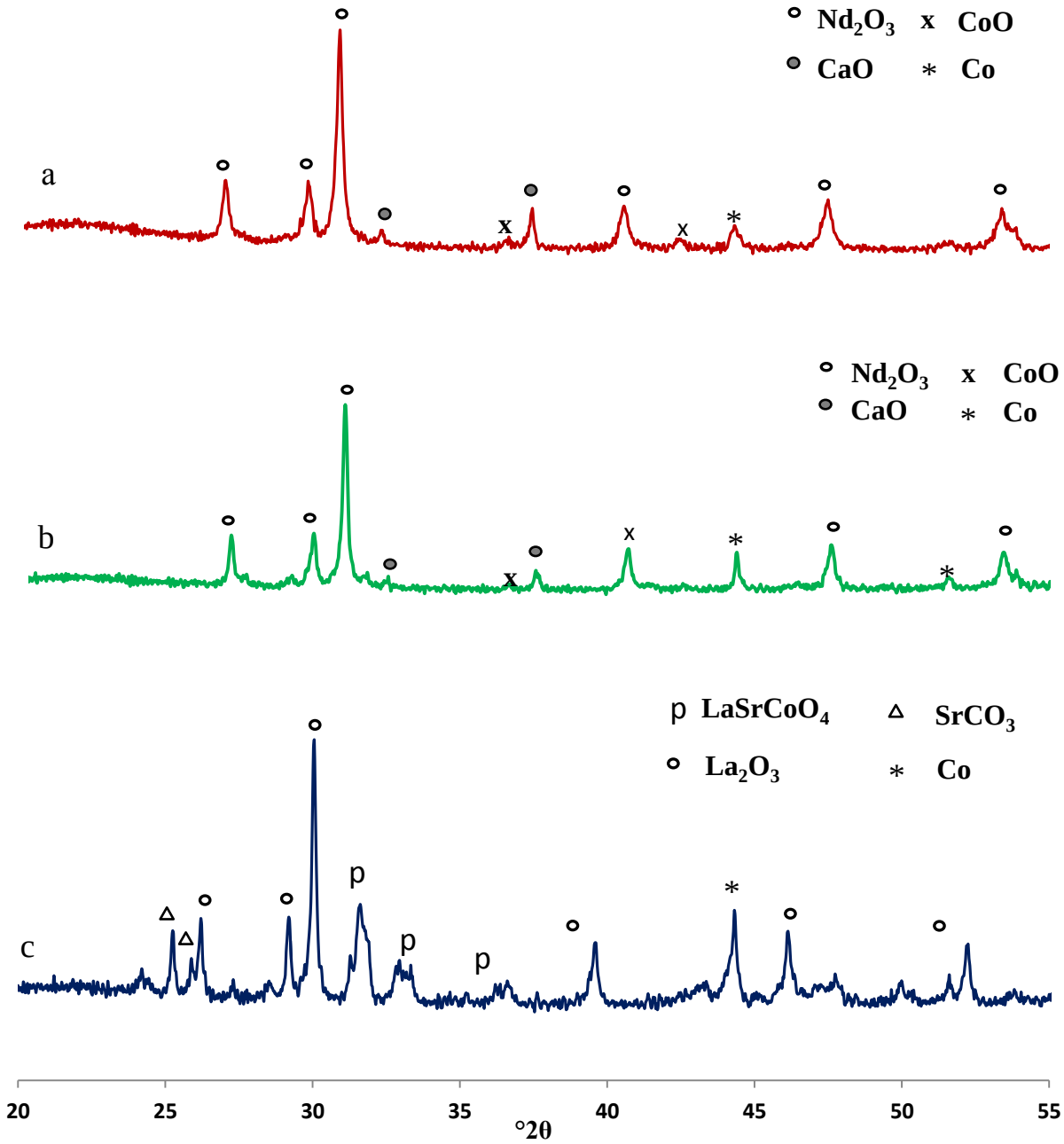


Figure 11 – Profils DRX des catalyseurs après la réaction OPM : a - $NdCaCoO_{3.96}$; b - $Nd_{1.25}Ca_{0.75}CoO_{4.04}$; c – $LaSrCoO_{4.00}$

L'étude des catalyseurs par la méthode de la microscopie électronique à transmission (Fig. 12) a montré qu'après la réduction et utilisation dans l'OPM $NdCaCoO_{3.96}$ formera la matière contenant les nanoparticules métalliques, tandis qu'en cas de $Nd_{1.25}Ca_{0.75}CoO_{4.04}$ et $LaSrCoO_{4.00}$ on ne réussit pas à fixer la formation des clusters semblables.

Les données expérimentales reçues dans notre travail, ont permis de supposer que OPM dans la

présence de $NdCaCoO_{3.96}$ passe notamment à l'interface de deux phases . Cela, à son tour, donne la raison de croire que le catalyseur $NdCaCoO_{3.96}$, actif et sélectif en OPM, peut aussi manifester l'activité en reformage du méthane à sec.

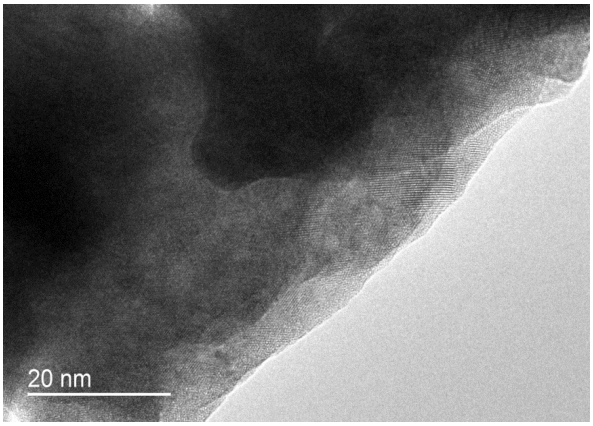


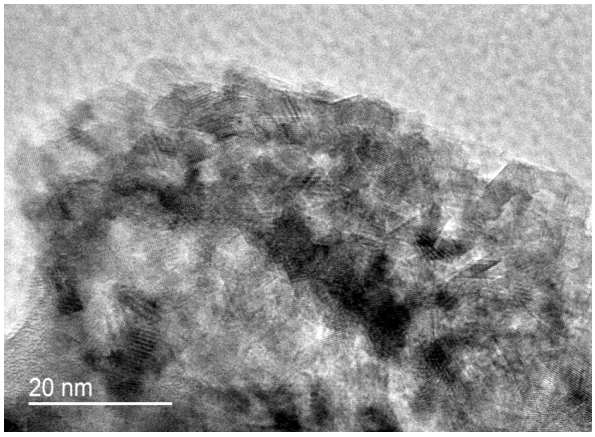


Figure 12 – Images MET des catalyseurs of catalysts after reduction in $H_2$ flow followed by partial oxidation of methane: a - $LaSrCoO_{4.00}$; b - $NdCaCoO_{3.96}$;

$NdCaCoO_{3.96}$ a été teste dans RMS à la présentation du mélange non dilués par le gaz inerte de $CH_4$ et $CO_2$. L'essai du catalyseur à la longueur de 50 h (le temps total du séjour du catalyseur dans les conditions du RMS sans compter la période de sa mise au régime dans le flux de réactifs) n'a pas révélé du changement important du rendement du gaz de synthèse (fig. 13)

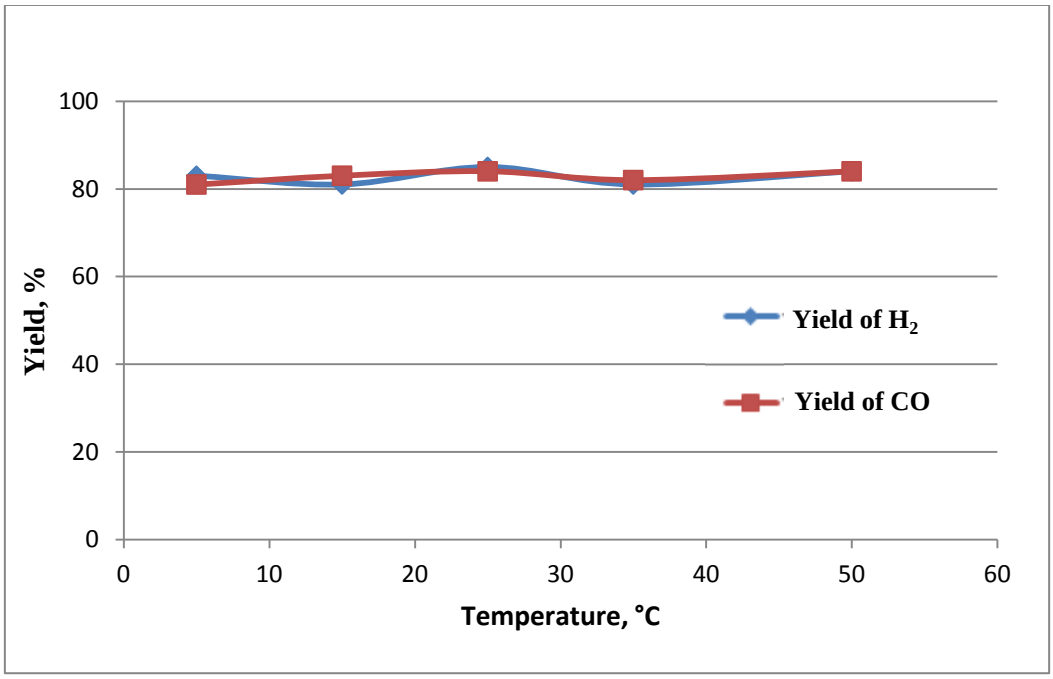


Figure 13 – Rendement de CO и $H_2$ en présence $NdCaCoO_{3.96}$ pendant le RMS en fonction de la température (T = 900ºC; $CH_4/CO_2$ = 1; W = 20 $L*g^{-1}*h^{-1}$)

.

Ainsi, le catalyseur $NdCaCoO_{3.96}$ a démontré la bonne stabilité dans le procédé de RMS, en

montrant le rendement du gaz de synthèse au niveau de 80% et la sélectivité proche de 100%. Les résultats acquis confirment indirectement le mécanisme d'OPM dans la présence de $NdCaCoO_{3.96}$ comme un mécanisme en deux étapes.

# UNIVERSITÉ DE STRASBOURG

*ÉCOLE DOCTORALE DE SCIENCES CHIMIQUES*
**L'Institut de chimie et procédés pour l'énergie, l'environnement et la santé**

# THÈSE présentée par :

**Dmitry KOMISSARENKO**

soutenue le : **24 septembre 2015**

pour obtenir le grade de : **Docteur de l'université de Strasbourg**
Discipline/ Spécialité : chimie

# OXYDATION CATALYTIQUE SELECTIVE DU METHANE EN GAZ DE SYNTHESE AVEC DES OXYDES MIXTES DE COBALT ET DES ELEMENTS DES TERRES RARES

**THÈSE dirigée par :**

| | |
|---|---|
| **Mme ROGER Anne-Cécile** | Professeur, Université de Strasbourg |
| **M DEDOV Alexey** | Professeur, Université d'État Gubkin du Pétrole et du Gaz |

**RAPPORTEURS :**

| | |
|---|---|
| **M ANISIMOV Alexander** | Professeur, Université d'État Lomonossov de Moscou |
| **Mme BATIOT-DUPEYRAT Catherine** | Professeur, Université de Poitiers |

---

**AUTRES MEMBRES DU JURY :**

| | |
|---|---|
| **M LOUIS Benoit** | Chargé de recherche CNRS, Université de Strasbourg |
| **Mme PARKHOMENKO Ksenia** | Chargé de recherche CNRS, Université de Strasbourg |
| **M LOKTEV Alexey** | Professeur, Université d'État Gubkin du Pétrole et du Gaz |

# Content

**Chapter 1. Literature review** ..... 22
1.1 Methods of oxidative methane conversion to synthesis gas ..... 22
1.1.1 Steam reforming of methane ..... 23
1.1.2 Dry reforming of methane ..... 26
1.1.3 Partial oxidation of methane ..... 28
1.2 Mechanism and catalysts of partial oxidation of methane ..... 30
1.2.1 Mechanism of partial oxidation of methane ..... 30
1.2.2 Catalytic materials of partial oxidation of methane ..... 40
**Chapter 2. Experimental section.** ..... 55
2.1 Initial reactants ..... 55
2.2. Methodic of catalytic tests performance ..... 55
2.2.1 Study of partial oxidation of methane and dry reforming of methane to synthesis gas. ..... 55
2.2.2 Analysis of products of partial oxidation of methane and dry reforming of methane ..... 57
2.3 Catalyst synthesis methods ..... 59
2.4 Physico-chemical analysis of the catalysts ..... 60
2.4.1 X-ray diffraction study ..... 60
2.4.2 X-ray photoelectron spectroscopy method ..... 60
2.4.3 Scanning electron microscopy with energy dispersive X-ray analysis. ..... 60
2.4.4 Transmission electron microscopy ..... 61
2.4.5 Hydrogen temperature programmed reduction ..... 61
2.4.6 Iodometric titration analysis ..... 62
**Chapter 3. Results and discussion** ..... 63
3.1 Study of partial oxidation of methane to synthesis gas over synthesized catalysts 65
3.2 Study of influence of physico-chemical properties of synthesized catalysts on the results of methane partial oxidation to synthesis gas. ..... 77
3.3 Evaluation of catalytic activity of $NdCaCoO_{3.96}$ in dry reforming of methane ..... 98

**Conclusions** ..... 102
**Bibliography**..... 103
**Annex**..... 115

# Introduction

Chemical processing of gas feedstock, primarily natural gas, is a very important task. Proven worldwide reserves of natural gas are about 187 trillion $m^3$. Russian Federation has the highest proven reserves of natural gas possessing about 30% (55 trillion $m^3$) of world reserves [1,2]. According to Russian Statistics (Rosstat), in 2014 the volume of gas produced in Russia was around 640 billion $m^3$ [3]. Nowadays, the largest amount of natural gas is used as a fuel and is not engaged to chemical processing. Natural gas is not only one of the most environmentally friendly feedstock but it also can be used as a raw material for the production of a numerous petrochemical products. The main component of natural gas is methane and its involvement in chemical processing is an urgent task.

Currently, the key area of chemical processing of methane is its conversion into synthesis gas [4-10]. Production of synthesis gas is a large-scale industrial process, on its basis major intermediates and products of the chemical industry are produced such as hydrogen, methanol, synthetic fuels and others. For instance, the worldwide methanol production capacity in 2014 exceeded 60 million tons [3]. According to experts, the most expensive stage in the petrochemical production chain from methane is synthesis gas production with about 70% of the costs. Any improvement in the process of synthesis gas production is an important problem.

Partial oxidation of methane (POM) and dry reforming of methane (DRM) are perspective processes for synthesis gas production. The major problem of these processes is a creation of selective and stable catalyst as well as a decreasing of the processes temperature. The solution of these problems is required studying of active sites nature of the catalysts.

The aim of current research is to improve the processes of partial oxidation and dry reforming of methane to synthesis gas by creating new selective and stable catalysts based on complex oxides with a layered perovskite-like structure, as well as to identify correlations between the composition and physico-chemical properties of the studied

catalysts and the methane oxidation processes. For that it was necessary to solve the following problems:

- synthesize the catalytic materials with layered perovskite-like structure;
- study their catalytic properties in POM and DRM;
- study of physico-chemical properties of the synthesized catalytic materials.

# Chapter 1. Literature review
# Oxidative methane conversion to synthesis gas

## 1.1 Methods of oxidative methane conversion to synthesis gas

In the literature devoted to gas feedstock processing mainly three methods of oxidative methane conversion to synthesis gas (mixture of carbon monoxide and hydrogen) have been discussed [6-10]:

- ***Steam reforming of methane (SRM)***

$CH_4+H_2O \leftrightarrow CO+3H_2$ $\Delta H^0_{298}$= +206 kJ/mole; (1)

- ***Partial oxidation of methane (POM)***

$2CH_4+ O_2 \leftrightarrow 2CO+4H_2$ $\Delta H^0_{298}$= -36 kJ/mole; (2)

- ***Dry reforming of methane (DRM)***

$CH_4 + CO_2 \leftrightarrow 2CO + 2H_2$ $\Delta H^0_{298}$= +247 kJ/mole (3)

The processes are characterized by different thermal effect and a different composition of the resulting synthesis gas. The proportion of obtained $H_2$ and CO, preferable for the synthesis of certain compounds can be achieved by adjusting the variation of oxidants. The methane steam reforming reaction produces a synthesis gas with a composition of CO: $H_2$ = 1: 3, containing a large amount of hydrogen used for ammonia. For the synthesis of methanol or hydrocarbons via the Fischer-Tropsch process synthesis gas with a ratio of CO: $H_2$ - 1: 2 is required. Partial oxidation of methane - the most preferred reaction to produce synthesis gas of this ratio. Dry reforming of methane produces synthesis gas composition, favorable for the synthesis of dimethyl ether and hydroformylation reaction. There are also examples of hydrocarbon conversion under the action of several oxidants - $H_2O$, $O_2$ and $CO_2$ [11,12], which allow to vary the composition of the resulting synthesis gas, and the thermal effect process.

Steam reforming of methane and dry reforming of methane are highly endothermic reactions, while the partial oxidation of methane is the exothermic

reaction. According to thermodynamic calculations, all three processes are required high temperatures, above 800°C, to achieve acceptable levels of $CH_4$ conversion and selectivity to CO and $H_2$ [13]. In addition to the thermodynamic limitations, providing high selectivity and yield of the synthesis gas is constrained by factors related to the occurrence of adverse reactions. Therefore it is particularly important to develop a catalyst capable of providing a high yield of the synthesis gas and to reduce the temperature of the methane oxidation. It should be noted that all three methods of oxidative conversion of methane to synthesis gas have common features – these processes are required high-temperature and occur mainly in the presence of Group VIII metals.

### 1.1.1 Steam reforming of methane

Currently, steam reforming of methane is the main industrial catalytic process for synthesis gas production from natural gas. The main reaction takes place at temperatures 900-1000 ºC, space velocity 1000 $hr^{-1}$ and an elevated pressure. In the process of steam reforming of methane, are mainly used catalyst materials based on nickel. In addition to the main reaction (1) at least two secondary reactions can proceed [8]:

water gas shift reaction (hydrogenation of $CO_2$)

$$CO_2 + H_2 \leftrightarrows CO + H_2O \quad \Delta H^0_{298} = +41 \text{ kJ/mole} \quad (4)$$

and Boudoir's reaction

$$2CO \leftrightarrows C + CO_2 \quad \Delta H^0_{298} = -171 \text{ kJ/mole} \quad (5)$$

A main problem of the steam reforming of methane is a reactivity and state of surface carbon which is formed by the first stage of the process - the dissociation of methane:

$$CH_4 + Ni \rightarrow Ni_n\text{-}CH_x \rightarrow Ni_m\text{-}C \rightarrow [C,Ni] \rightarrow \text{filamentous C}$$

Formation of the desired reaction products - CO and $H_2$, takes place by the interaction of $CH_4$ dissociation products with surface hydroxyl groups:

$$Ni_n\text{-}CH_x + Ni\text{-}OH_y \rightarrow Ni + CO + H_2$$

$$Ni_m\text{-}C + Ni\text{-}OH_y \rightarrow Ni + CO + H_2$$

The process of methane dissociation on Ni is structurally sensitive. The use of transmission electron microscopy (TEM) in situ allowed a detailed examination of the mechanism of activation of methane on Ni and deactivation of active sites [14]. $CH_4$ molecules interact with “steps” on Ni nanocrystals and form of graphite clusters, which are then rearranged in a multi-layer carbon nanotube. Simultaneously with the growth of nanotubes nickel particle are also reconstructed which changes their shape and size. After complete encapsulation of Ni the growth of nanotube is done and the catalyst is deactivated. A comparison of the reactions taking place on the smooth surface of a Ni (111) single crystal and Ni (211) stepped surface, indicated that the activation energy of all stages of the sequence

$$CH_4 \rightarrow CH_{3s} \rightarrow CH_{2s} \rightarrow CH_s \rightarrow C_s \rightarrow CO$$

on the stepped surface lower than that on a smooth one but for different links of the sequence of activation energy is different. Ni (111) edge exhibits a catalytic activity in the reaction of SRM but it is inactive in carbon deposition processes, while Ni (211) edge active in both carbon deposition and catalytic reaction. It is noted that in general the steps are disadvantageous for steam reforming of methane.

In addition to Ni other metals of VIII group such as Rh, Ru, Ir, Pt, Pd, Co, Fe are able to catalyze steam reforming of methane [6,7]. However, iron and cobalt in SRM are often oxidized and deactivated whereas the noble metals are quite expensive. Therefore, despite the large number of studies devoted to the selection of SRM catalysts nowadays in industry nickel supported catalysts are mainly used. As a support such oxides as $\alpha$-$Al_2O_3$, MgO, ZrO are generally used. $\alpha$-$Al_2O_3$ has high mechanical strength and stability, but has low specific surface area and suffer from coking. Magnesium oxide is less susceptible to coking than $Al_2O_3$. Introduction of additives alkali metal prevents the formation of coke, but it decreases the catalyst activity. For a better mass transfer catalysts are used in the form of small beads or rings. The main drawback of the Ni catalysts is the ability to form carbon fibers in SRM. In addition to catalyst deactivation the growth of such filaments reduces the strength of the catalyst and leads to its destruction, the gas flow impedes interaction with the surface and deteriorates the heat exchange [8]. To improve the mechanical strength of the catalyst cementitious binder containing free of $SiO_2$, for

example $CaAl_2O_3$was proposed. However, these catalysts lose activity due to formation $NiAl_2O_3$ spinel during operation.

Increasing of synthesis gas yield in SRM could be achieved by removal $H_2$ or CO from reaction zone [15]. Removal of CO can be done by its absorption for instance by CaO:

$$CH_4 + 2H_2O + CaO \rightarrow 4H_2 + CaCO_3 \quad (6)$$

In this case, the regeneration of the sorbent is required for example by decomposition of calcium carbonate. For hydrogen removal metal membrane can be used, which also can prevent the poisoning of the catalyst caused by hydrogen sulphide contained in methane. It is to note that the deposition of the $Ni/Al_2O_3/Al$ catalyst on thick layer of the reactor walls can lead to significant improvement of heat transfer. In [15] a tubular heat exchange SRM reactor was proposed. The reactor allows combining two processes - total oxidation of methane realized on Ni-Cr-foam supported on the perovskite and steam reforming of methane took place on the Ni-catalyst. Thus, by combining exothermic and endothermic reactions the oxidation of methane to synthesis gas can reach of the total thermal effect closed to zero. The Velosys Incorporation has developed a technology of SRM [8] which uses the MRT-reformer (MRI - Microprocessing Technology). The reactor consists of a large number of mutually intersecting microchannels with diameter less than 1 micron. Layers where heat-transfer agent and the layers in which the conversion of natural gas successively alternate. This combination results in a significant increase in heat transfer and reduce the size of equipment compared to conventional devices of SRM.

The main disadvantages of the process of steam reforming of methane are using very large amounts of superheated steam and an excess amount of $CO_2$ caused by secondary process [5]. The synthesis gas with $H_2/CO$ ratio obtained by SRM is not favorable for further using in synthesis of methanol or hydrocarbons via the Fischer-Tropsch. For this purpose during SRM $O_2$ or $CO_2$ are added to reaction system resulting to formation of syngas with the desired ratio.

### 1.1.2 Dry reforming of methane

The interest in dry reforming of methane consist in possibility of obtaining synthesis gas with $H_2$/CO ratio favorable to synthesis of hydrocarbons, dimethyl ether, formaldehyde and involvement in the process of such source of raw material as carbon dioxide. Recently, the issue of reducing industrial $CO_2$ emissions becomes especially important and as a result there is an intensive growth of research devoted to DRM. In comparison with steam reforming of methane DRM is even more endothermic and is carried out at temperatures above 900°C generally in the presence of transition metal elements and its oxides.

Selectivity and conversion closed to 100% are achieved at temperatures about 1000-1100ºC. The Gibbs free energy is zero at 640ºC. Below this temperature the methanation of CO is preferable and the equilibrium is shifted toward the formation of $CH_4$ and $CO_2$. Besides of the main reaction (2) in a mixture of $CH_4$ and $CO_2$ formation of carbon occurs:

$$CH_4 + 2CO_2 \rightarrow C + 2CO + 2H_2O \quad (7)$$

Also in the presence of $CO_2$ oxidative coupling of methane can takes place:

$$2CH_4 + CO_2 \rightarrow C_2H_6 + CO + H_2O \quad (8)$$

At 800ºC $C_2H_6$ yield is close to 13%. Formation if $C_{2+}$ углеводородов –products was observed mainly over oxide catalysts.

It was shown that mechanism of dry reforming of methane involves stages of formation of C, H, O and CO adsorbed species on the surface of a catalyst followed by CO and $H_2$ formation [17-19]:

$$CO_2 + (S) \leftrightarrow CO + O(S)$$

$$CH_4 + (S) \leftrightarrow CH_x(S) + (4\text{-}x)H(S) \leftrightarrow C(S) + 2H_2$$

$$C(S) + O(S) \leftrightarrow CO + (S)$$

$$CO(S) \leftrightarrow CO + (S)$$

As in the case of SRM the most widely known catalysts for DRM are nickel-based ones. Co, Fe, Pt, Pd, Rh, Ir supported on different substrates are also active [6-8]. It was noted the supports with basic properties like MgO or $La_2O_3$ can participate in the

activation of $CO_2$. On this sort of supports adsorbed $CO_2$ reacts with carbon via reverse Boudoir's reaction.

On the Ni/α-$Al_2O_3$ [20], Co/α-$Al_2O_3$ [21] and Pt/α-$Al_2O_3$ [22] catalysts dry reforming of methane was studied in both flowing and pulsed modes. It has been shown that practically methane does not react with the oxides of nickel and cobalt but is actively engaged with the reduced metal to form a surface $H_2$ and carbon which is able to react slowly with lattice oxygen and rapidly with surface adsorbed one. Also, surface carbon quickly reacts with $CO_2$ to form CO and slowly with metal particles (Me) forming CO and MeO. Thus, it is proved that the main route to the DRM on Ni/α-$Al_2O_3$ and Co/α-$Al_2O_3$ catalyst includes chemisorption of methane to form C + $2H_2$ and interaction of carbon with CO2 via inverse Boudoir's reaction:

$C + CO_2 \leftrightarrows 2CO$ (9)

Secondary routes are the interaction of chemisorbed C and $H_2$ with lattice oxygen of the catalyst and dissociative adsorption of $CO_2$ on the metal. The competitive reaction of carbon with surface oxygen decreases the conversion of $CO_2$ in the main reaction. The addition of $O_2$ into reaction causes a decrease in $CH_4$ + CO2 reaction rate (oxygen poisoning of the catalyst).

Cobalt catalysts are comparable to nickel ones in terms of activity and stability [23]. The most active is Co/MgO/$SiO_2$. Co/γ-$A1_2O_3$ is characterized by the same features as Ni/γ-$A1_2O_3$. The stability and activity of the catalyst depends on the Co content and calcination temperature. High cobalt content promotes deactivation caused by coke deposition. The activity of Co/$TiO_2$ catalyst strongly depends on the temperature of its reduction [24]. Only the catalyst reduced at T> 850°C has high activity and stability. Addition of small amounts of Pt and Ru improves these figures.

In addition to the metal catalysts complex oxides with perivskite-like structure are highly active in DRM. For example, in the case of using the compounds of the $LaNi_xFe_{1-x}O_3$ composition complete conversion of $CH_4$ and $CO_2$ was achieved at 800°C [25]. The authors indicate that during the reaction the catalyst perovskite-like structure is destroyed. For catalyst with x = 0.3 - 0.8 Ni-Fe alloys are formed. It is assumed that

the formation of alloys prevents carbon deposition on the catalyst by inhibiting the diffusion of carbon through the particle Ni.

Authors [26] was studied $La_{1-x}Sr_xNiO_3$ (x = 0.01, 0.1) and $La_{2-x}Sr_xNiO_4$ (x = 0.1), with perovskite-like structure. It was found that their catalytic activity and resistance to coke formation at 600°C and atmospheric pressure dependent on the anion sublattice defectiveness. $La_{0.9}Sr_{0.1}O_3$ and $La_{1.8}Sr_{0.2}NiO_4$ had maximal activity among strontium substituted catalysts. According to XRD data under DRM catalyst converted into a mixture $La_2O_2SO_2$, $SrCO_3$ and metallic Ni. The authors have suggested that the high activity of the catalysts due to the presence of two centers: $La_2O_3$ which is responsible for activation of $CO_2$ and Ni activating $CH_4$.

The main difficulty for the industrial use of DRM is strong coking of metal catalysts [6-8]. To reduce the poisoning of nickel catalysts Haldor Topsoe suggests using as a raw material mixture of $CH_4$, $CO_2$ and $H_2O$. There is also a process of steam reforming of methane in which part of the steam is substituted by $CO_2$ which cen reduce the $H_2$/CO ratio from 2.7 to 1.8. The process proceeds at 915-945ºC and 9 at. Into the reactive gases sulfur vapor added to passivate the nickel catalyst and prevent carbon formation. Sulfur prevents the formation of large ensembles of carbon, and thus inhibits coke formation reaction is stronger than the DRM process. A disadvantage of this process is the formation of $C_2$-products.

DRM is a promising method for synthesis gas production but nowadays it has not been realized in industry, primarily because of the difficulties associated with catalyst coking.

### 1.1.3 Partial oxidation of methane

The partial oxidation of methane (POM) - slightly exothermic process [5-10]. From this viewpoint, POM is more preferable in comparison with the endothermic processes of SRM and DRM. The resulting synthesis gas composition ($H_2$/CO = 2) is preferred for the synthesis of methanol or hydrocarbons by Fischer-Tropsch synthesis. In addition, POM does not require supply of large amounts of superheated steam as the SRM.

Along with the steam and carbon dioxide reforming of methane (reaction 1 and 3, respectively), during the partial oxidation of methane can also tale place following reactions [27]:

$CH_4 + 2O_2 \rightarrow CO_2 + 2H_2O$ (10)

$CH_4 + O_2 \rightarrow CO_2 + 2H_2$ (11)

$CH_4 \leftrightarrow C + 4H_2$ (12)

$2CO \leftrightarrow CO_2 + C$ (13)

$CO + H_2O \leftrightarrow CO_2 + H_2$ (14)

$CO + H_2 \leftrightarrow C + H_2O$ (15)

$CO + 0.5O_2 \rightarrow CO_2$ (16)

$H_2 + 0.5O_2 \rightarrow H_2O$ (17)

Partial oxidation of methane can be carried out in a homogeneous way without using a catalyst. In this case, in order to achieve high yields of synthesis gas high temperature is requires that can reach 1300°C [5]. As oxidant can act air, oxygen-enriched air or pure oxygen can be used. However, large scale production is preferable to use pure oxygen generators, not only to reduce the size of equipment as to avoid costly purification procedure of a mixture of CO and $H_2$ from nitrogen. In industry, the homogeneous partial oxidation of methane is realized at the factory for production of diesel oil company Shell, which uses a homogeneous non-catalytic process [5-10]. The reaction takes place at 1150-1300 ° C and pressures in the range of 25-80 atm. After purification of $H_2S$ and $CO_2$ Synthesis gas with $H_2$: CO = 1: 2 composition was converted into a mixture of high molecular waxy hydrocarbons. Then on zeolite catalysts they are subjected to cracking and hydrocracking to produce diesel. A disadvantage of the homogeneous POM is a high reaction temperature.

Catalytic pilot plans at atmospheric pressure temperature of POM exceeds750°C [5,6]. In practice, it preferred to use higher pressures. With increasing pressure high yields are achieved at higher temperatures. For example at a pressure of 10 atm 80% methane conversion occurs at a temperature above 900°C. When the temperature exceeds 30 atm this conversion level is required 1000°C. By adding steam the temperature can be reduced to 950°C and increase $CH_4$ conversion.

To reduce the cost of the synthesis gas and reducing the risk of explosion in recent years technology has developed based on the use of high-oxygen-conductive ceramic membrane [5,6]. This allows you to combine the generation of synthesis gas as well as air separation and exclude the technological scheme of expensive equipment to produce oxygen. However, the use of membrane reactors for POM has a number of obstacles to their commercialization. They must be resistant to poisoning, corrosion, deformation and to withstand high differential pressures. But the main drawback of this systems that in this case conversion of methane and selectivity to synthesis gas limited by the diffusion of oxygen inside the membrane, thereby affecting the very poor productivity of such materials.

## 1.2 Mechanism and catalysts of partial oxidation of methane

### 1.2.1 Mechanism of partial oxidation of methane

Nowadays the mechanism of POM is still controversial. In the literature two basic mechanisms of the partial oxidation of methane have been discussing [5-10]. The first involves the direct oxidation of methane molecules by oxygen and formation of hydrogen and carbon monoxide. The indirect or combustion-reforming mechanism involves the initial total oxidation of methane to carbon dioxide and water which are then react with an excess of methane to form the desired products. The combustion-reforming mechanism was suggested based on a consideration of the temperature profiles in the flow reactor [28-30], where there was a strong heating of front part of catalyst bed due to the high exothermicity of the reaction of total oxidation and subsequent cooling of the end of catalyst bed caused by the endothermic reaction of steam and dry reforming of methane. At high flow rates and larger ratios of $O_2/CH_4$ selectivity to $CO_2$ and $H_2O$ increases, that is, under these conditions the conversion is preceded by a fast reaction of total oxidation. Nowadays, there are experimental data which show in favor of indirect and direct formation of CO and $H_2$ and one can speak about a number of factors that affect the mechanism of the POM. It is the nature and state of the catalyst (dispersion of metal, oxidation state, nature of the interaction the

metal with carbon, oxygen, hydrogen and carrier), and process conditions (the ratio of $CH_4/O_2$, actual temperature profile of the catalyst bed and others.). The variety of these factors and the ability to change the state of the catalyst under the influence of the reaction medium is often impedes clear distinction between the mechanisms of the POM. It is very likely that the POM is a collection of many of the reactions that take place simultaneously in a heterogeneous system ($CH_4$ + $O_2$)-catalyst-(CO + $H_2$ + $H_2O$ + $CO_2$ + C).

Oxidation of methane through a direct mechanism involves the steps of adsorption and dissociation of $CH_4$ and $O_2$ molecules on the surface of the catalyst and further reacting the components of the surface followed by desorption of products. Based on measurements of the temperature profile and the oxidation of methane in a pulsed mode, in [31] it was proposed a one-step mechanism of oxidation of methane on $Ni^0$ formed during the reaction from $Ca_{9.5}Ni_{2.5}(PO_4)_6$ (Fig. 1).

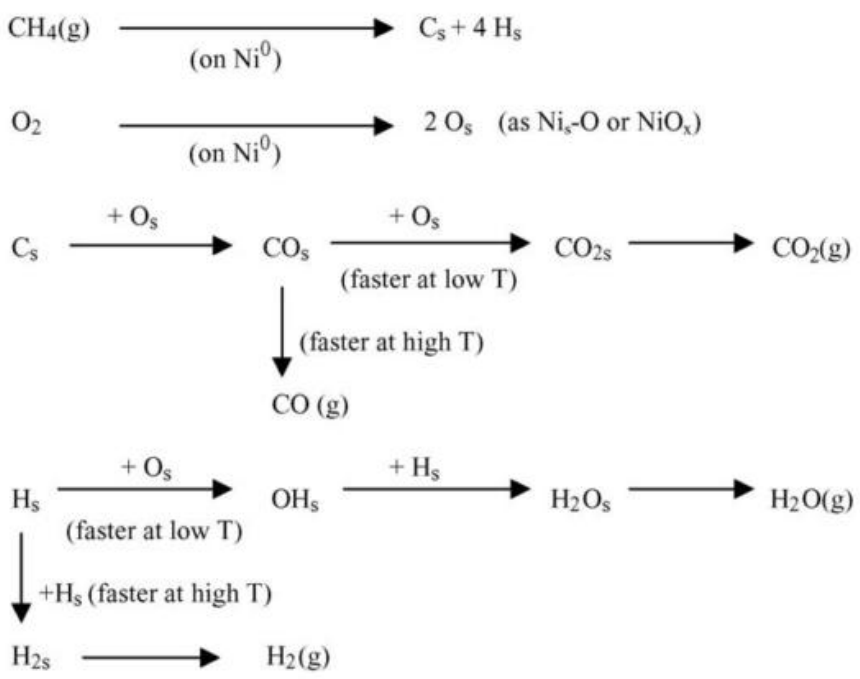


Figure 1 – Possible pathways of methane oxidation on $Ni^0$ [31].

Initially, methane dissociates on metallic nickel on the catalyst surface forming carbon and hydrogen. The resulting carbon is oxidized to CO by lattice oxygen of the catalyst followed two possible pathways - desorption of carbon monoxide in the gas phase or its further oxidation to $CO_2$. At lower temperatures most probably further oxidation of CO to $CO_2$ molecules whereas higher temperature promotes desorption of CO in the gas phase. A similar pattern can be taken into account in the analysis and desorption of hydrogen oxidation. It is noted that the reduced catalyst in a stream of $H_2$ was less active than the catalyst reduced in a mixture of $CH_4/O_2$.

Extended scheme of POM mechanism was given in [32]. The scheme involves 19 reactions for which the values of the pre-exponential factor and the activation energy were calculated. The reaction is initiated from an irreversible dissociation of methane, after that all four hydrogen atoms is immediately cleaved. The way in which a hydrogen atom is cleaved by surface oxygen

$$CH_x + O_{пов} \rightarrow CH_{1-x} + OH_{пов}$$

considered as less possible because this route leads to formation of $CO_2$ and $H_2O$ but at elevated temperatures $H_2$ и CO were predominantly formed. The main reactions of scheme are pyrolysis of methane, desorption of hydrogen and carbon oxidation. Calculations of selectivity and conversion based on the found constants did not much deviate from the experimental data. A model in accordance with the experiment predicted a higher selectivity for the Rh than Pt catalyst due to different rates of reactions:

$$H_s + O_s \rightarrow OH_s$$

$$OH_s \rightarrow H_s + O_s$$

$$OH_s + H_s \rightarrow H_2O$$

On the Pt potential barrier the formation of OH (2.5 kJ/mol) lower than that on rhodium (40 kJ / mol). The authors [32] observed that the surface OH is less stable on the Rh, than on Pt, which slows down the reaction of $H_2O$ formation and makes more preferable the desorption of $H_2$

$$2H_s \rightarrow H_2$$

As shown by theoretical calculation, the adsorbed oxygen favors to a greater extent to the dissociation of methane on Pt, Cu, Ag and Au, and to a lesser extent - on Ru, Rh, Os, Ir and Pd. The differences in the selectivity to $H_2$ are associated with different stability of surface OH groups on metals. A higher selectivity to $CO_2$ approaches on the surface enriched by oxygen. $CO_2$ is easily formed on the Ir, Pt or Pd, Rh than or Ru [33]. This is also confirmed in [34] where it was shown that the adsorbed oxygen on the metal surface has a positive effect on the activation of the methane molecule.

One of the recent methods for studying the mechanism of methane oxidation is using of the TAP (temporal analysis of products) reactor. It is a reactor with time-resolved analysis of the products. In a fixed-bed microreactor very short pulses of reactants feeds (a typical pulse duration is 0.00015 second) containing from $10^{13}$ to $10^{19}$ molecules. The response to a pulse is measured by a sensitive mass spectrometer.

Using such a reactor allows for example to fix the various forms of oxygen involved in the oxidation process. Thus, on the surface of $Pt/SiO_2$ type 2 types of active oxygen have been discovered [8]. At 600-1000ºC on Pt/MgO in the TAP reactor pulses of $CH_4$ and $O_2$ alternately injected with a significant time interval. As the reaction products mainly of CO and $H_2$ were formed with a selectivity of 94 and 95%, respectively. By feeding pulses of $CH_4 + O_2$ main reaction products were $CO_2$ and $H_2O$. Based on these data it was concluded that on Pt both stable subsurface oxygen and labile surface oxygen were formed. The last was engaged in total oxidation of methane. It was also found that methane dissociates on partially reduced platinum. Adsorption of $CO_2$ involves the formation of the weakly bound intermediate which is then converted to carbonate and bicarbonate. Under the reaction conditions CO is in two states - mobile and weakly bound chemisorbed. CO oxidation takes place on the islands of surface bound oxygen. Under the reaction conditions the surface oxygen can be converted into the subsurface and vice versa. The activity of Pt supported on $Ce\text{-}ZrO_2$ associated with the ability to supply and to store oxygen. $CeO_x$ facilitates to remove carbon from the catalyst.

The participation of lattice oxygen in the oxidative conversion of methane is proved by the example of $ZrO_2$ and $ZrO_2$ doped by $Y_2O_3$ (YSZ) [35]. On both catalysts the reaction proceeds according to the Mars - van Crevelen mechanism which involves alternating oxidation and reduction of the catalyst surface. Pulsed reaction with using $^{18}O^{18}O$ isotope clearly demonstrated the participation of lattice oxygen in the catalytic oxidation. In the case of YSZ as the products $C^{16}O$, $C^{16}O_2$, $H_2{}^{16}O$ and $H_2$ were exclusively recorded. In the case of undoped $ZrO_2$ products with gas-phase oxygen $^{18}O$ were also fixed.

In [36] the catalytic activity of $Mn_3O_4$ and $Er_2O_3$ in POM have compared. A oxygen enriched mixture of 0.8% (v) $CH_4$, 21% $O_2$ and 78.2% Ar was fed into the reactor. It was shown that over manganese oxide the only total oxidation of methane took place whereas over $Er_2O_3$ the yield of $H_2$ was 10%. Moreover, $Er_2O_3$ was completely inactive in carbon dioxide reforming. Therefore, hydrogen on this catalyst was formed by a direct mechanism of POM due to the participation of lattice oxygen. Based on the results of studies POM in pulsed reactor with oxygen $^{18}O^{18}O$ in [37,38] it was observed that the lattice oxygen plays a key role in the process of methane oxidation over 1% $Rh/(Ce_{0.56}Zr_{0.44})O_{2-x}$ and $1\%Rh/(Ce_{0.91}Gd_{0.09})O_{2-x}$. The authors discuss the possibility of the reaction proceeding at the same time by direct and indirect mechanisms.

The question of whether the dissociation of methane on the surface of the catalyst is limiting step of POM or not is debatable. According to IR spectroscopy and isotopic exchange ($^{16}O_2$-$^{18}O_2$) for the $Ru/TiO_2$ modified by $Ca^{2+}$ the limiting step is the interaction of $CH_4$ with the Ru surface with the consequent formation of $CH_x$ [8]. Neighboring Ru-centers and atomic oxygen are involved in the subsequent hydrogen abstraction from $CH_x$. It is assumed that initially the CO molecule is formed by reacting of carbon with oxygen on Ru-centers and $CO_2$ - by the oxidation of CO on oxidized centers. The IR spectra were also detected bands of the OH groups (3600 $cm^{-1}$) and a broad band at 1995 $cm^{-1}$ ascribed to the carbonyl hydrides - H-Ru-CO or $H_2$-Ru-CO. At the same time, in a study on the POM over $Ni/SiO_2$ by isotope exchange method, it was shown that the rate-limiting step of the reaction was not the dissociation of methane but

the oxidation of carbon on the catalyst surface. While 28% of the methane ($CH_4$, $CD_4$) was converted to CO and $CO_2$, 65% of methane was involved in the isotope exchange reaction (3% $CH_4$, 31% $CH_3D$, 38% $CH_2D_2$, 20% $CHD_3$ and 8% $CD_4$) which meant that the dissociation of methane is faster than its oxidation. On unreduced $NiO/SiO_2$ it was found only $CH_4$ and $CD_4$ molecules without any trace $CD_xH_y$. Thus, the nickel oxide does not occur isotope exchange and methane is oxidized directly without prior dissociation [39].

Many studies have indicated that the mechanism of oxidation of methane depends on oxidation sate of the metal in the catalyst. In [40] indicates that the CO is directly formed on the 1% $Rh/SiO_2$ whereas on rhodium oxide total oxidation proceeds. At the same time in the reaction conditions on 1% $Ru/SiO_2$ of methane oxidizes to $CO_2$ on both reduced catalyst and its oxide. Authors [41] have investigated the mechanism of the catalytic POM on $Ru/\gamma Al_2O_3$ using in situ XAS and in situ TGA-MS (Fig. 2).

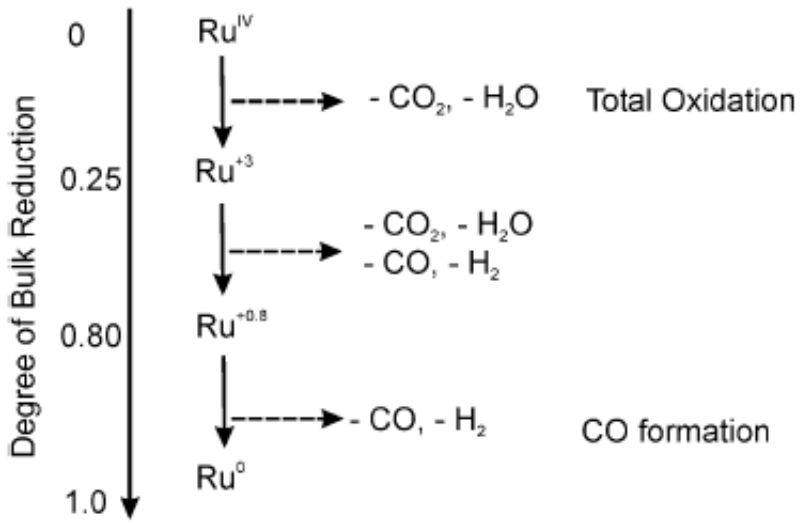


Figure 2 – Interaction of methane with $RuO_2$ [41].

It was shown that total oxidation occurs over the fully oxidized catalyst covered with $RuO_2$. At a bulk reduction degree of 25%, the evolution of carbon monoxide started. At a bulk reduction degree of 90%, CO was formed exclusively.The paper also postulated two routes reactions: direct oxidation of methane to CO in the reduced catalyst and a combustion-reforming mechanism on the oxide. The use of TAP-reactor and IR spectroscopy also revealed [42,43] that the reaction of POM on 1% $Rh/Al_2O_3$

and Rh-black strongly depends on the oxidation state of rhodium. On metallic Rh the dissociative adsorption of methane takes place followed by formation of surface carbon and hydrogen. $C_s$ reacts quickly with $CO_2$ by inreverse Boudoir's reaction providing CO selectivity of 96%. In the absence of carbon dissociation of $CO_2$ is not observed. On the oxidized parts of the catalyst the total oxidation of methane to $CO_2$ and $H_2O$ is predominant. In the steady state the following reactions occur:

$CH_4 + (Rh) \rightarrow CH_x(Rh) + (4\text{-}x/2)H_2$ (methane actication)

$CH_x(Rh) \rightarrow C(Rh) + x/2H_2$

$O_2 + Rh \rightarrow 2O(Rh)$

$C(Rh) + O(Rh) \rightarrow (Rh) + CO$

$CH_x(Rh) + O(Rh) \rightarrow CO_2 + x/2(H_2O/OH) + (Rh)$ (total oxidation)

$CH_x(Rh) + CO_2 \leftrightarrow 2CO + x/2H_2 + (Rh)$ (inreverse Boudoir's reaction)

$CH_x(Rh) + H_2O/OH \leftrightarrow CO + (x/2 +1)H_2 + (Rh)$

$(Rh) + O_2 \rightarrow 2O(Rh)$ (re-oxidation)

A detailed study of the mechanism of the POM in situ by IR and Raman spectroscopy allowed to observe the CO, $CO_2$ and other oxygen compounds directly during the reaction. On Rh /$SiO_2$ various forms of adsorbed CO were observed whereas on Ru/$SiO_2$ - adsorbed large amounts of $CO_2$ and $O_2$. It was concluded that on the rhodium catalyst POM proceeds through a  the direct pathway while on ruthenium through indirect one [8]. At the same time, the measurement of the temperature profile showed that during pulses puffing of $2CN_4 + O_2$ on Rh/$TiO_2$ and Rh/$Al_2O_3$ exothermic effect was observed in the front part of the catalyst bed which means reaction apparently passed through indirect mechanism. On Ir/$TiO_2$ exothermic effect was observed at the end of the catalyst bed.

The authors in [44] analyzed the IR spectra obtained in situ during POM  on Ru/$\alpha Al_2O_3$ and Ru/$\gamma Al_2O_3$ and found superficial compound with absorption bands of 2000 $cm^{-1}$. Its concentration is correlated with the rate of formation of CO. It has been suggested that oxidation of $CH_4$ proceeds via the formation of hydride surface species H-Ru-CO. The active sites are partially reduced clusters of $Ru^+$. Between Ru and OH groups the hydrogen spillover takes place.

In [45] used a pulsed method for studying the mechanism of POM on nickel supported on alumina. It has been found that the selectivity to synthesis gas increased with the number of pulses of $CH_4$ and proportional decreasing of oxygen on the catalyst surface. The mechanism of POM on $Ni/Al_2O_3$ and $NiO/Al_2O_3$ was also studied in a pulsed reactor [46]. After the first pulse of $CH_4$ very low conversion was observed on NiO and as reaction products were recorded exclusively of $CO_2$ and $H_2O$ which suggested that the methane can not dissociate on nickel oxide to form $H_2$ and C. At the same time on the surface of the partially reduced $Ni^0/NiO$ catalyst methane decomposes into C and $H_2$. After the second pulse, there was a significant increase in conversion of methane and as the reaction products were mainly recorded CO and $H_2$. Thus, on NiO methane activation took place in two stages – at first methane reacts with nickel oxide and oxidized to $CO_2$ and $H_2O$ with simultaneous reduction of the NiO to metallic state followed by dissociation of methane on the metallic surface to form Ni···C:

$$NiO + CH_4 \rightarrow CO_2 + H_2O + Ni^0$$

$$CH_4 + Ni^0 \rightarrow Ni\cdots C + H_s$$

$$H_s + H_s \rightarrow H_2$$

Formed Ni···C species can interact with two sort of oxygen species - $Ni^{\delta+}\cdots O^{\delta-}$ which can form due to oxygen activation on $Ni^0$ and $Ni^{2+} – O^{2-}$ generated on $Ni^0/NiO$:

$$Ni \cdots C + Ni^{\delta+} \cdots O^{\delta-} \rightarrow 2Ni^0 + CO$$

$$Ni \cdots C + 2Ni^{2+} – O^{2-} \rightarrow 3Ni^0 + CO_2$$

Thus, the authors note that the energy of the Ni-O plays an important role in the oxidation of methane. $Ni^{2+}–O^{2-}$ groups have a strong oxidizing potential and oxidize methane to carbon dioxide and water while $Ni^{\delta+}\cdots O^{\delta-}$ species having weaker oxidizing properties allow to oxidize methane to CO and $H_2$.

Based on the results of experiments in pulsed reactor, temperature-programmed surface reaction (TPPR) as well as measurements of the temperature profile of the catalyst bed following model of POM on the $NiO/Al_2O_3$ has been put forward [46]:

$$CH_4 + O_2 \rightarrow CO_2 + H_2O \text{ (on NiO)}$$

$$CH_4 + NiO \rightarrow CO_2 + H_2O + Ni^0$$

$CH_4 + Ni^0 \rightarrow Ni\cdots C + 4H_{пов}$

$H_{пов} + H_{пов} \rightarrow H_2$

$O_2 + Ni^0 \rightarrow Ni^{\delta+}\cdots O^{\delta-}$

$Ni\cdots C + Ni^{\delta+}\cdots O^{\delta-} \rightarrow 2Ni^0 + CO$

$2H_{пов} + Ni^{\delta+}\cdots O^{\delta-} \rightarrow H_2O$

$CO + Ni^{\delta+}\cdots O^{\delta-} \rightarrow CO_2$

Similar conclusions are also reached by the authors [47] studying the $Ni/Al_2O_3$ and $Pd/Al_2O_3$ by thermo-programmed surface reaction (TPPR) (Fig. 3). The flow quartz reactor supplied stoichiometric mixture of $CH_4/O_2$, diluted by inert nitrogen and the reaction products were recorded using a mass spectrometer.

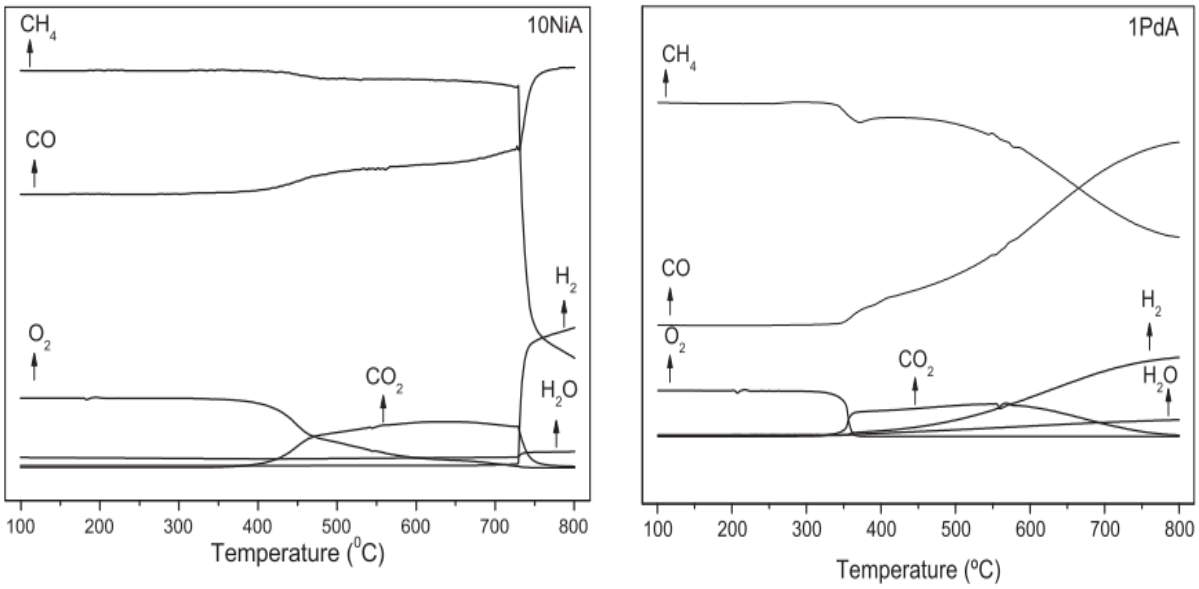


Figure 3 - TPS reaction of POM over $Ni/Al_2O_3$ (left plot) and $Pd/Al_2O_3$ (right plot) [47].

It was found that on nickel a indirect combustion-reforming pathway of methane oxidation is realized through Ni-C species formation followed by their interaction with $Ni^{\delta+}\cdots O^{\delta-}$ species. On Pd reaction occurs simultaneously in a direct and indirect routes and formation of $H_2$, CO, $CO_2$ and $H_2O$. In [49] the following model of the catalytic POM over $Ni/La_2O3$ formed from $LaNiO_3$ precursor has proposed (Fig. 4):

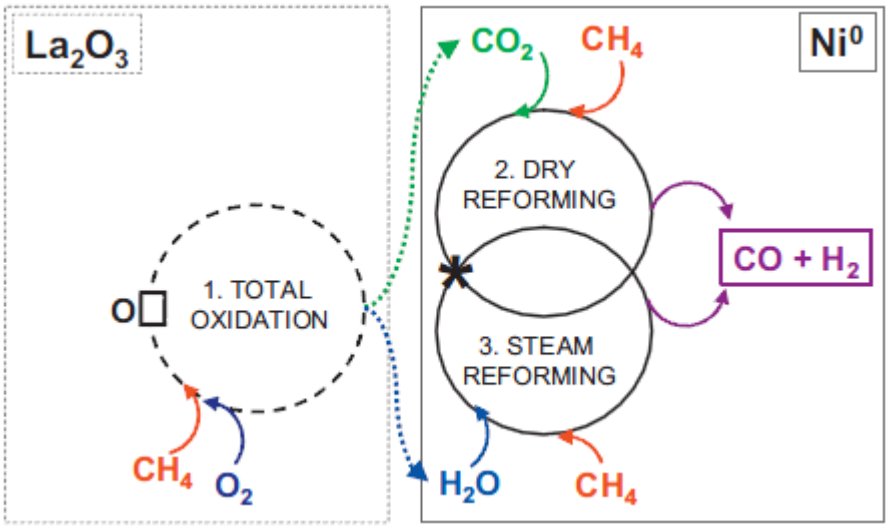


Figure 4 – Scheme of catalytic POM over $Ni/La_2O_3$ [49].

In this model, as the active sites are the anionic vacancies of $La_2O_3$ on which total oxidation of methane to $CO_2$ and $H_2O$ is realized. Simultaneously, $CH_4$ dissociates on metal sites of $Ni^0$ forming the active carbon that reacts with the products of total oxidation with formation of CO and $H_2$.

Thus, the partial oxidation of methane to synthesis gas goes through a direct pathway is usually promoted by high temperature, high space velocity and reduction of the catalyst to the metallic state. On the oxidized surface of supported catalysts, at low space velocity methane oxidation occurs mainly though a combustion-reforming mechanism.

### 1.2.2 Catalytic materials of partial oxidation of methane

As catalysts of POM are mainly Group VIII metals and their oxides [27]. The most widely studied catalyst are based on nickel and the noble metals, especially Rh, Ru and Pt. Such catalysts may provide high selectivity and yield of the synthesis gas. The main problem of these materials is to stabilize the catalytic active metallic sites [10]. Deactivation of such centers is often associated with coking, sintering and formation of inactive compounds during the reaction.

#### 1.2.2.1 Nickel based catalysts

One of the most studied catalysts of POM are based on nickel. Thus, nickel supported on alumina can achieve yields of synthesis gas closed to 100%. However, the catalyst is easily deactivated caused by coking and formation of $NiAl_2O_4$ spinel [28], inactive in the reaction POM.

The main problem of the nickel catalytic systems is intense deposition of carbon. Nickel particles accumulated on the carbon can sliver the active metal from surface which leads to a significant reduction in catalyst activity [49]. There are a number of studies [27, 46-53] devoted to the creation of materials that would prevent the deposition of coke on the catalyst surface. Since the formation of carbon fibers is extremely sensitive to the particle size of Ni, one of the ways of prevent coking is a change of crystallite size of Ni. Also the stabilization of Ni particles is very important that would prevent their sintering. Modifying the properties of the catalyst can be carried out through the use of various methods of synthesis such as microemulsion, sol-gel or co-precipitation.

The impregnating of the support by active component is one of the most popular synthesis methods. At the same time, in [50] using the microemulsion method of Ni-catalyst supported on silica preparation it was found that such a material has a high activity and selectivity in the formation of synthesis gas and exhibits increased

resistance to coke formation in comparison with $Ni/SiO_2$ prepared by conventional impregnation.

In [51] studied the effect of the preparation method of $Ni/\alpha\text{-}Al2O_3$ on its catalytic properties. As initial components $Ni(NO_3)_2$ and Ni acetylacetonate were chosen. Catalysts showed similar activity and selectivity but both deactivated. Investigation of spent catalysts has shown that in the case of Ni prepared from its nitrate precursor carbon fibers were found while the particles of the catalyst synthesized using organic precursor were sintered during reaction.

$Ni/\alpha\text{-}Al_2O_3$ activated in the plasma has been studied in [52]. It was shown that the activation process prevented the formation of coke on the catalyst surface and thus prolongs its lifetime. Similar results were obtained for $Ni/\gamma\text{-}Al_2O_3$ and Ni-Fe alloy $/Al_2O_3$ which are also subjected to plasma treatment previously [53,54].

In [49, 55, 56] the coking and sintering processes are suppressed by using the sol-gel technique for the synthesis of nickel catalyst. Investigation of spent catalysts by EXAFS showed that a sample obtained by sol-gel synthesis contained Ni, with 9-coordinated atoms unlike 12-coordinated nickel in a sample obtained by impregnation. This shows that in the first case, the nickel particles were smaller.

Also modification of Ni particle size may be effected either by changing the nature of the support or by adding promoters to a catalyst system in a variety of metals or oxides.

The authors [57] revealed high activity of $Ni/TiO_2$ in POM reaction but according to the XRD material is rapidly deactivated due to the formation $NiTiO_3$ phase. At the same time this material showed high stability in the dry reforming of methane and its activity was constant for at least 100 hours of operation. In [58] it was found that the formation of $NiTiO_3$ during the reaction complicates its subsequent reduction. However, the formation of inactive nickel titanate phase can be prevented by introduction into the system of Ce which also can increase oxygen conductivity of the catalyst and significantly reduce the formation of coke. $Ni/TiO_2$ is also studied in [59] in a temperature range of 300-750ºC. Twenty-hour test of the stability of the catalyst showed that the material rapidly lose its activity due to coke formation.

Partial oxidation of methane in the presence of nickel supported on strontium phosphate have been studied in [60]. Study of catalyst by XRD revealed that the synthesized catalyst contained in the structure phases of strontium phosphate, strontium hydroxyapatite and Ni-substituted strontium phosphate. The last phase during the reaction decomposed and on the surface of material finely Ni was formed which led to excellent performance of POM with selectivity to synthesis gas of 100%.

The authors [61] by using Fe/Cr/Al/Si/Y alloy as a support for a mixture of NiO-MgO obtained yields of synthesis gas closed to 100%. Based on scanning electron microscopy and energy dispersive analysis data it was proved interaction of active NiO-MgO component with Cr on the surface of the support.

Catalytic materials based on Ni/SiC with different nickel loading were studied in POM in a temperature range of 500-850ºC. It has been found that the best catalyst was 10% Ni. The catalyst showed high activity but deactivated caused by coking. The regeneration of the catalyst carried out in air showed that the material is completely restored to its original activity [62].

POM in the presence of calcium aluminosilicate coated with a Ni, Cr, Co, Fe or Cu has been studied in [63]. A Ni containing catalyst provides high yields of synthesis gas while the other materials were mainly catalyzed total oxidation reaction with only minor yields of CO and $H_2$.

The positive effect of promotion 18.7% $Ni/Al_2O_3$ by noble metals has been observed in [64]. Addition of 0.1% of the noble metal lowers the temperature of the POM reaction from 790 ºC to 605 ºC in the case of Pt and to 520ºC if Pd. With further increasing of load to 0.5% the initial reaction temperature decreased to 530ºC in the case of Pt and to 460ºC when Pd used as a promoter. Reduction of the reaction temperature in the promotion of the Ni-Pt catalyst has also been documented in [65]. Adding chromium to the $Ni/Al_2O_3$ increased its stability due to formation Ni-Cr alloy [66].

Influence of additives like Ce, La and Ca on the behavior of $Ni/\gamma\text{-}Al_2O_3$ and $Ni/\alpha\text{-}Al_2O_3$ in POM was studied in [67]. Adding all three promoters to $Ni/\alpha\text{-}Al_2O_3$ increases both $CH_4$ conversion and selectivity of the synthesis gas while on the N $/\gamma\text{-}Al_2O_3$ high

levels achieved without the addition of promoters. Improving the catalytic properties of Ni/α-$Al_2O_3$ with the introduction of Na, Sr, La and especially Ce was explained by the increase of nickel reducibility.

In [68] the activity of Ni and NiB supported on a calcium modified γ-$Al_2O_3$ has been investigated. NiB was subjected to coking in a smaller extent than Ni which was explained by the increase of dispersion of nickel particles in: 35-75 nm for 10% Ni/ $Al_2O_3$, 15-25 nm for 10% Ni/CaO/$Al_2O_3$ and 12 nm at 10% NiB/CaO/$Al_2O_3$. On 1% NiB/CaO/$Al_2O_3$ carbon was not detected. This material showed 85% conversion of methane and high stability at 15 atm and 800°C.

Introduction of Co to Ni/$Yb_2O_3$, Ni/$Zr_2O_3$ and Ni/$Th_2O_3$ allows to reduce the rate of carbon deposition on catalysts as well as the reaction temperature of POM [69].

Rare earth oxides have been widely studied as promoters of nickel catalysts. For example, the addition of $La_2O_3$ to NiO/$Al_2O_3$ leads to decreasing of the reaction temperature and preventing inactive $NiAl_2O_4$ spinel phase formation [70]. Furthermore, the amount of carbon formed on the surface of 2% $La_2O_3$/NiO /$Al_2O_3$ was less than on lanthanum undoped NiO/$Al_2O_3$. However, increasing the amount of La in the catalyst resulted in the increase of coke formation rate on the catalyst surface. At the same time, the introduction into the system of CaO completely inhibited the process of coking.

Influence of Li as a promoter on the POM was studied on Ni/$La_2O_3$ and Ni/ $La_2O_3$ /$Al_2O_3$ [71-73]. Adding of Li favored to the proceeding of an oxidative coupling of methane, increasing the selectivity of $C_{2+}$-products, especially on the Ni/$La_2O_3$. Increasing the concentration of Li resulted in a significant decrease in the selectivity of CO and $H_2$ and increase the ratio of ethylene/ethane. Ni/Li/$La_2O_3$/$Al_2O_3$ catalyst showed higher activity and selectivity to the desired product with values close to 100%. Substitution by K, Li or Na [74] led to a slight increase in the selectivity of $CO_2$ whereas replacing nickel by Co or Fe resulted in a sharp decrease of conversion of $CH_4$, 35-40% and the selectivity of CO to 30-35%. The time of stream test on Ni /Li/$La_2O_3$ /$Al_2O_3$ catalyst showed that the sample did not lose activity over 200 hours of work in the POM environment at 850°C [75].

The element that can decrease process of coking is Ir. For example, on 0.25%Ir/ 0.5% Ni/$La_2O_3$ already at 600°C $CH_4$ conversion reached 25% with a selectivity to CO and $H_2$ of 80% [76]. However, further raising the temperature to 800°C resulted in an increase of conversion only up to 32% and the selectivity of CO formation to 90%. Use $Y_2O_3$, $Al_2O_3$, $Zr_2O_3$, MgO and $SiO_2$ as supports is required higher temperatures for activation of the methane molecule. Adding SrO to Ni/$La_2O_3$ increased the rate of the oxidative coupling of methane and only a very high loading of Ni prevents the formation of $C_{2+}$-products [77].

Ni/$CeO_2$ strongly deactivated due to the formation of carbon on its surface but the introduction of La could prevent catalyst deactivation. 4% La/5%Ni/$CeO_2$ remained active at least for the 100 hours of operation at 650°C [78]. As shown in [79], the presence of Ce in $Ce_{1-x}Ni_xO_y$ (x = 0.05-0.6) caused an increase in their efficiency and stability. The greatest effect of adding cerium oxide was achieved at x = 0.4, where selectivity to CO and $H_2$ were 80% and 90%, respectively.

### 1.2.2.2 Cobalt based catalysts

Cobalt catalysts are also widely studied in the partial oxidation of methane to synthesis gas. Co/Al2O3 allows to achieve high values of methane conversion and selectivity to the desired product but it deactivates very fast. Deactivation of the catalyst in this case is largely associated with the process of oxidation of Co that has been found in the study of a fresh-prepared and spent catalysts by $H_2$-TPR. The authors in [80], studying the Co/γ-$Al_2O_3$, found that the active metallic Co was in cubic form and deactivated during the formation of the inactive $CoAl_2O_3$ phase.

Preventing the formation of $CoAl_2O_3$ spinel can be achieved through the use of supports different from aluminum oxide. One such system is the magnesium oxide which can form solid solutions due to interaction with CoO. Pre-reduced solid solution of CoO-MgO (Co/Mg = 1-10) showed high efficiency in the partial oxidation of methane, while pure MgO and CoO were completely inactive and favored total oxidation to $CO_2$ and $H_2O$ [81]. High levels of activity and stability of the POM has also been achieved on the solid solution of CoO-MgO/$Al_2O_3$ prepared by co-precipitation

[82]. However, for solid solutions of CoO-MgO promoted the formation of hot spots - the actual temperature in the catalyst bed can reach very high values, up to 1300 °C [83].

In [84] studied the partial oxidation and dry reforming of methane on Co/MgO, Co/CaO and Co/$SiO_2$. On Co/CaO and Co/$SiO_2$ synthesis gas formation did not occur while the Co/MgO remained stable over 110 hours of operation with selectivity to CO and $H_2$ at a level of 94-95%. According to the XRD, during calcination at 800°C CoO-MgO solid solution was formed.

Activity of Co/MgO in POM reaction was confirmed in [85]. XRD analysis revealed the presence of $Co_3O_4$ together with the solid solution CoO-MgO phases after reaction. It has also been shown that Co/BaO and Co/SrO deactivated after the first hours of operation. Deactivation was associated with oxidation of cobalt metal during catalysis. Study of Co/CaO showed that the catalyst is able to provide the oxidation of methane with selectivity to CO of 50-55% but the conversion of methane does not exceed 40% and the selectivity to $H_2$ fell down from 80 to 60% for 25 hours.

In [86] the catalytic activity of Co/$ThO_2$ and CoO/$UO_2$ was compared with activity of NiO supported on $ZrO_2$, $ThO_2$, $UO_2$, $TiO_2$, and CoO-NiO supported on oxides of zirconium, thorium and uranium. In comparison with nickel, cobalt catalysts were generally less active and selective for the formation of synthesis gas. In [87] it is shown that Co/$Al_2O_3$ and Co/$SiO_2$ contributed substantially to total oxidation of methane unlike nickel catalysts on the same support. Similar results were obtained in Co deposited on the oxidized diamond [88]. Thus, on Co catalyst carbon formation was not detected while on Ni deposited on this support 3% carbon was found.

Since the loss of activity of cobalt catalysts is most likely due to its ability to oxidize. One of the main requirements for promoters of cobalt catalysts is to inhibit the ability of Co oxidation. Bimetallic of Pt-Co supported on $Al_2O_3$ have been studied in [89]. It is shown that the conversion of methane and selectivity to synthesis gas was higher compared to the unpromoted Pt systems. Introduction of Pt also reduces coke deposition - after 80 hours of time on stream on the surface of the catalyst only a monolayer of carbon monoxide was found. $H_2$-TPR and XPS analysis revealed that the

presence of platinum in the system may also improve the resistance of Co to oxidation. Similar results were obtained on $Co/Al_2O_3$ promoted by Pt [90, 91]. The introduction of platinum over 0.2% does not significantly increase the yield of synthesis gas.

Studying of $Co/Al_2O_3$ promotion by various noble metals [92] it was found that the additives Pt-group metal can reduce the temperature of the POM reaction (outlet temperature of the catalyst bed was below 450 ° C) presumably due to the catalyst ability to enhance reducibility. Promotion of $Co/Al_2O_3$ by various oxides as $Fe_3O_4$/ $Cr_2O_3$, $La_2O_3$, $SnO_2$ and $K_2O$ does not lead to an improvement POM except lanthanum oxide which is able to stabilized Co particles. Promotion of catalyst by potassium oxide or iron leads to an increase of coke formation and the introduction of $SnO_2$ leads to the formation of inactive forms of $SnO_x$ on Co surface.

Cobalt catalysts modified by Ni, Fe, Cr, Re, V, Ta, Mo, W and Re oxides were studied in [93]. XPS and hydrogen chemisorptions analyses showed that the addition of W, Mo, V and Ta decreased the amount of metallic Co active sites on the catalyst surface which in turn decreased the activity and selectivity. The presence in the Fe led to the formation of carbon on the active surfaces of the catalyst during the POM. The values of $CH_4$ conversion and syngas selectivity closed to 100% have been achieved on $Co/\alpha\text{-}Al_2O_3$. $Co/\alpha\text{-}Al_2O_3$ modified by nickel showed the same results at higher space velocity. Introduction of Cr, Mn and Re does not affect the yield of the synthesis gas.

The authors [94] investigating the effect of calcium addition on the activity of $Co/Al_2O_3$ showed that unmodified calcium catalyst provided high yields of synthesis gas only with high content of Co - 12%. However, this material is very rapidly deactivated due to the formation of $CoAl_2O_3$ spinel. Introduction of Ca could prevent the formation of inactive spinel phase and a dispersion enhancing Co metal on the support. $CH_4$ conversion and selectivity for CO and $H_2$ closed to 90% were achieved at 6 Co/6%Ca/$Al_2O_3$. The catalyst remained stable over 120 hours of time on stream.

### 1.2.2.3 Precious metal based catalysts

Catalysts based on noble metals are the most active in the POM. Furthermore, unlike the Ni catalyst, such compounds are highly resistant to coking processes and may operate at short contact times. However their industrial application is complicated because of high cost.

The ability of Rh catalysts exhibit high activity and selectivity in the formation of CO and $H_2$ is strongly dependents on the type of support [8]. Rhodium supported on oxides with high reducibility such as $CeO_2$, $Nb_2O_5$, $Ta_2O_5$, $MnO_2$ or $UO_2$ are not achieved such high selectivity as using MgO, $La_2O_3$ or $Y_2O_3$. During deposition of on the supports intermediates are formed, ease of formation of which varies among $MgRh_2O_4$ > $LaRhO_3$ > $YRhO_3$>$RhTaO_4$. Rh/MgO and Rh/$La_2O_3$ kept constant activity over 100 hours of time on stream whereas the Rh/$Y_2O_3$ and the Rh/$Ta_2O_5$ rapidly deactivated.

The authors [95] as a support for Rh suggest using a ternary system where the first component is an alkaline earth metal oxides, the second - the oxides of elements of scandium, yttrium and the lanthanides; the third - zirconium oxide. The highest level of activity was achieved on the Rh/MgO-$ZrO_2$-$CeO_2$. Conversion on the catalyst was 80%, with a selectivity of $H_2$ and CO of 91.2% and 91.5%, respectively. When Rh and Pt deposited on the $Al_2O_3$ were examined it was was found that Rh provided higher selectivity to hydrogen (85%) than Pt (60%) at a ratio of methane/oxygen = 1.6.

It was shown [6] that 1%Pd/γ-$A1_2O_3$, $Y_2O_3$, $La_2O_3$, $TiO_2$, $ZrO_2$, $HfO_2$ approach selectivity to synthesis gas of 99% with $CH_4$ conversion of 35-66%. Over Pd/$SiO_2$ conversion of $CH_4$ was 35-66%. Maximal selectivity to syngas of 99,5% was achieved over Pd/γ-$Al_2O_3$. Pt-gauze in temperature range of 200-900°C and short contact time 0.21-0.442 мс did not reveal selectivity to synthesis gas. The only CO, $CO_2$ and $H_2O$ products were detected [27]. The increase of temperature and decrease of contact time led only to an increase of the concentration of $C_{2+}$-products. In a following up 10%Pt Rh gauze was studied in the temperature range 200-1100 ° C and a contact time of 0.5-1.5 ms. The presence of Rh improved the selectivity to synthesis gas with up to 30%

selectivity to hydrogen, as compared to the pure Pt gauze where in significant amounts of hydrogen was detected. It was indicated the difference in stability of the Pt–10% Rh gauze as compared to the pure Pt gauze after 8 h on stream. The Pt gauze was found to decompose either by volatilization or by redox-cycling leading to degradation and loss of catalytic material from phase transformation as $PtO_2$ was formed on the surface.

Using TAP reactor revealed that elimination of gas-phase oxygen produces synthesis gas on Pt selectivity to CO and $H_2$ of 97 and 96%, respectively [6]. It has been found that in this case the residence time of CO and $H_2$ on the Pt catalyst was less than the time required for oxygen diffusion from the bulk to the catalyst surface, which prevents further oxidation of CO and $H_2$ to $CO_2$ and $H_2O$, respectively. Thus, it was shown that this catalyst may be accompanied by a direct reaction mechanism, by passing the stage of formation of $CO_2$ and $H_2O$ due to the elimination of gas phase oxygen and oxygen on the catalyst surface.

Introduction of $CeO_2$ into $Pt/Al_2O_3$ resulted in an increase of dispersion of platinum on the alumina surface and simultaneously increase the selectivity of CO and $H_2$ [27]. High dispersion was observed already at 1-2% $CeO_2$, however, further increase in the concentration of cerium oxide did not lead to an increase of dispersion fo Pt or selectivity to synthesis gas.

### 1.2.2.4 Catalysts based in oxides with perovskite structure

Instead of metallic supported catalysts as alternative complex oxides with perovskite structure with general formula $ABO_3$ could be used. Usually in A-sites cations of rare-earth elements are located whereas in B-sites – cations of transition elements (Fig.5)

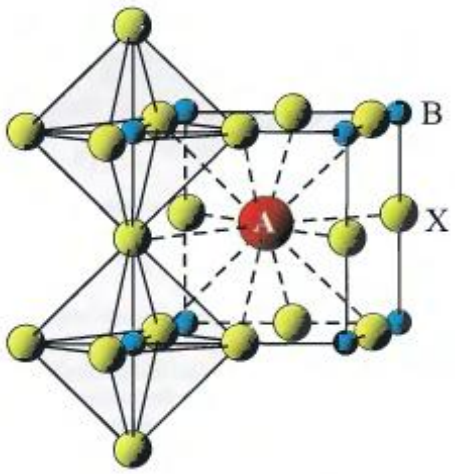


Figure 5 – Perovskite structure of complex oxides of general formula $ABO_3$ [96]

One of the main feature of such systems is the possibility of heterovalent substitution of cations in A and/or B position which allows to create defects for example vacancies in anion sublattice and as a result increase of its mobility. This feature of the complex oxides with a perovskite structure makes them attractive as oxygen conductive membranes and catalysts of redox processes. Several works have been devoted to the study of the energy of the B-O bound and its influence on the catalytic properties. It has been found that the catalytic properties of perovskite oxides largely depend on how much oxygen is easily released from the surface of these materials during the redox processes [97]. Another feature of the complex oxides with the perovskite structure is that these systems in a reducing atmosphere can be formed on the surface fine particles of transition metal elements [27]. Such particles can be very active for a numerous of processes, including the partial oxidation of methane to synthesis gas. In addition, several authors noted [26, 98-102] that metal sites formed in this way may be resistant to the sintering process and coke formation making perovskite oxides are promising catalysts for POM.

Among perovskite catalysts for POM lanthanum nickelates with different choice of substitution in the A and B positions have been widely studied [101-104]. In [102] the effect of substitution of Ni by Co in $LaNiO_3$ perovskites on the performance of POM have been studied. The best results were achieved on the unsubstituted $LaNiO_3$ that allows to achieve the selectivity of the synthesis gas closed to 100% at a $CH_4$

conversion of 60%. By increasing the degree of substitution of Ni by Co methane conversion and selectivity to the desired product decreased significantly while $LaCoO_3$ was absolutely inactive in the POM. This trend is in accordance with the $H_2$-TPR analysis, the results of which showed a decrease in the reducibility of synthesize materials with increasing content of Co. Moreover, according to XPS and $O_2$-TPD data, unsubstituted lanthanum nickelate was able to release more oxygen compared to Co-substituted counterpart that was explained by energy of Ni-O bond which was lower than that for Co.

In [103] an increase in the reduction temperature of $LaNi_{1-x}Co_xO_3$ perovskite oxides with increasing degree of substitution of Ni by Co associated with the formation Co-Ni alloy in the reduction. In contrast to [102], in this paper all catalysts passed activation step in a $H_2$ flow in order to form the metallic phase of $Ni^0/Co^0$ active in the POM. As in the previous case, the most active catalyst were materials formed from unsubstituted $LaNiO_3$ precursor. At the same time, the XRD results indicated that $Ni^0$ partially oxidized to NiO during catalysis whereas introduction of Co allowed to suppress the oxidation of active $Ni^0$. The authors of [104] compared the catalytic activity of Co and Pt-substituted lanthanum nickelates with 5%Ni/γ-$Al_2O_3$. The reactor was a Inconel alloy tube. The reaction was initiated by the partial oxidation of methane at 920°C and then proceeded autothermally. The results of catalytic experiments showed that the perovskite catalysts were significantly less active and selective compared to 5% Ni/γ-$Al_2O_3$, which reminded the values of $CH_4$ conversion and selectivity to CO and $H_2$ of 90%, even when the space velocity was high. Based on the XRD and TGA-MS results, the authors have suggested that the low catalytic activity of the Co-and Pt-substituted lanthanum nickelates could be related to the formation of inactive $LaOH_3$ phase during the reaction.

Catalytic systems based on $Ca_{0.8}Sr_{0.2}Ti_{1-y}Ni_yO_3$ were examined in [105]. It was observed that the catalysts with a degree of substitution of y=1 show good activity in total oxidation of methane at temperatures of 600°C but at higher temperatures up to 800°C a sharp increase in the concentration of the synthesis gas in the outlet gases was observed. $Ca_{0.8}Sr_{0.2}Ti_{0.8}Ni_{0.2}O_3$ catalyst with a degree of substitution of y = 2 was more

active in both the total oxidation of methane (at 600°C) and in the partial oxidation of methane to CO and $H_2$ (at 800°C). As in the case of Ni /γ-Al2O3 in [104] in [105] combustion-reforming mechanism of POM has postulated.

The authors of [106] exploring the $LaMO_3$ (M - Rh, Ni, Co) systems was also noted that during the POM perovskite structure is completely decomposed to $La_2O_3$ and the metal transition element phases. LaRhO3 was the most active and stable catalyst provided 95% methane conversion and selectivity to CO of 98% constant for at least 120 hours of time on stream. $LaNiO_3$ deactivated after 17 hours of operation probably due to the formation of coke and on $LaCoO_3$ mainly total oxidation of methane took place. But after 30 h in POM reaction LaCoO3 catalyst was reduced forming $Co^0$ dispersed on the surface of the $La_2O_3$ matrix after that the reaction shifted towards the formation of CO and $H_2$. However, in the next 50 hours of time on strream the catalyst gradually deactivated.

In [99] the method of temperature-programmed surface reaction (TPPR) combined with mass spectrometry revealed that $LaCoO_3$ under the reaction mixture of $CH_4/O_2$/ He = 2/1/37 highly diluted by an inert gas is able to oxidize methane to CO and $H_2$ at temperatures in excess of 900°C. According to the XRD the multiphase system of $La(OH)_3$, $La_2O_3$, $Co_3O_4$, $La_2CoO_4$ and partially preserved perovskite phase $LaCoO_3$ were formed during the reaction. Increasing the concentration of methane in the gas stream ($CH_4/O_2$/He = 5/1/64) can significantly increase the concentration of CO and $H_2$ in the outlet gases as well as reduce the reaction temperature. In this case XRD data indicated the total destruction of the original perovskite structure and the occurrence of $Co^0$ during the reaction. Despite the fact that increasing the concentration of reducing agent in the system allows to increase the yield of CO and $H_2$, it also leads to intensive coking of material which was confirmed by TGA, electron microscopy and Raman spectroscopy. However, the partial substitution of Co by Cu ions allowed to not only prevent coke formation and subsequent catalyst deactivation but also to reduce the temperature of the partial oxidation of methane.

In [107] the effect of the nature of the rare earth element cations on the catalytic properties of $LnCoO_3$ (where Ln - La, Pr, Nd, Sm and Gd) was investigated. According

to XRD activation $LnCoO_3$ precursor in $H_2$ flow led to the formation of metallic cobalt, distributed on the surface of the oxide matrix $Co^0/Ln_2O_3$. It should be noted that according to the hydrogen chemisorption and XPS data no differences in the dispersion of Co was observed. Nevertheless, results of catalytic experiments showed a significant difference to their activity in POM. It was found that increasing the yield of the synthesis gas is inversely proportional to the ionic radius of Ln (Fig. 6).

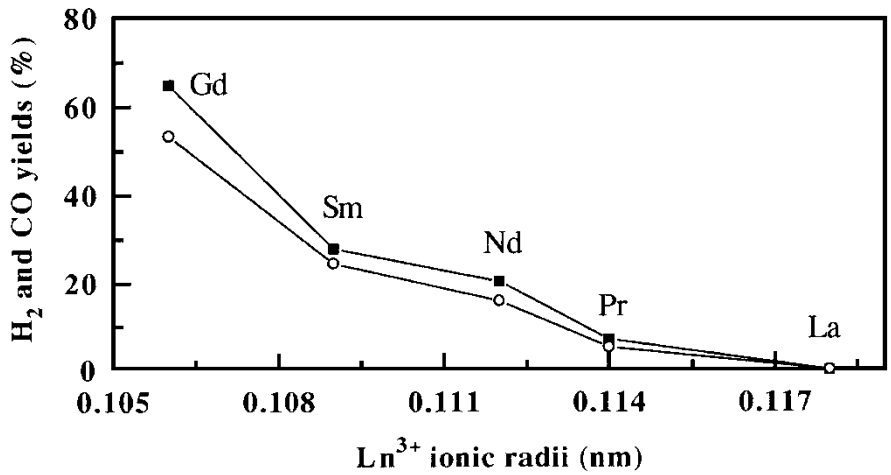


Figure 6 – Yield of CO and $H_2$ as a function of ionic radii of rare earth cations.

$GdCoO_3$ was the most active and selective - $CH_4$ conversion was 73% and the selectivity to CO and $H_2$ were 79 and 81%, respectively. XRD data after the experiment showed the presence of two phases in the sample - $Co^0$ and $Gd_2O_3$ indicating catalyst resistance to re-oxidation. $NdCoO_3$ was less active and selective, and during reaction a partial re-oxidation of Co took place. In case of LaCoO3 the catalyst was able to produce only trace amounts of CO and $H_2$ while XPS and XRD data revealed complete re-oxidation of Co into initial perovskite structure. According to $H_2$-TPR data it was also pointed the influence of the nature of the rare earth cation on the reducibility of cobalt. Tolerance factor t (criterion of Goldschmidt), calculated for $LnCoO_3$ decreases in the series - $LaCoO_3$> $PrCoO_3$> $NdCoO_3$> $SmCoO_3$> $GdCoO_3$. It means the most stable $LaCoO_3$ system formed in the presence of the largest rare earth cations (Fig. 6).

TPR-$H_2$ profiles also indicated that $LaCoO_3$ was the most difficult to reduce in the series. In contrast, $O_2$-TPO analysis showed that re-oxidation into perovskite structure is preferable for large cations.

Therefore, catalyst deactivation of the catalysts based on perovskite oxides often occurs not only due to sintering and coking processes but also because of the re-oxidation of the active phase of the transition element into the initial perovskite structure.

Despite the fact that a number of studies have noted low activityof $LaCoO_3$ in POM, a recent study showed that partial substitution of La by Sr can significantly increase the yield of synthesis gas [108]. In [109] $La_{0.9}M_{0.1}Ni_{0.5}Fe_{0.5}O_3$ has been investigated in a carbon dioxide reforming of methane and it was also indicated positive effect of Sr and Ca introduction which can prevent the deposition of coke and increase the activity of the catalyst in the oxidation of methane to synthesis gas. The next mechanism on the promoted catalysts has been suggested:

$SrO + CO_2 \rightarrow SrCO_3$

$La_2O_3 + SrCO_3 \rightarrow La_2O_2CO_3 + SrO$

$La_2O_3 + CO_2 \rightarrow La_2O_2CO_3$

$C + La_2O_2CO_3 \rightarrow La_2O_3 + 2CO$

$CaO + CO_2 \rightarrow CaCO_3$

$CaCO_3 + C \rightarrow CaO + 2CO$

In the study of complex oxide catalysts of POM the most attention is paid to systems with $ABO_3$-type perovskite structure. At the same time, the possibility of the use of two-dimensional counterparts of such systems, for instance, oxides with a layered perovskite structure (structure type $K_2NiF_4$) for POM has not been studied extensively. There are only few examples of the possibility of using such systems in the partial oxidation of methane to synthesis gas. For example, $(La_{0.5}Sr_{0.5})_2Ni_{1-x}Fe_xO_{6+\delta}$ as a precursor formed during the reaction a composite of nano-sized clusters of $Ni^0$ dispersed on the support with $K_2NiF_4$, nickel oxide and $SrCO_3$ [98]. Methane conversion and selectivity toward CO and $H_2$ in this catalyst were ~ 99%. However, it should be noted that these results were achieved in the experimental conditions under high dilution of the reaction mixture by inert gases ($CH_4$:$O_2$:$N_2$:He - 2:1:4:38).

***

The catalytic partial oxidation of methane and dry reforming of methane are promising processes for production of synthesis gas. One of the main problems in the implementation of these processes is to provide high selectivity and stability of the catalyst, the activity of which may be reduced due to the coke formation and transformations of the active components into inactive compounds. Currently, reduction of coke formation is mostly achieved by introducing into a conventional nickel catalysts are transition metals, including the platinum group. Also, promotion of catalysts may be due to the introduction of rare earth and alkaline earth elements. Another approach involves the development of catalytic systems based on complex oxides with a perovskite structure. Such systems may have a high lattice oxygen mobility and under reducing atmosphere formed fine particles of transition metals. Formed in this manner metal centers may have an increased resistance to agglomeration and deposition of coke.

Thus, the main point of current research is to improve the process of partial oxidation of methane and dry reforming of methane to synthesis gas by creating new selective and stable catalysts based on complex oxides with layered perovskite-like structure containing cobalt ions, rare earth elements and alkaline earth elements.

# Chapter 2. Experimental section.

## 2.1 Initial reactants

For catalytic tests conducting the followed chemicals were used:

- Methane, 51-841-87, volumetric fraction of methane in terms of dry matter 99.99%. (Joint stock company «Moscow gas processing plant»).
- Oxygen, ultra high purity, 6-21-10-83, volumetric fraction of methane in terms of dry matter 99.999%. (Joint stock company «Moscow gas processing plant»).
- Carbon dioxide, volumetric fraction of methane in terms of dry matter 99.9%. (Joint stock company «Moscow gas processing plant»).
- Lanthanum oxide $La_2O_3$, Produced by «Fluka».
- Neodymium oxide $Nd_2O_3$, Produced by «Fluka».
- Strontium carbonate $SrCO_3$, Produced by «Fluka».
- Calcium carbonate $CaCO_3$, Produced by «Fluka».
- Cobalt oxide $Co_3O_4$, Produced by «Fluka».

## 2.2. Methodic of catalytic tests performance

### 2.2.1 Study of partial oxidation of methane and dry reforming of methane to synthesis gas.

Partial oxidation of methane and dry reforming of methane was performed by using a single-pass plug flow setup (Fig. 7) including a flow-fixed bed reactor (8 mm internal diameter, 650 mm length). The reactor is equipped with an internal pocket for a thermocouple (∅ = 4 mm).

Catalytic tests were carried out at atmospheric pressure in the temperature range 800 – 950°C with space velocity (W) 10 – 75 $L \cdot g^{-1} \cdot h^{-1}$ feeding either $CH_4$:$O_2$ or $CH_4$:$CO_2$ in range 1.8:1 ÷ 4.6:1 without any dilution by inert gas. The catalyst was placed in a hot zone of the reactor at a distance of 500 mm from the inlet. The reactor was filled with quartz glass inserts to reduce the free volume upstream and downstream the catalyst. These quartz inserts were tightly held in the thermocouple pocket.

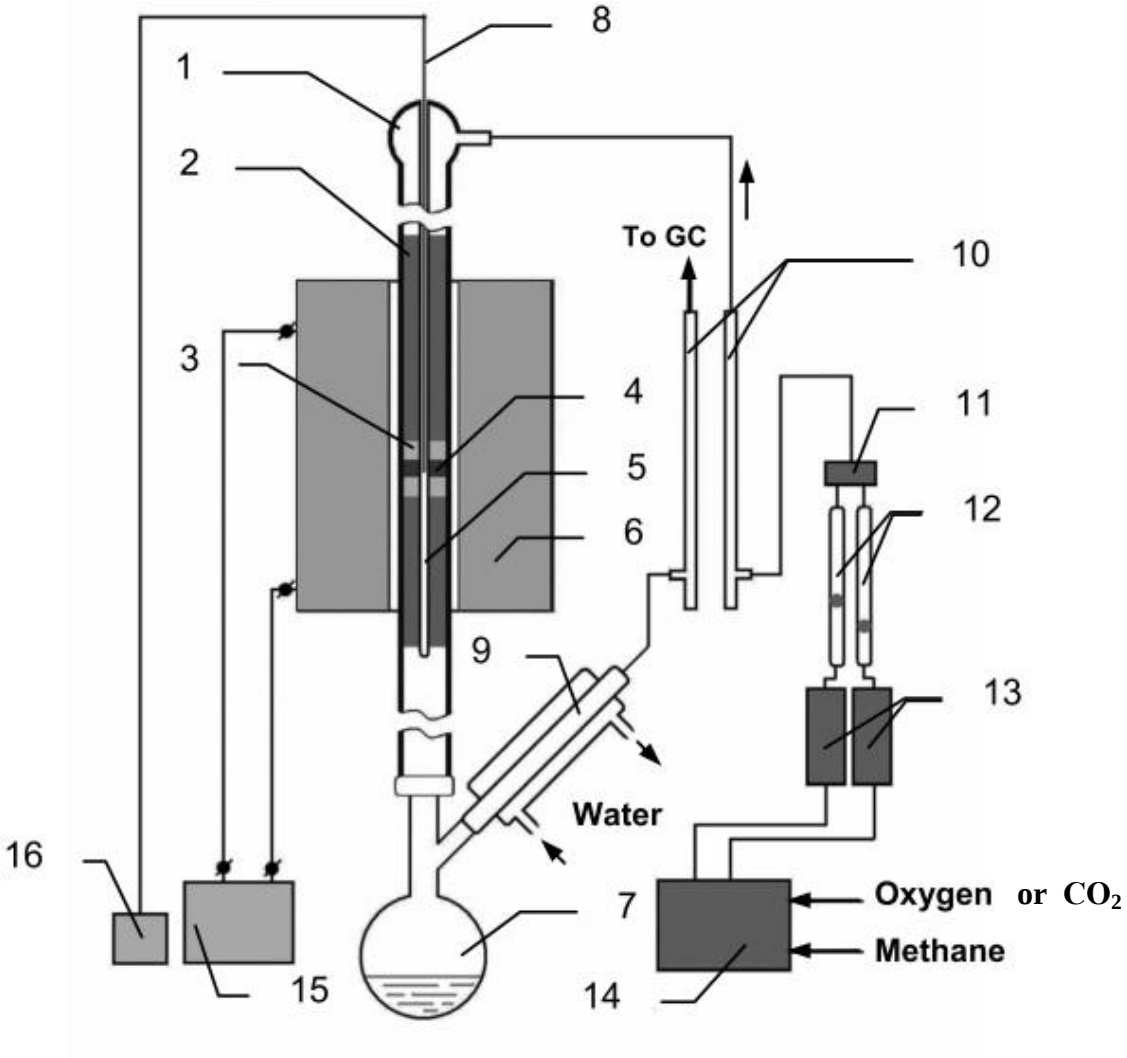


Fig. 7. Single-pass plug-flow setup. (1) Quartz reactor, (2) quartz-glass insert, (3) quartz wool, (4) catalyst, (5) internal pocket for thermocouple, (6) electric furnace, (7) condensate receiver (round-bottom flask), (8) thermocouple, (9) water cooler, (10) flow meters, (11) gas mixer, (12) ball-in-tube flow meters, (13) adsorbent, (14) gas flows from META-CHROM, (15) furnace controller, and (16) temperature indicator.

5 mm quartz wool layers (mixer-filter) were placed at the inlet of the reactor and upstream and downstream the layer of catalyst. The catalyst bed height was approximately 1–2 mm. All tests were carried out with 0.1 g of the catalyst. The catalysts were tested in the temperature range of 850–940 °C with the GHSV 10–75 $L \times g^{-1} \times h^{-1}$. The 140 h run of catalyst was carried out periodically. Catalyst was heated and cooled several times in a gas flow mixture. 140 h total runtime corresponds to the

time of POM after achieving a steady state reaction conditions, not including a heating and cooling time.

The employed method of catalytic test performance is required of using quartz wool in free reactor volume. The experiments of conversion of methane/air mixture in the reactor with only quartz wool loaded instead of catalyst were carried out in order to estimate properly the activity of synthesized materials. The tests revealed that in the employed conditions at 950°C quartz wool contribution to methane conversion is not visible (less than 1 %).

### 2.2.2 Analysis of products of partial oxidation of methane and dry reforming of methane

The initial gas mixture and outlet gas were analyzed using two gas chromatographs. Helium was used as a carrier gas in both chromatographs. The first chromatograph was equipped by TCD and two stainless columns, 3 m in length and 3 mm in diameter. The first column was filled with Porapak Q (50–80 mesh, Waters Assoc., USA) and was used to determine the content of air, methane, $CO_2$, ethane and ethylene. The second column was filled with 8% $Na_2CO_3$ supported on alumina and was used to determine the content of air, methane, ethane, ethylene and $C_{3+}$ hydrocarbons. The temperature of columns during analysis was 80 ◦C. The chromatograms were treated by an internal normalization method with a correction for the molecular weight of components. The second chromatograph was equipped by TCD and a column with NaX zeolite (Gazprom Neftekhim Salavat, Russia), 2 m in length and 3 mm in diameter. This column works at an ambient temperature and allows the determination of the contents of hydrogen, oxygen, nitrogen, carbon monoxide and methane. Due to the small difference in thermal conductivities of He and $H_2$, negative $H_2$ peaks can be observed sometimes. In order to solve this problem we used the $H_2$ peak inversion procedure and special software for $H_2$ content calculation, based on the results of analysis of model gas mixtures. The methane conversion (X), product selectivity (S) and the yield (Y) of products are defined as follows:

Methane conversion $C_{CH_4}$ (%) was calculated as a ratio between reacted methane $W_{CH_4}$ to total amount of methane fed into reactor $W_{CH_4}{}^0$:

$$C_{CH_4} = \frac{W_{CH_4}}{W_{CH_4}{}^0} \times 100\%$$

Carbon dioxide conversion $C_{CO_2}$ was calculated as a ratio between reacted methane $W_{CO_2}$ to total amount of methane fed into reactor $W_{CO_2}{}^0$:

$$K = \frac{W_{CO_2}}{W_{CO_2}{}^0} \times 100\%$$

The same calculations were performed to estimate oxygen conversion.

Selectivity S of CO formation was calculated as ratio between molar fraction of methane converted toward CO $W^{CO}$ to amount of reacted methane $W_{CH_4}$ :

$$S = \frac{W^{CO}}{W_{CH_4}} \times 100\%$$

Selectivity $S$ of $H_2$ formation was calculated as a ratio between molar fraction of methane converted to hydrogen $W^{H_2}$ to double amount of converted methane $W_{CH_4}$:

$$S = \frac{W^{H_2}}{2 \cdot W_{CH_4}} \times 100\%$$

Yield of CO (%) was determined as product of methane conversion on selectivity of CO formation:

$$Y_{CO} = \frac{C_{CH_4} \cdot S}{100\%}$$

Yield of $H_2$ (%) was determined as product of methane conversion on selectivity of $H_2$ formation:

$$Y_{H_2} = \frac{C_{CH_4} \cdot S_{H_2}}{100\%}$$

To evaluate measurement errors the data of 10 experiments performed under the same conditions were chosen, followed by calculation of conversion and selectivity (Table. 1).

Table 1 – Measured values of methane conversion and CO selectivity

| Number of measurement | $CH_4$ conversion, % | CO selectivity,% |
|---|---|---|
| 1 | 77 | 92 |
| 2 | 78 | 97 |
| 3 | 85 | 98 |
| 4 | 79 | 98 |
| 5 | 79 | 98 |
| 6 | 78 | 98 |
| 7 | 77 | 100 |
| 8 | 79 | 99 |
| 9 | 77 | 96 |
| 10 | 79 | 97 |

Data of table 1 were used for calculation:

Table 2 - The arithmetic mean value:

| $\bar{x}$ | For $CH_4$ conversion | For CO selectivity |
|---|---|---|
| $\bar{x} = \frac{1}{n}\sum_{i=1}^{n} x_i$ | 78,8 | 97,3 |

Table 3 – Absolute error:

| $\Delta x_i$ | For $CH_4$ conversion | For CO selectivity |
|---|---|---|
| $\Delta x_i(\max) = \lvert x_i - \bar{x} \rvert$ | $\pm 2\%$ | $\pm 2\%$ |

## 2.3 Catalyst synthesis methods

The $La_{2-x}Sr_xCoO_{4\pm\delta}$ (x = 0.75; 1.0) and $Nd_{2-x}Ca_xCoO_{4\pm\delta}$ (x = 0.75; 1.0) layered perivskite-type cobaltates as catalysts for both partial oxidation and dry reforming of methane were prepared using solid-state technique.

The following oxides and carbonates were taken as a initial chemicals for silid-satte synthesis: $La_2O_3$, $Nd_2O_3$, $SrCO_3$ и $CaCO_3$. Lanthanum and neodymium oxides as well as calcium and strontium carbonates before synthesis were calcinated for 4 h at800ºC и 400°C, respectively. Then appropriate quantity of reagents for each composition were mixed and grinded in a planetary ball mill for 30 min with addition of heptane. After heptane evaporation the powder precursors were calcinated in air at 1100°C for 24hours. Then precursors were grinded again in planetary ball mill, pressed into pills and calcinated at 1200°C for 10 hours.

## 2.4 Physico-chemical analysis of the catalysts

### 2.4.1 X-ray diffraction study

The phase composition of as-prepared and spend catalysts was determined by X-ray diffraction alalysis (XRD) using both Huber IMAGE FOIL G670 diffractometer ($CuK_{\alpha1}$ radiation, Image Plate detector) and Bruker AXS D8 Advanced Powder Diffraction System ($CuK_{\alpha1}$ irradiation, VANTEC detector). Scanning was performed in 2θ angle region from 10° to 80° with 0.01° step. For the analysis of XRD patterns and refinement of unit cell parameters the “WinXpow” software (STOE) and International Center for Diffraction Data (ICDD) were used.

### 2.4.2 X-ray photoelectron spectroscopy method

The chemical composition of the particle surface and oxidation state of elements were analyzed by X-ray photoelectron spectroscopy (XPS) using a ThermoScientific Multilab 2000 employing Al $K_{\alpha1}$and Mg $K_{\alpha1}$ radiations at a residual pressure of $10^{-9}$ mbar. The binding energy spectra were calibrated using the C1s line (E = 284.6 eV) internal standard.

### 2.4.3 Scanning electron microscopy with energy dispersive X-ray analysis.

SEM analysis with secondary and backscattered electrons was performed in order to determine chemical bulk composition as well as surface microstructure of

synthesized catalytic materials. For this purpose LEO-SUPRA 50 VP scanning electron microscope with a field emission cathode at U = 10–20 kV was used. The powder of the sample was fixed at the copper substrate using a carbon-based conducting adhesive. Magnification was in a region ×1000- ×20000. EDX analysis at U = 15 kV was performed by means of an energy dispersive INCA x-SIGHT spectrometer attached to a scanning electron microscope.

### 2.4.4 Transmission electron microscopy

Transmission electron microscopy was carried out on a transmission electron microscope JEOL JEM 2010 UHR with $LaB_6$ radiation source. The accelerating voltage was 200 kV. Images resolution of 4008 × 2672 pixels have been received in the Gatan Orius SC1000 chamber. Processing micrographs was performed using DIGITAL MICROGRAPH software. Prior to analysis, samples were milled in an agate mortar and then dispersed in ethanol and passed sonication treatment. After that the dispersed samples were deposited on a carbon film placed on a copper grid.

### 2.4.5 Hydrogen temperature programmed reduction

The behavior of the catalysts in a reducing environmental was studied by hydrogen thermo-programmed reduction ($H_2$-TPR) using the Micromeritics Autochem II Chemisorption Analyzer RS232 Status. Record of hydrogen consumption curves and processing of the data was performed using a standard software instrument - Autochem II 2920 V. 3.50.

The test sample was placed in a special U-shaped quartz cell layer on the quartz fiber (quartz wool). Mass of the loaded sample was 0.1 g.

To sample reduction gas mixture of the composition of 10%$H_2$/ 90% Ar was used. The flow rate of the gas mixture was 50 ml $min^{-1}$. The sample was heated with ramp 15°C/min up to temperature of 900°C and held at this temperature for 30 minutes.

The registration of the experimental data (sample temperature, duration of the experiment and the difference in hydrogen content of the initial and final gas mixture) was carried out with a frequency of 1 $sec^{-1}$. The experimental data are displayed as a

plot of hydrogen consumption of the sample temperature or of time of the experiment. The total peak area of hydrogen consumption corresponds to the amount of hydrogen that consumed to reduce the sample throughout the experiment.

### 2.4.6 Iodometric titration analysis

The oxygen content in as-prepared catalysts was calculated according to oxidation state of cobalt which was determined by iodometric titration. A sample was dissolved in diluted hydrochloric acid in the presence of potassium iodide. This is accompanied by following reactions:

$$Co^{+3} + Cl^{-} \rightarrow Co^{+2} + 1/2Cl_2$$

$$Co^{4+} + 2Cl^{-} \rightarrow Co^{+2} + Cl_2$$

$$Cl_2 + 2I^{-} \rightarrow 2Cl^{-} + I_2$$

Then, the formed iodine was titrated by 0.1 M solution of sodium thiosulfate:

$$I_2 + 2Na_2S_2O_3 \rightarrow 2NaI + Na_2S_4O_6$$

$Co^{3+}/Co_{total}$ ratio was calculated according to formula:

$$n = \frac{c_{Na_2S_2O_3} V_{Na_2S_2O_3} M}{m} + 2,$$

where $c_{Na_2S_2O_3}$ and $V_{Na_2S_2O_3}$ – concentration and volume of thiosulfate solution engaged to titration, respectively. $M$ – catalyst molar mass, $m$ – mass of sample.

During calculations of oxygen content it was taken into account that oxidation state of rare earth cations is 3+ and alkaline earth is 2+.

# Chapter 3. Results and discussion

According to literature review, development of new catalytic materials for partial oxidation of methane and dry reforming of methane is very important problem. In the most studies devoted to this problem the design of new catalysts is focused on the materials which could provide high activity, selectivity and resistance to deactivation.

The most widely used catalysts of POM and DRM are nickel-based materials supported on different oxides. However, these materials suffer from deactivation most likely due to coking, sintering and formation of inactive compounds during catalytic process. Introduction of noble metals into nickel supported catalyst can prevent deactivation.

The alternative way is application of mixed oxides with perovskite structure. It is known that these systems can form nano-size particles of transition metals dispersed on the oxide support in reducing environment. Formed in this way metallic particles can provide high activity as well as prevent deactivation. In the literature review it was shown that high selectivity and conversion can be mostly achieved at perovskite oxides contains precious metals, for example on $LaRhO_3$ or with strong dilution of reacting system by inert gases.

Presence in perovskite oxide structure of transition elements, varying oxidation state due to heterovalent substitution, provides the ability to create a high concentration of defects in the anion sublattice (oxygen vacancies or overstoichiometric atoms of oxygen). Such defects can increase the mobility of lattice oxygen and affect the catalytic activity of perovskite oxides.

Two-dimensional counterparts of perovskites (layered perovskites of $K_2NiF_4$ structure type) are characterized by high oxygen mobility [110-113]. The structure of these compounds can be described as an intergrowth of the perovskite structure with rock salt structure. For example, the mobility of lattice oxygen of the $LaSrCoO_4$ layered perovskite oxide significantly higher than the mobility of $LaCoO_3$ perovskite [110]. Lattice oxygen of $NdSrCu_{1-x}Co_xO_{4-\delta}$ and $Sm_{1.8}Ce_{0.2}Cu_{1-x}Co_xO_{4+\delta}$ cobaltates determines the high catalytic activity of these oxides in the total oxidation of methane to $CO_2$ and

$H_2O$ [111]. Most of known studies devoted to catalytic properties of layered perovskite oxides have been generally focused on the total oxidation of methane (in environmental with very high dilution of reaction mixture by oxygen and at relatively low temperature). Catalytic properties of these compounds in oxidative conversion of methane to synthesis gas (in highly reducing environmental) have not been carefully studied. Therefore, detailed study of the catalytic properties of layered perovskite oxides in the oxidation of methane to synthesis gas - oxygen partial oxidation and carbon dioxide reforming of methane is very important.

In the current research we focused on the study of partial oxidation of methane and dry reforming of methane to synthesis gas

$$2CH_4 + O_2 \leftrightarrow 2CO + 4H_2$$

$$CH_4 + CO_2 \leftrightarrow 2CO + 2H_2$$

over complex oxides with layered perovskite-like structure: $NdCaCoO_{3.96}$, $Nd_{1.25}Ca_{0.75}CoO_{4.04}$, $LaSrCoO_{4.00}$ and $La_{1.25}Sr_{0.75}CoO_{4.03}$.

Generally synthesis of a single-phase layered perovskite structure requires high temperatures and long time of calcination needed to reach equilibrium. The most common method for the preparation of such compounds is a solid-state synthesis that includes physical homogenization of the initial components followed by thermal treatment. The main advantages of this approach are the simplicity of implementation and wastelessness.

Thus, to achieve the goal of the present work, a series of catalysts were synthesized and tested in the selective catalytic oxidation of methane to synthesis gas.

## 3.1 Study of partial oxidation of methane to synthesis gas over synthesized catalysts

In this work the partial oxidation of methane to syngas over layered perovskite oxides $NdCaCoO_{3.96}$, $Nd_{1.25}Ca_{0.75}CoO_{4.04}$, $LaSrCoO_{4.00}$ and $La_{1.25}Sr_{0.75}CoO_{4.03}$ was studied for the first time.

The values of $CH_4$ conversion and products formation selectivity as a function of temperature are shown in Fig. 8,9,10 and 11 ($CH_4/O_2$ = 2:1; space velocity (W) = 22 $L*g^{-1}*h^{-1}$). According to these data, at T < 850°C $CH_4$ conversion is very low for all catalysts and does not exceed 25%. At this temperature, the full oxidation of $CH_4$ to $CO_2$ dominates over the POM reaction and the amount of $CO_2$ produced is higher than the corresponding amounts of CO and $H_2$. Over all four catalysts the methane conversion increases with increasing temperature. Conversion of oxygen varied similarly. The selectivity of the synthesis gas also increases with temperature with simultaneous decreasing $CO_2$ selectivity. As shown in Fig. 8, 9, 10 and 11 the most efficient catalyst for partial oxidation of methane to syngas is $NdCaCoO_{3.96}$. Increase temperature from 850 ºC to 870 ºC led to rapid increase of CO selectivity from 1% to 76% and $CH_4$ conversion from 25% to 62% (Fig.8). At 910°C conversion of $CH_4$ approached 90% and did not changed with further temperature increase. Selectivity of CO and $H_2$ formation was closed to 100% at 925°C.

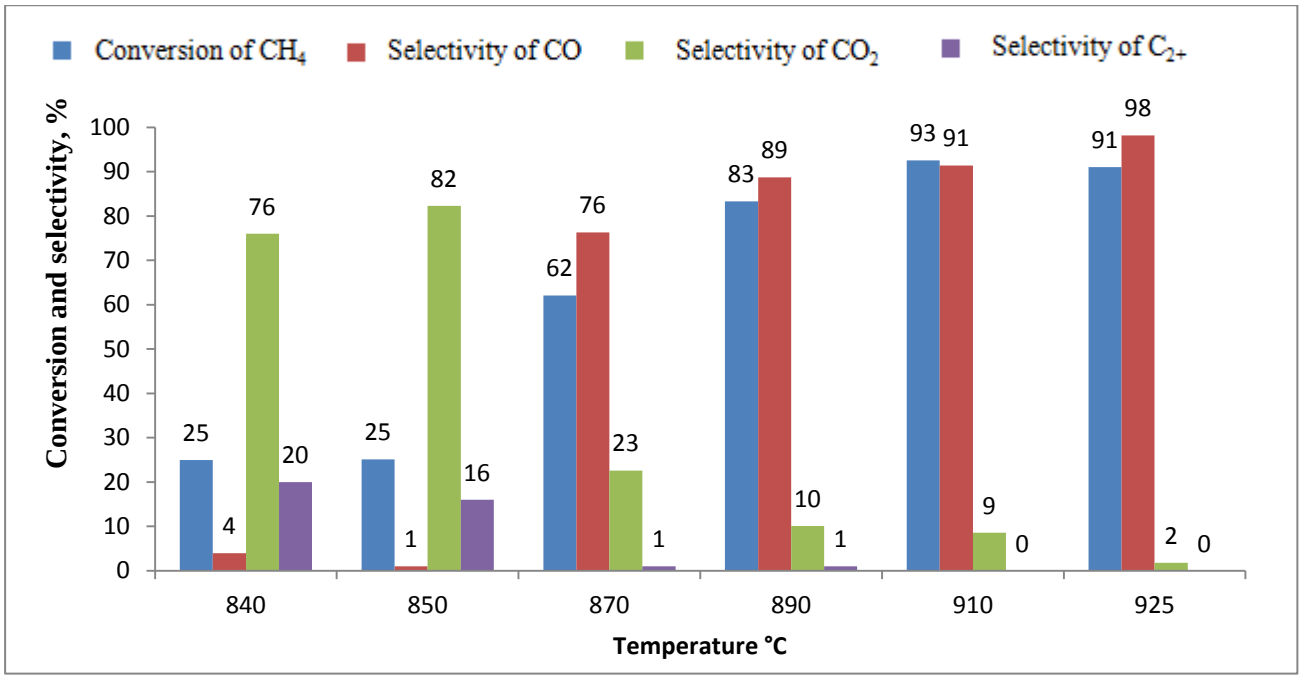


Figure 8 – $CH_4$ conversion and products formation selectivity as a function of temperature ($NdCaCoO_{3.96}$; CH4/$O_2$ = 2; W = 22 L*$g^{-1}$*$h^{-1}$).

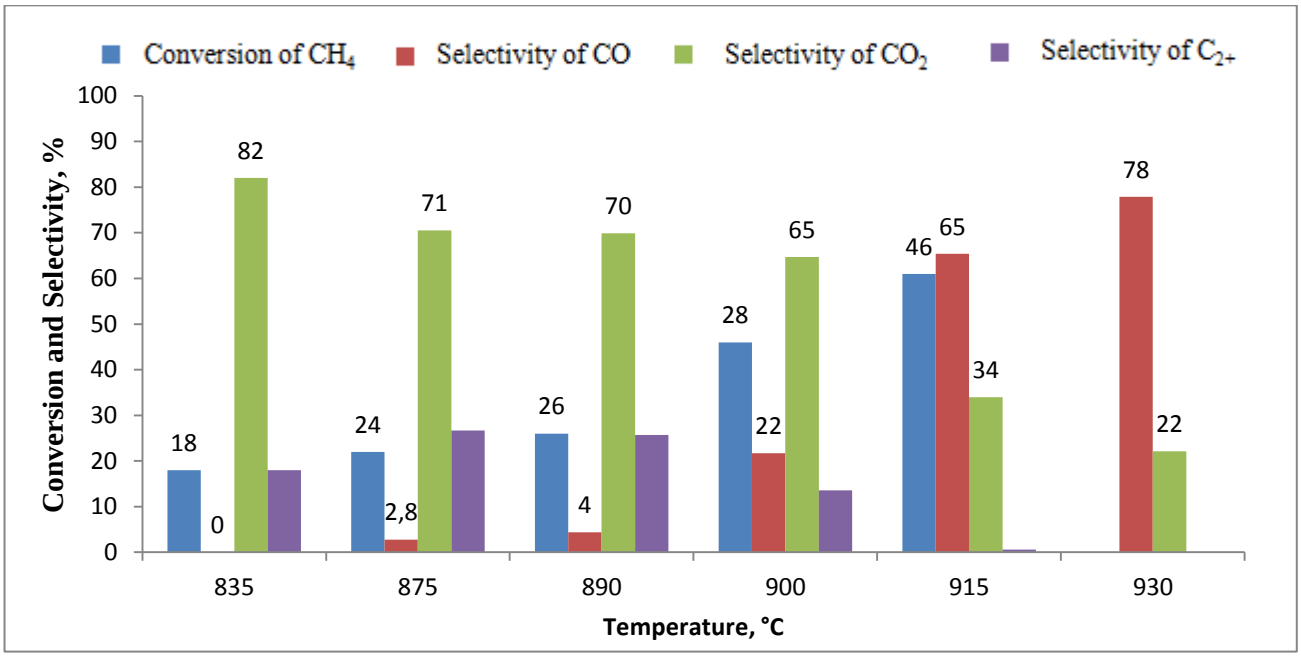


Figure 9 – $CH_4$ conversion and products formation selectivity as a function of temperature ($Nd_{1.25}Ca_{0.75}CoO_{4.04}$; $CH_4/O_2$ = 2; W = 22 L*$g^{-1}$*$h^{-1}$).

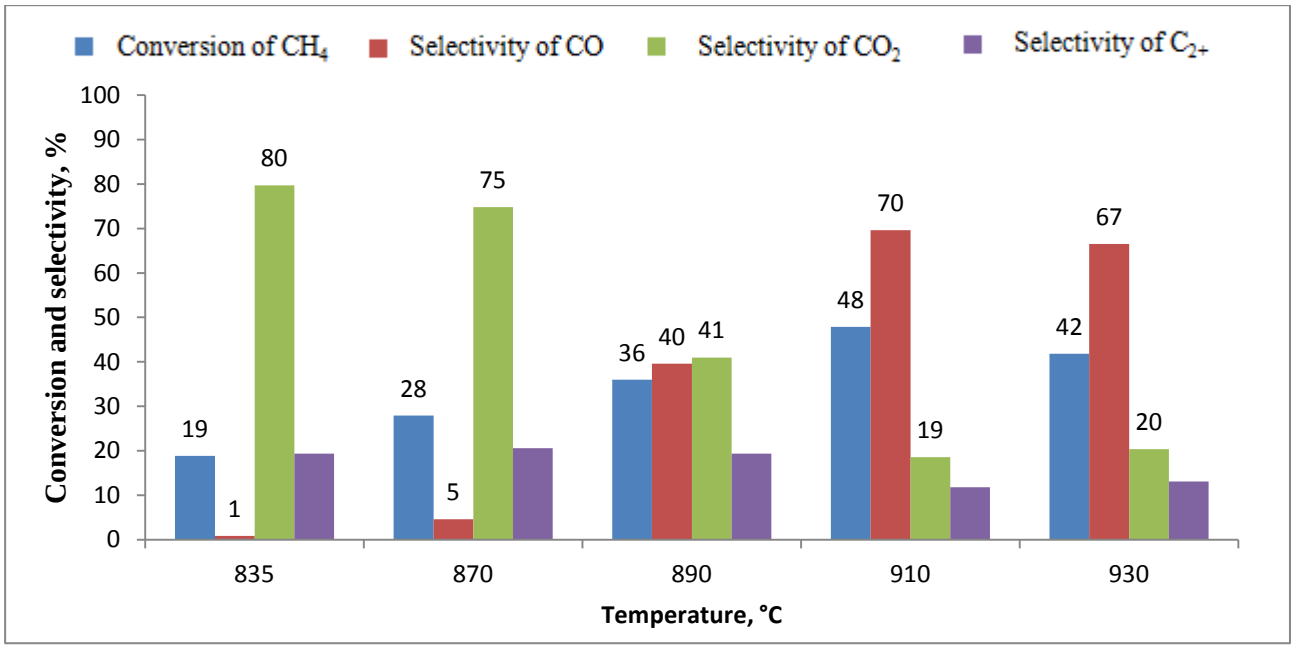


Figure 10 – $CH_4$ conversion and products formation selectivity as a function of temperature ($LaSrCoO_{4.00}$; $CH_4/O_2$ = 2; W = 22 $L*g^{-1}*h^{-1}$).

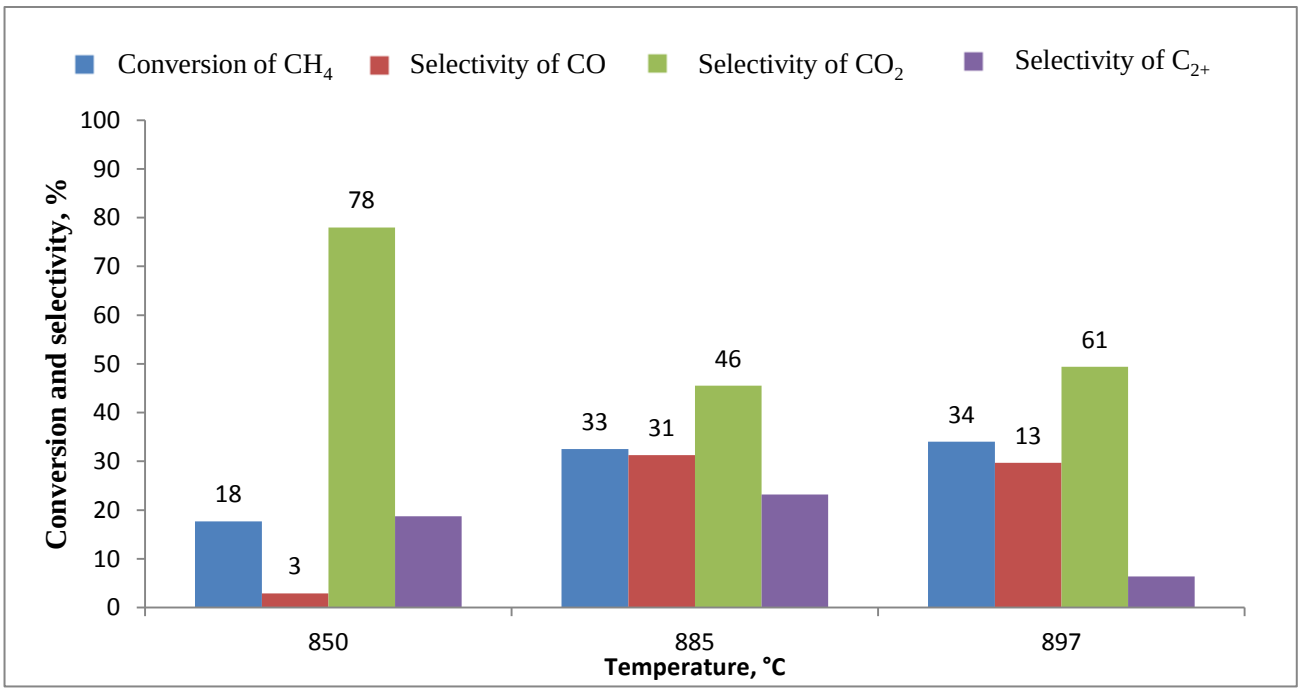


Figure 11 – $CH_4$ conversion and products formation selectivity as a function of temperature ($La_{1.25}Sr_{0.75}CoO_{4.03}$; $CH_4/O_2$ = 2; W = 22 $L*g^{-1}*h^{-1}$).

In case of $Nd_{1.25}Ca_{0.75}CoO_{4.04}$ (Fig. 9) the methane conversion and the selectivity toward synthesis gas were significantly lower than those for $NdCaCoO_{3.96}$. Thus, over $Nd_{1.25}Ca_{0.75}CoO_{4.04}$ the methane conversion increased from 18% to 28% with rising of reaction temperature from 835$^{o}$C to 900$^{o}$C. With further increase of reaction temperature up to 930°C the methane conversion approached only 61%. Although higher temperatures are also accompanied by an increase of selectivity of the synthesis gas and decreasing the selectivity of $CO_2$ and $C_{2+}$-products, but the maximum selectivity of CO and $H_2$ at 930$^{o}$C did not exceed 78%.

Lanthanum and strontium-based materials were also less active and selective than $NdCaCoO_{3.96}$ in partial oxidation of methane. Over $LaSrCoO_{4.00}$ maximal values of $CH_4$ conversion did not exceed 50% and selectivity toward synthesis gas 70% at 910°C (Fig. 10). Further rising of reaction temperature did not lead to increase neither methane conversion nor synthesis gas selectivity. At 930°C the selectivity of $CO_2$ and $C_{2+}$-products formation were 20% and 13%, respectively. The catalyst $La_{1.25}Sr_{0.75}CoO_{4.03}$ was even less active than $LaSrCoO_{4.00}$ - rising temperature from 850°C to 897°C led to an increase of $CH_4$ conversion level from 18% to 34% (Fig. 11). Selectivity of synthesis gas formation at 897°C was only 13%.

The obtained experimental results were in agreement with finding in [107] where unsubstituted by alkaline-earth elements perovskite $NdCoO_3$ was much more active than $LaCoO_3$. The activity of catalytic materials in [107] increased with decreasing of rare-earth element radii with the follow trend - $LaCoO_3 > PrCoO_3 > NdCoO_3 > SmCoO_3 > GdCoO_3$. Over the most active $GdCoO_3$ catalyst the $CH_4$ conversion was about 73% while the selectivities of CO and $H_2$ formation were 79 and 81%, respectively. Over $NdCoO_3$ highest $CH_4$ conversion level did not exceed 40% with the selectivity to CO and $H_2$ around 55%. In contrast to data in [107] for $NdCoO_3$, over $NdCaCoO_{3.96}$ catalyst with layered perovskite-like structure and partial substitution of Nd on Ca the selectivity toward synthesis gas was close to 100% with the $CH_4$ conversion around 90%.

One of the most important criteria for investigation of catalysts efficiency is its lifetime on stream. Over the most active and selective $NdCaCoO_{3.96}$ catalyst the time on

stream test in POM was done. As it shown in Fig. 12, synthesis gas selectivity was close to 100% and did not change for at least 140h with a constant level of methane conversion about 90%. No trend to catalyst deactivation was observed.

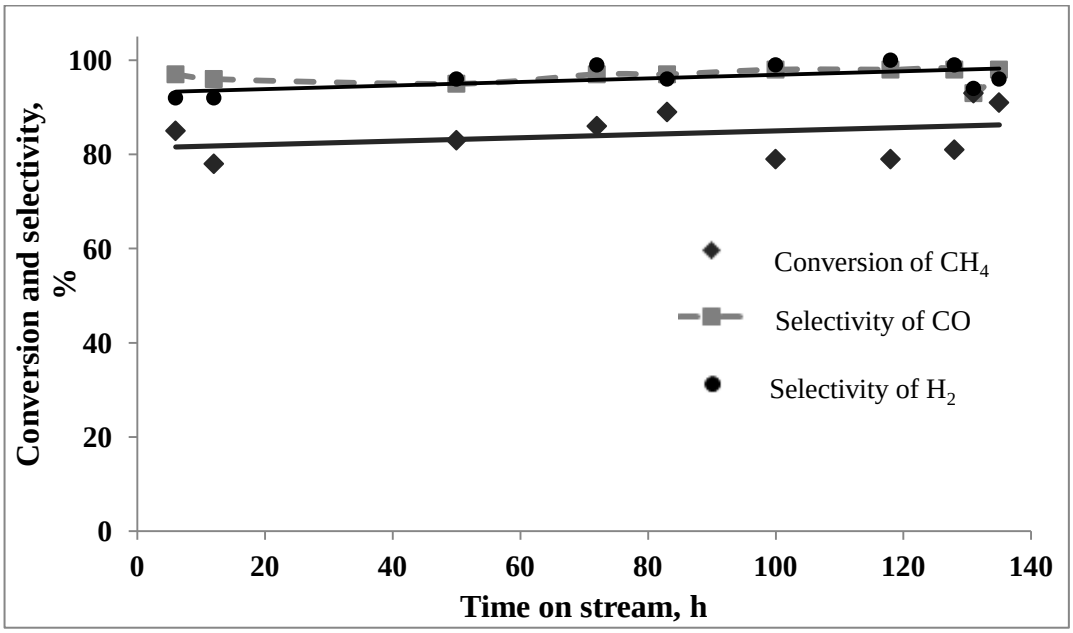


Figure 12 – Conversion of $CH_4$ and selectivity of CO and $H_2$ formation as a function of time on stream over $NdCaCoO_{3.96}$

(T = 915 - 925°C; $CH_4/O_2$ = 2-2.7; W = 20-22 $L*g^{-1}*h^{-1}$).

The results of POM reaction in terms of $CH_4$ and $O_2$ conversions and products formation selectivity as a function of operation conditions are shown in table 4. These data also show that the reaction temperature is one of the key factors determining the possibility to achieve high values of selectivity to synthesis gas. At the same time it should be noted that the temperature in the catalyst bed depends on the ratio of methane/oxygen in the feed gas to the reactor, as well as the space velocity.

Table 4 – Partial oxidation of methane over $NdCaCoO_{3.96}$

| № | T, °C | Conversion, % | | Selectivity, % | | | |
|---|---|---|---|---|---|---|---|
| | | $CH_4$ | $O_2$ | $C_{2+}$ | $CO_2$ | CO | $CO_x$ |
| Ratio $CH_4/H_2$ = 1.8, W = 18 $L\cdot g^{-1}\cdot h^{-1}$ | | | | | | | |
| 1 | 851 | 27 | 97 | 15 | 83 | 2 | 85 |
| 2 | 865 | 69 | 98 | 0 | 23 | 77 | 100 |
| 3 | 886 | 70 | 98 | 3 | 17 | 80 | 97 |

| | | | | | | | |
|---|---|---|---|---|---|---|---|
| 4 | 890 | 81 | 98 | 0 | 17 | 83 | 100 |
| 5 | 903 | 78 | 98 | 0 | 18 | 82 | 100 |
| 6 | 915 | 90 | 98 | 0 | 13 | 87 | 100 |
| Ratio $CH_4$/ $O_2$ = 1.9, W = 61 $L \cdot g^{-1} \cdot h^{-1}$ | | | | | | | |
| 1 | 875 | 25 | 92 | 9 | 88 | 3 | 91 |
| 2 | 910 | 32 | 93 | 6 | 63 | 31 | 94 |
| 3 | 922 | 38 | 97 | 7 | 56 | 37 | 93 |
| 4 | 942 | 47 | 99 | 5 | 39 | 56 | 95 |
| Ratio $CH_4$/ $O_2$ = 2, W = 17 $L \cdot g^{-1} \cdot h^{-1}$ | | | | | | | |
| 1 | 864 | 87 | 98 | 0 | 8 | 92 | 100 |
| 2 | 888 | 93 | 98 | 0 | 7 | 93 | 100 |
| 3 | 911 | 96 | 98 | 0 | 6 | 94 | 100 |
| 4 | 923 | 69 | 98 | 0 | 0 | 100 | 100 |
| Ratio $CH_4$/ $O_2$ = 2, W = 39 $L \cdot g^{-1} \cdot h^{-1}$ | | | | | | | |
| 1 | 857 | 22 | 95 | 14 | 85 | 1 | 86 |
| 2 | 878 | 22 | 95 | 12 | 86 | 2 | 88 |
| 3 | 900 | 25 | 97 | 9 | 76 | 15 | 91 |
| 4 | 910 | 40 | 99 | 2 | 38 | 60 | 98 |
| 5 | 925 | 63 | 99 | 1 | 15 | 84 | 99 |
| Ratio $CH_4$/ $O_2$ = 2, W = 49 $L \cdot g^{-1} \cdot h^{-1}$ | | | | | | | |
| 1 | 860 | 21 | 91 | 10 | 88 | 1 | 89 |
| 2 | 888 | 23 | 92 | 10 | 83 | 7 | 90 |
| 3 | 926 | 59 | 100 | 5 | 17 | 78 | 95 |
| Ratio $CH_4$/ $O_2$ = 2.1, W = 37 $L \cdot g^{-1} \cdot h^{-1}$ | | | | | | | |
| 1 | 879 | 22 | 95 | 11 | 87 | 2 | 89 |
| 2 | 900 | 25 | 97 | 11 | 77 | 12 | 89 |
| 3 | 910 | 45 | 99 | 4 | 31 | 65 | 96 |
| 4 | 930 | 74 | 99 | 2 | 4 | 94 | 98 |
| Ratio $CH_4$/ $O_2$ = 2.1, W = 44 $L \cdot g^{-1} \cdot h^{-1}$ | | | | | | | |
| 1 | 860 | 21 | 95 | 11 | 88 | 1 | 89 |
| 2 | 884 | 23 | 95 | 10 | 86 | 4 | 90 |
| 3 | 902 | 36 | 99 | 5 | 45 | 50 | 95 |
| 4 | 909 | 53 | 99 | 3 | 22 | 75 | 97 |
| 5 | 925 | 63 | 99 | 2 | 14 | 84 | 98 |
| Ratio $CH_4$/ $O_2$ = 2.2, W = 20 $L \cdot g^{-1} \cdot h^{-1}$ | | | | | | | |
| 1 | 860 | 22 | 97 | 17 | 81 | 2 | 83 |
| 2 | 895 | 86 | 98 | 0 | 3 | 97 | 100 |
| 3 | 918 | 89 | 98 | 0 | 3 | 97 | 100 |
| Ratio $CH_4$/ $O_2$ = 2.2, W = 26 $L \cdot g^{-1} \cdot h^{-1}$ | | | | | | | |
| 1 | 856 | 22 | 97 | 13 | 78 | 9 | 87 |
| 2 | 882 | 24 | 98 | 11 | 77 | 12 | 89 |
| 3 | 892 | 74 | 99 | 0 | 9 | 91 | 100 |
| 4 | 912 | 86 | 99 | 0 | 4 | 96 | 100 |
| Ratio $CH_4$/ $O_2$ = 2.2, W = 30 $L \cdot g^{-1} \cdot h^{-1}$ | | | | | | | |

| | | | | | | | |
|---|---|---|---|---|---|---|---|
| 1 | 884 | 25 | 98 | 10 | 78 | 12 | 90 |
| 2 | 905 | 55 | 99 | 5 | 23 | 72 | 95 |
| 3 | 928 | 83 | 99 | 0 | 5 | 95 | 100 |
| Ratio $CH_4$/ $O_2$ = 2.3, W = 16 $L \cdot g^{-1} \cdot h^{-1}$ | | | | | | | |
| 1 | 855 | 80 | 98 | 0 | 6 | 94 | 100 |
| 2 | 878 | 83 | 98 | 0 | 3 | 97 | 100 |
| 3 | 895 | 86 | 98 | 0 | 2 | 98 | 100 |
| Ratio $CH_4$/ $O_2$ = 2.3, W = 20 $L \cdot g^{-1} \cdot h^{-1}$ | | | | | | | |
| 1 | 858 | 27 | 98 | 12 | 67 | 21 | 88 |
| 2 | 864 | 62 | 98 | 0 | 17 | 83 | 100 |
| 3 | 872 | 62 | 98 | 0 | 15 | 85 | 100 |
| 4 | 873 | 60 | 98 | 1 | 18 | 81 | 99 |
| 5 | 895 | 84 | 98 | 0 | 4 | 96 | 100 |
| 6 | 900 | 85 | 99 | 0 | 3 | 97 | 100 |
| 7 | 914 | 85 | 99 | 0 | 3 | 97 | 100 |
| Ratio $CH_4$/ $O_2$ = 2.4, W = 20 $L \cdot g^{-1} \cdot h^{-1}$ | | | | | | | |
| 1 | 897 | 79 | 98 | 0 | 2 | 98 | 100 |
| 2 | 912 | 78 | 98 | 0 | 1 | 99 | 100 |
| 3 | 918 | 85 | 98 | 0 | 2 | 98 | 100 |
| Ratio $CH_4$/ $O_2$ = 2.5, W = 20 $L \cdot g^{-1} \cdot h^{-1}$ | | | | | | | |
| 1 | 865 | 85 | 97 | 0 | 1 | 99 | 100 |
| 2 | 871 | 82 | 98 | 0 | 1 | 99 | 100 |
| 3 | 873 | 58 | 98 | 1 | 16 | 83 | 100 |
| 4 | 905 | 65 | 98 | 0 | 8 | 92 | 100 |
| 5 | 923 | 74 | 98 | 0 | 3 | 97 | 100 |
| 6 | 932 | 84 | 98 | 0 | 2 | 98 | 100 |
| Ratio $CH_4$/ $O_2$ = 2.6, W = 20 $L \cdot g^{-1} \cdot h^{-1}$ | | | | | | | |
| 1 | 865 | 80 | 98 | 0 | 3 | 77 | 80 |
| 2 | 889 | 77 | 98 | 0 | 2 | 98 | 100 |
| 3 | 915 | 79 | 98 | 0 | 2 | 98 | 100 |
| 4 | 936 | 77 | 98 | 0 | 2 | 98 | 100 |
| 5 | 957 | 78 | 98 | 0 | 1 | 99 | 100 |
| Ratio $CH_4$/ $O_2$ = 2.7, W = 20 $L \cdot g^{-1} \cdot h^{-1}$ | | | | | | | |
| 1 | 890 | 77 | 98 | 0 | 3 | 97 | 100 |
| 2 | 892 | 78 | 98 | 0 | 2 | 98 | 100 |
| 3 | 911 | 85 | 97 | 0 | 0 | 100 | 100 |
| 4 | 915 | 79 | 98 | 0 | 2 | 98 | 100 |
| 5 | 925 | 79 | 98 | 0 | 2 | 98 | 100 |
| Ratio $CH_4$/ $O_2$ = 2.8, W = 60 $L \cdot g^{-1} \cdot h^{-1}$ | | | | | | | |
| 1 | 871 | 39 | 99 | 1 | 23 | 76 | 99 |
| 2 | 930 | 51 | 100 | 3 | 11 | 86 | 97 |
| 3 | 868 | 18 | 95 | 7 | 82 | 11 | 93 |
| 4 | 890 | 42 | 99 | 1 | 19 | 80 | 99 |
| 5 | 917 | 47 | 99 | 1 | 14 | 85 | 99 |

| Ratio $CH_4$/ $O_2$ = 4.5, W = 20 $L \cdot g^{-1} \cdot h^{-1}$ | | | | | | | |
|---|---|---|---|---|---|---|---|
| 1 | 879 | 63 | 98 | 0 | 0 | 100 | 100 |
| 2 | 895 | 62 | 98 | 0 | 0 | 100 | 100 |
| 3 | 898 | 61 | 98 | 0 | 1 | 99 | 100 |
| 4 | 895 | 48 | 97 | 1 | 0 | 99 | 99 |
| 5 | 897 | 48 | 97 | 1 | 0 | 99 | 99 |

Results of the influence of $CH_4/O_2$ ratio on the partial oxidation of methane over $NdCaCoO_{3.96}$ presented in Figure 13. It can be seen that the ratio of methane/oxygen has an appreciable effect on the conversion of methane which naturally decreases with increasing its concentration in the gas stream. Increase of the ratio of $CH_4/O_2$ from 2.1 to 2.7 led to methane conversion decreasing from 90 to 80%. Further increase in the methane concentration to a ratio of $CH_4/O_2$ = 4.6 decreased the $CH_4$ conversion to 50%. Selectivity toward syngas and the ratio $H_2$/CO remained stable in the range of $CH_4/O_2$ - 2.1/4.6.

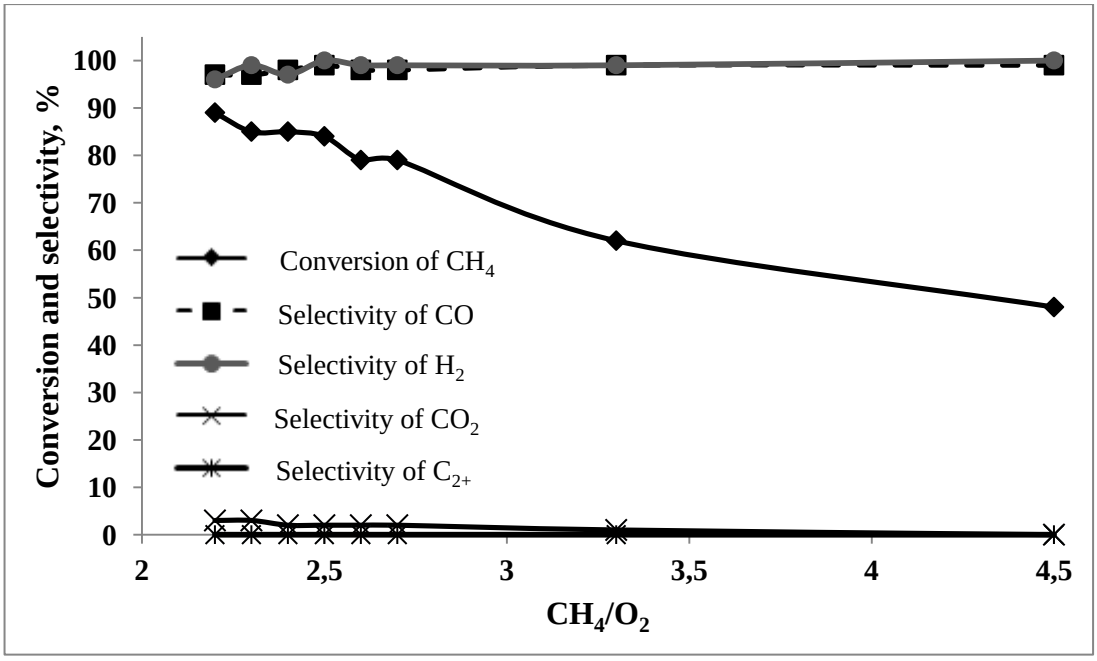


Figure 13 - Conversion of $CH_4$ and selectivity of CO and $H_2$ formation as a function of $CH_4/O_2$ ratio ($NdCaCoO_{3.96}$; T = 915 - 925°C; W = 20 $L*g^{-1}*h^{-1}$)

The contact time of the reactants with the catalyst surface substantially affects the POM results. The highest $CH_4$ conversion value was observed at GHSV $\leqslant$ 17 L*

$g^{-1}*h^{-1}$. A further increase in the space velocity causes a significant decrease in the methane conversion (Fig. 14). In addition to $CH_4$ conversion, the variations in the selectivity at 17–37 L* $g^{-1}*h^{-1}$ were negligible (Fig. 14). However, a further increase in the flow rate resulted in a substantial decrease in the CO and $H_2$ selectivity and a corresponding increase in the selectivity to $CO_2$. Similar trends were also observed in [104] using a perovskite-like lanthanum cobaltate nickelates and in [94] over the $Co/Ca/Al_2O_3$.

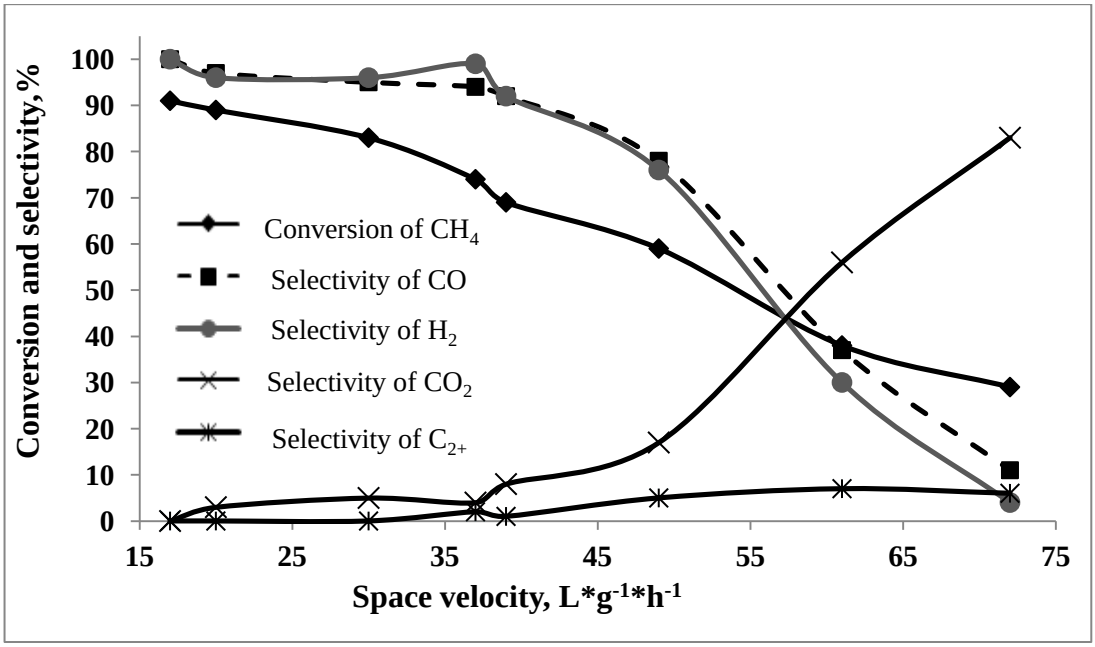


Figure 14 - Conversion of $CH_4$ and selectivity of CO and $H_2$ formation as a function of space velocity ($NdCaCoO_{3.96}$; T = 920 - 925 °C; $CH_4/O_2$ = 2-2.2).

The results of study of space velocity effect on methane conversion and products formation selectivity in POM over $LaSrCoO_{4.00}$ are shown in Table 5. By increasing the space velocity the $CH_4$ conversion and the selectivity toward synthesis gas in the presence $LaSrCoO_{4.00}$ also decreased as it was in the case of $NdCaCoO_{3.96}$. Increase of space velocity from 24 to 60 $L*g^{-1}*h^{-1}$ led to decreasing of the methane conversion from 35% to 22% and the selectivity of synthesis gas formation from 42% to 5% in the temperature range of 890°C-900°C. At the same time the selectivity toward $CO_2$ was increased from 52 % to 88% and the selectivity of $C_{2+}$-products formation did not change a lot and was around 6-7%.

Table 5 – Conversion of $CH_4$ and selectivity of CO and $H_2$ formation as a function of space velocity over $LaSrCoO_{4.00}$

| № | $CH_4/O_2$ | W, L/g/h | T, $^oC$ | C $CH_4$,% | S $O_2$,% | Selectivity, % | | |
|---|---|---|---|---|---|---|---|---|
| | | | | | | $C_{2+}$ | $CO_2$ | CO |
| 1 | 2 | 24 | 890 | 35 | 97 | 6 | 52 | 42 |
| 2 | 2 | 24 | 910 | 42 | 98 | 2 | 40 | 58 |
| 3 | 2 | 24 | 933 | 47 | 98 | 1 | 33 | 66 |
| 4 | 2 | 60 | 800 | 15 | 69 | 3 | 97 | 0 |
| 5 | 2 | 60 | 840 | 19 | 78 | 4 | 95 | 1 |
| 6 | 2 | 60 | 900 | 22 | 83 | 7 | 88 | 5 |

As it was noted in the literature review (chapter 1), there are two different mechanisms of partial oxidation of methane – a direct oxidation of methane to CO and $H_2$ and a combustion-reforming mechanism when $CH_4$ is firstly oxidized to $CO_2$ and $H_2O$; then the reforming reactions of $CH_4$ with steam and $CO_2$ lead to desire products formation as it is shown at the following Scheme 1:

$$\begin{tikzcd} & CO + H_2 \\ CH_4 + O_2 \arrow[ur] \arrow[dr] & \\ & CO_2 + H_2O \arrow[uu, "CH_4"'] \end{tikzcd}$$

Experiments in pulsed reactors show that high temperatures, short contact times and reduction of oxide catalysts to metal state favor proceeding of POM through a direct route. At lower space velocity values, lower temperatures and on oxidized surfaces indirect combustion-reforming mechanism of POM generally takes place. At the same time, in flow reactors it seems difficult proceeding of POM reaction only through the direct pathway since the reaction of total oxidation of methane is most favorable.

The obtained results of experiments with the space velocity variation indicates an increase in the contribution of the total oxidation of methane with a decrease of the contact time, indicating that the combustion-reforming mechanism of the reaction of partial oxidation of methane over $NdCaCoO_{3.96}$ is probably preferable. This is also in the agreement with [94, 104]. At short contact time the total oxidation of methane is

favored, while the proceeding of following steps is quite complicated at the high space velocity values.

In a numerous publications with the comparison of the catalytic activity in the total oxidation of methane to $CO_2$ and $H_2O$ it is proposed to compare the temperatures at which the $CH_4$ conversion achieves certain values [110-114]. Using this approach we compared the temperatures at which the conversion of methane achieved 25% over $LaSrCoO_{4.00}$, $La_{1.25}Sr_{0.75}CoO_{4.03}$, $Nd_{1.25}Ca_{0.75}CoO_{4.04}$ and $NdCaCoO_{3.96}$ (Fig. 15). It can be seen that over $NdCaCoO_{3.96}$ methane conversion approached 25% at 840°C, over $LaSrCoO_{4.00}$ at 865°C, while over $Nd_{1.25}Ca_{0.75}CoO_{4.04}$ and $La_{1.25}Sr_{0.75}CoO_{4.03}$ catalysts conversion of $CH_4$ achieved 25 % only at 890°C and 895°C, respectively. When it comes to the reaction products formation at these temperatures it has shown that oxidation reactions occurs unselectively (Fig. 16). In the outlet gases the $CO_2$ и $C_{2+}$-products are predominating. Over the most active $NdCaCoO_{3.96}$ at 840°C the selectivity toward $CO_2$ was 76%, $C_{2+}$ 20% while selectivity of CO formation did not exceed 4%. At the same time over $La_{1.25}Sr_{0.75}CoO_{4.03}$ catalyst, which indicated the lowest activity and selectivity toward synthesis gas, at 25% level of $CH_4$ conversion selectivity toward $CO_2$ was 61% and CO - 13%.

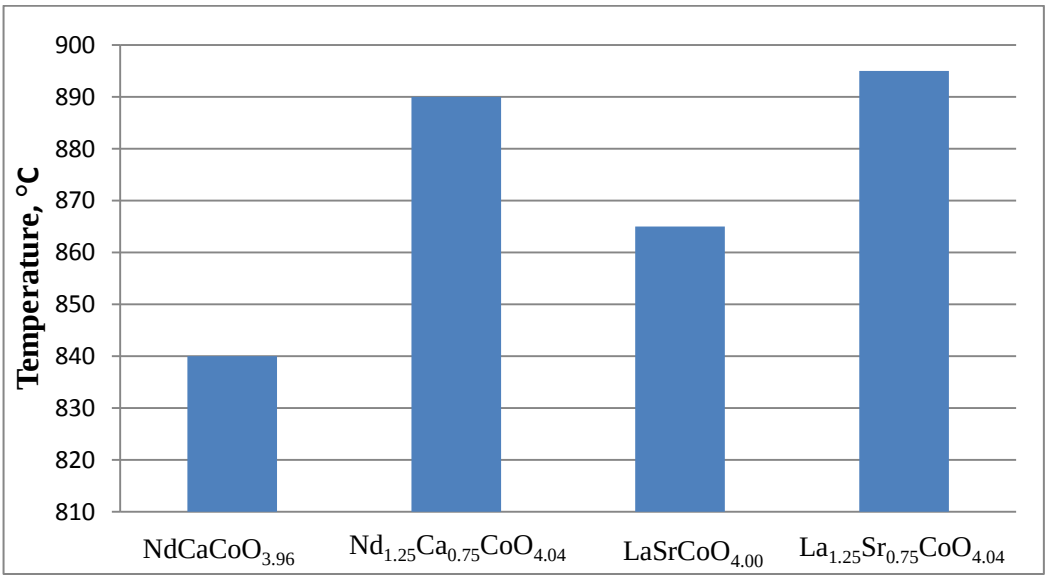


Figure 15 – Temperature of approaching of 25% $CH_4$ conversion in partial oxidation of methane over synthesized catalysts ($CH_4/O_2$ = 2; W = 22 $L*g^{-1}*h^{-1}$)

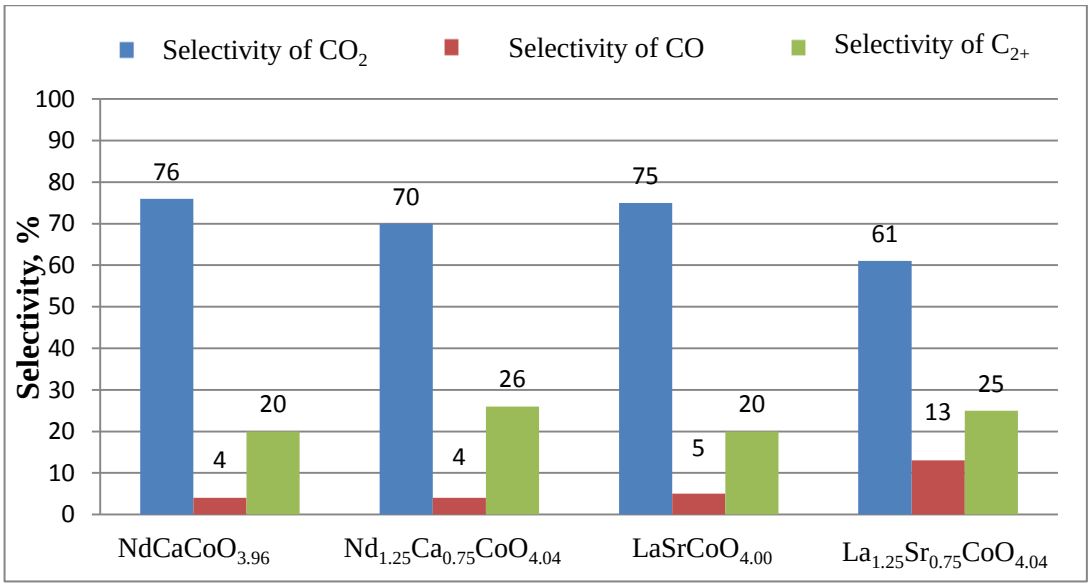


Figure 16 – Products formation selectivity at 25% level of $CH_4$ conversion in partial oxidation of methane over synthesized catalysts ($CH_4/O_2$ = 2; W = 22 $L*g^{-1}*h^{-1}$)

Analysis of the literature review indicates that the active sites of oxidative methane conversion to synthesis gas are mostly metal particles of transition elements on which the primary methane molecule dissociation is performed [27]. It is also known that oxidation products composition can be determined by both nature of active oxygen species, which are involved in an oxidation process, and by the binding energy of active oxygen with catalyst surface. Several authors consider that the lattice oxygen of the catalyst can play a crucial role in methane oxidation to synthesis gas [34-38]. It can be suggested that adsorbed oxygen, which is more active, is responsible for total oxidation of methane to $CO_2$ и $H_2O$ (the first step of methane oxidation to syngas according to indirect mechanism). In a partial oxidation of organic substances to oxygenates an oxygen which has a strong interaction with catalyst surface is involved[7].

Considering the proceeding of partial oxidation of methane to synthesis gas through combustion-reforming process, it can be proposed that the reaction is initiated over sites which are responsible for total oxidation of methane to $CO_2$ и $H_2O$. Oxygen vacancies can be associated with this kind of sites [115]. Hence the defects of oxide catalyst can affect catalytic properties.

Based on the obtained results it can be proposed that lower activity and selectivity of $LaSrCoO_{4.00}$, $La_{1.25}Sr_{0.75}CoO_{4.03}$ and $Nd_{1.25}Ca_{0.75}CoO_{4.04}$ in POM is most likely due to their ability to form active sites. In this connection, it was necessary to estimate physico-chemical properties of synthesized catalytic materials in order to give more insight more into relationship between the composition and the catalytic properties of the catalysts of POM.

## 3.2 Study of influence of physico-chemical properties of synthesized catalysts on the results of methane partial oxidation to synthesis gas.

According to XRD data, all synthesized cobaltates are single-phases (Fig. 17) and have layered perovskite structure ($K_2NiF_4$-type structure). No patterns which could be assign to initial oxides or other phases was observed (Annex).

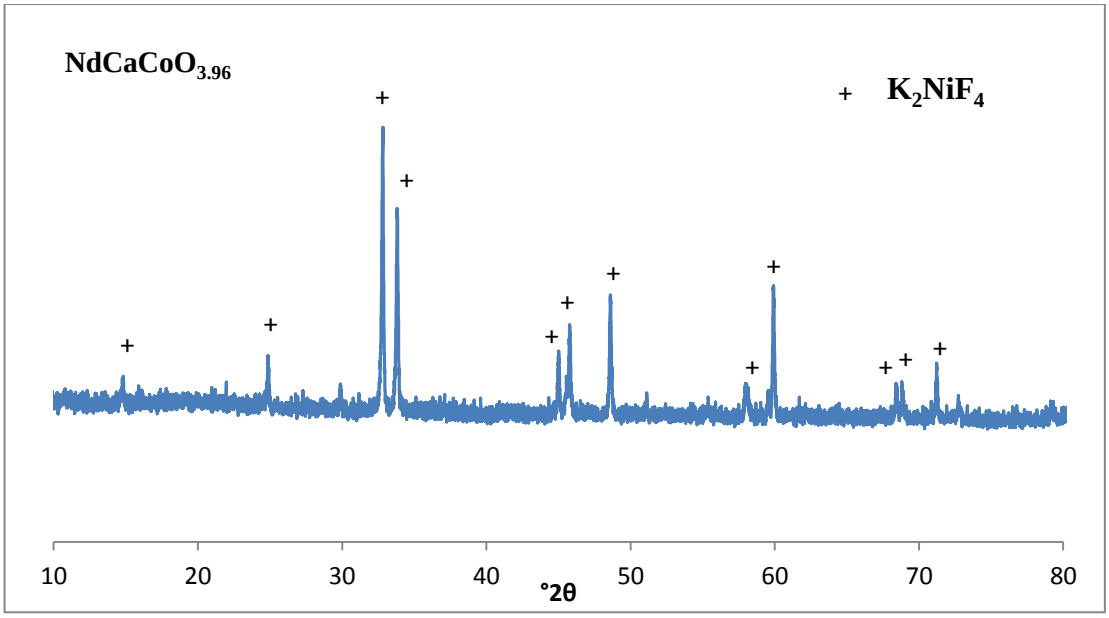

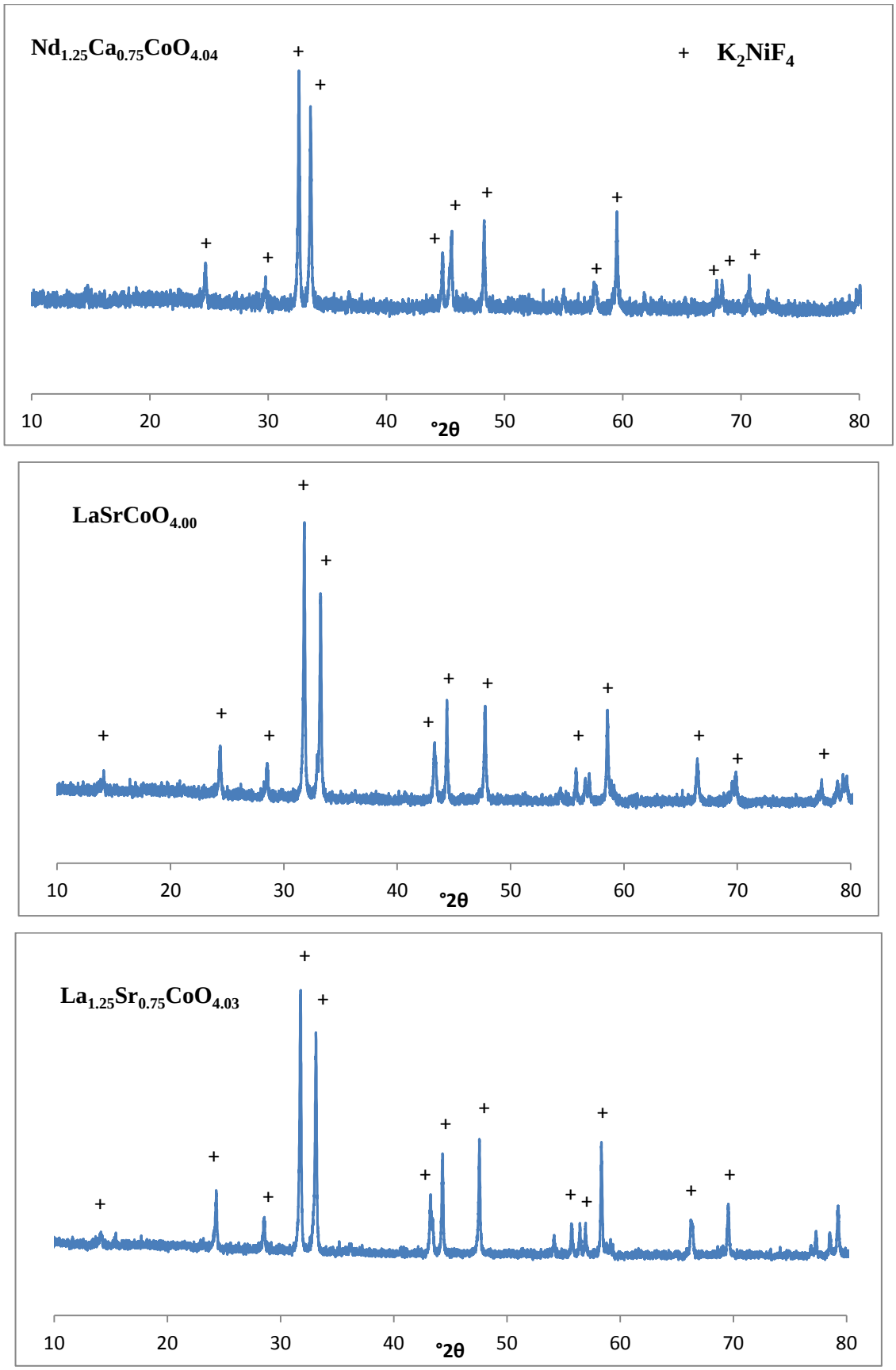


Figure 17 – X-ray diffraction patterns of synthesized catalysts: $NdCaCoO_{3.96}$, $Nd_{1.25}Ca_{0.75}CoO_{4.04}$, $LaSrCoO_{4.00}$ and $La_{1.25}Sr_{0.75}CoO_{4.03}$

Based on the X-ray diffraction analysis data the cell parameters of the obtained were also calculated (Table 6). One can see from Table 6, in the lanthanum-strontium cobaltate ***a*** cell parameter decreases with increasing the degree of substitution of lanthanum to strontium. Reduction of ***a*** parameter with increasing strontium content can not be explained by the changing composition of the A-sublattice because there is a substitution of the cation $La^{3+}$ on the cation with larger radius ($Sr^{2+}$ - 1,44 Å, $La^{3+}$ - 1,36 Å). Perhaps, in this case the major role is played by the electronic configuration of the cobalt ions

Table 6 – Lattice parameters and oxidation state of cobalt in synthesized catalysts

| Composition | Lattice parameters | | $Co^{3+}/Co_{total}$ |
|---|---|---|---|
| | *a*, Å | *c*, Å | |
| $LaSrCoO_{4.00}$ | 3.8041(7) | 12.476(6) | 1.00 |
| $La_{1.25}Sr_{0.75}CoO_{4.03}$ | 3.8174(6) | 12.535(3) | 0.81 |
| $NdCaCoO_{3.96}$ | 3.7358(3) | 11.912(2) | 0.92 |
| $Nd_{1.25}Ca_{0.75}CoO_{4.04}$ | 3.7667(9) | 11.992(4) | 0.82 |

The unit cell parameters of $Nd_{2-x}Ca_xCoO_{4\pm\delta}$ (Table 2) decrease with increasing calcium content. As in the case of lanthanum strontium cobaltate, reduction of parameters is probably due to a change in the electronic configuration of the cobalt ions but not by changing in the composition of A-sublattice. Substitution of neodymium cations (r = 1,09 Å) occurs to $Ca^{2+}$ cations with the larger ionic radius (1,18 Å) [117]. A detailed study of the features of phase formation of layered perovskite cobaltate series $Nd_{2-x}Ca_xCoO_{4\pm\delta}$ is given in [118].

There are also in Table 6 values of $Co^{3+}/Co_{total}$ cation ratio, which were calculated according to iodometrical titration experiment results. The oxygen nonsoichiometry of the catalysts is also presented in Table 6.

Apparently the oxidation state of cobalt cations in lanthanum-strontiuom cobaltate is +3 and the amount of oxygen appropriate to stoichiometrical (Table 6). On the other hand $NdCaCoO_{3.96}$, synthesized in the same conditions and with the same ratio between

Nd and Ca, contains cobalt with oxidation state +3 as well as +2. Because of this the electro- neutrality of the $NdCaCoO_{3.96}$ molecule neutralize by the creation of vacancies in the oxygen sublattice.

In $La_{1.25}Sr_{0.75}CoO_{4.03}$ and $Nd_{1.25}Ca_{0.75}CoO_{4.04}$ there is a significant amount of cobalt cations in oxidation state +2 and over-stiochiometrical amount of oxygen.

It is well known that the presence in complex oxides of anion vacancies can increase the mobility of oxygen sublattice and promote active oxygen migration to adsorbed methane on the active sites. The lattice oxygen can make a contribution in oxidation of methane to CO and $H_2$. On the other hand, high concentration of defects in anion sublattice can increase the amount of adsorbed oxygen species, which are generally responsible for total oxidation of methane to $CO_2$ and $H_2O$ [110-114].

Perhaps high concentration of anion defects in the $NdCaCoO_{3.96}$ catalyst favored proceeding of total oxidation of methane at relatively low temperatures compare to other catalysts. Apart from $NdCaCoO_{3.96}$, on the catalysts with overstoichiometrical oxygen the temperature of methane oxidation to $CO_2$ and $H_2O$ was higher than 890°C.

Data of both bulk and surface chemical composition, obtained from EDAX and XPS, are presented in Fig. 18. When it comes to EDAX experiments it is observed that bulk composition is close to stoichiometrical for all synthesized catalysts, while chemical composition of catalysts surface is strongly enriched by alkaline-earth elements – calcium and strontium.

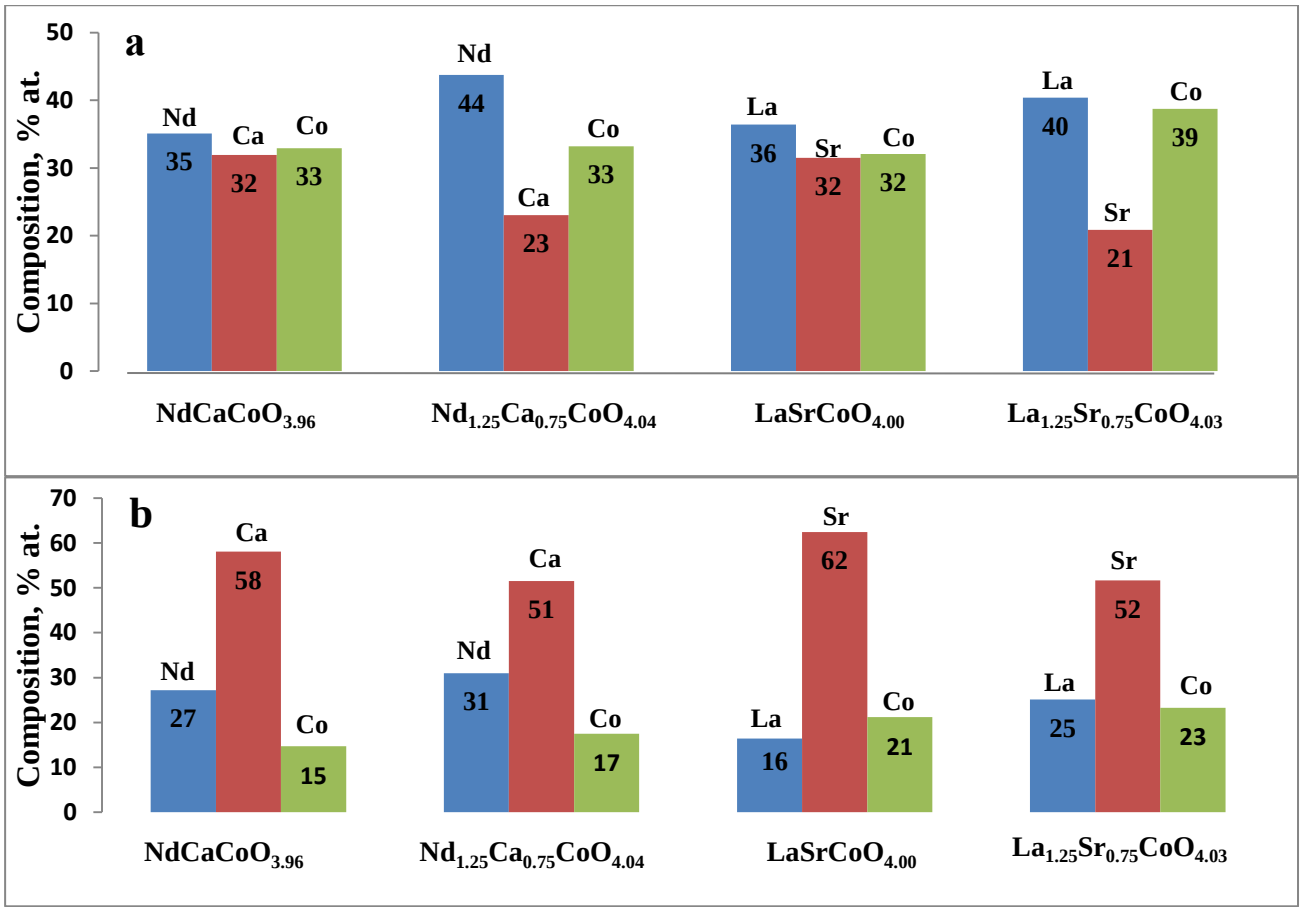


Figure 18 – Chemical composition of synthesized catalytic materials based on EDAX - a; XPS – b

The same phenomena was observed in [119,120] for Sr-substituted lanthanum ferrites and it was explained by the tendency of alkaline-earth elements to form carbonates. Alkaline-earth cations migrate from the bulk of the catalyst to its surface followed by interaction with adsorbed $CO_2$ species.

The XPS spectra of La-containing samples in the La $3d_{5/2}$ zone consist of two peaks (Fig. 19). Positions of their centers correspond to the binding energies of 833.8 eV and 836.4 eV. Analysis of literature data showed that the first value corresponds quite well to La (III). The appearance of La $3d_{5/2}$ peaks with higher binding energies could be attributed to the formation of hydroxo-groups at the surface of the particles [119].

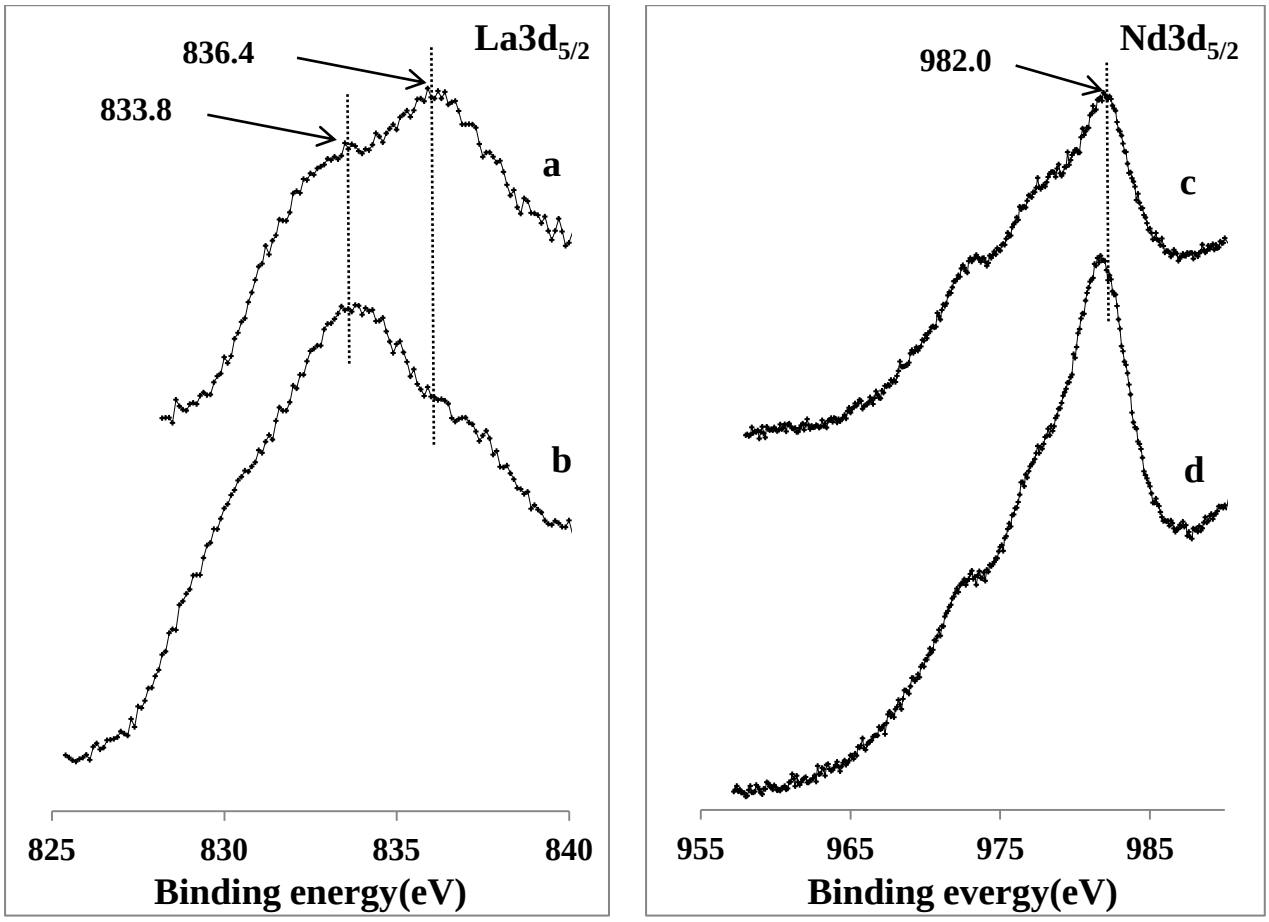


Figure 19 – XPS spectra of $La3d_{5/2}$ and $Nd3d_{5/2}$ region of catalysts : a – $LaSrCoO_{4.00}$, b – $La_{1.25}Sr_{0.75}CoO_{4.03}$, c – $NdCaCoO_{3.96}$, d – $Nd_{1.25}Ca_{0.75}CoO_{4.04}$

Authors [107], studied the $LnCoO_3$ perovskite family (Ln – La, Pr, Nd, Sm, Gd) in partial oxidation of methane to syngas have was found by XPS the presence of hydroxo-groups on the surface of the oxide support which was formed after reduction of $LaCoO_3$ perovskite. They pointed out that the presence of these OH-groups could promote Co metal particles reoxidation to initial perovskite structure. The catalyst formed from $LaCoO_3$ precursor showed lowest activity in POM to synthesis gas and was active in total methane oxidation to carbon dioxide and water [107]. It was also in agreement with the study of $Rh/Al_2O_3$ in POM [107]. It was supposed that OH-groups adsorbed on the $Al_2O_3$ surface could participate in the methane oxidation process. Several authors also pointed out that hydroxo-groups formed during methane dissociation process could be a key intermediate in the oxidation of methane to $H_2O$ [36, 47].

XPS spectra of both Nd-containing samples are fully identical with a center of a single peak at 982 eV (Fig. 19) that is common for Nd (III) oxidation state [111]. No peak corresponded to HO-grounds was observed for both $Nd_{2-x}Ca_xCoO_{4\pm\delta}$ samples.

XPS spectra of Co2p region (Fig. 20) indicated the presence of both cobalt 2+ and 3+ cations in synthesized samples apart from $LaSrCoO_{4.00}$.

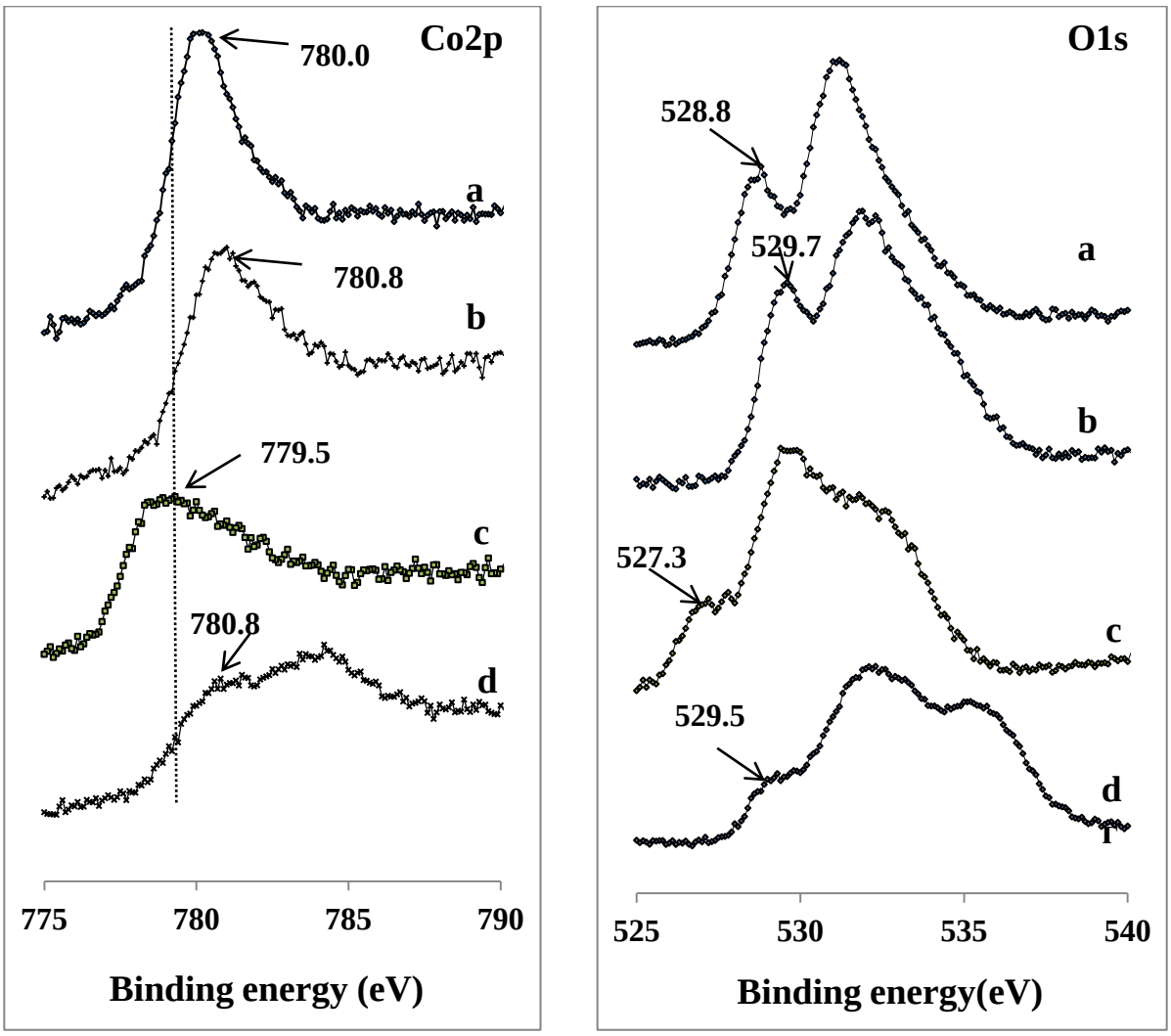


Figure 20 – XPS spectra of $Co2p_{3/2}$ and O1s regions of synthesized catalysts: a – $NdCaCoO_{3.96}$, b – $Nd_{1.25}Ca_{0.75}CoO_{4.04}$, c – $LaSrCoO_{4.00}$, d – $La_{1.25}Sr_{0.75}CoO_{4.03}$

The XPS spectra in Co 2p area are slightly different for Nd- and La- containing samples. However, the position of main peaks for $LaSrCoO_{4.00}$ and $NdCaCoO_{3.96}$ (799.5 – 780.0) can be attributed to Co(III) [121]. Meanwhile, progressive substitution of Nd and La with alkaline earth elements causes a systematic shift of Co spectrum to the

higher values of binding energy, more pronounced in the case of $La_{1.25}Sr_{0.75}CoO_{4.03}$. It is shown [121] that the binding energy of Co in $Co_3O_4$ is 779.6 eV while the corresponding value for CoO is 780.5 eV. Hence, the observed shift of Co spectra of $Nd_{1.25}Ca_{0.75}CoO_{4.04}$ and $La_{1.25}Sr_{0.75}CoO_{4.03}$ to the higher values of binding energy correlates quite well with the appearance of Co(II) in their lattice confirmed by the iodometric titration (Table 6). Similar behavior was observed also in [122] for $Ca_{1-x}Nd_{1+x}CoO_4$ solid solutions when the increase of Ca amount in the lattice was accompanied by the systematic increase of Co(II) content.

Binding energies of O1s region in studied catalytic materials (Fig. 20) change depending on catalyst composition. In the same time [122] binding energy of O1s region in $Ca_{1-x}Nd_{1+x}CoO_4$ cobaltates was 532.0 eV and did not depend on Nd/Ca ratio. It can be seen from the spectra on Fig. 20 that several maxima corresponded to different lattice and adsorbed oxygen species on the catalysts. Thus, binding energy between 527.3-529.7 eV most likely due to lattice oxygen, while higher values of binding energies could be assign to different adsorbed species on the surface [111, 113,119].

Study of the most active $NdCaCoO_{3.96}$ by XRD after experiments in partial oxidation of methane indicated the modification of initial layered perovskite-type (Fig. 21).

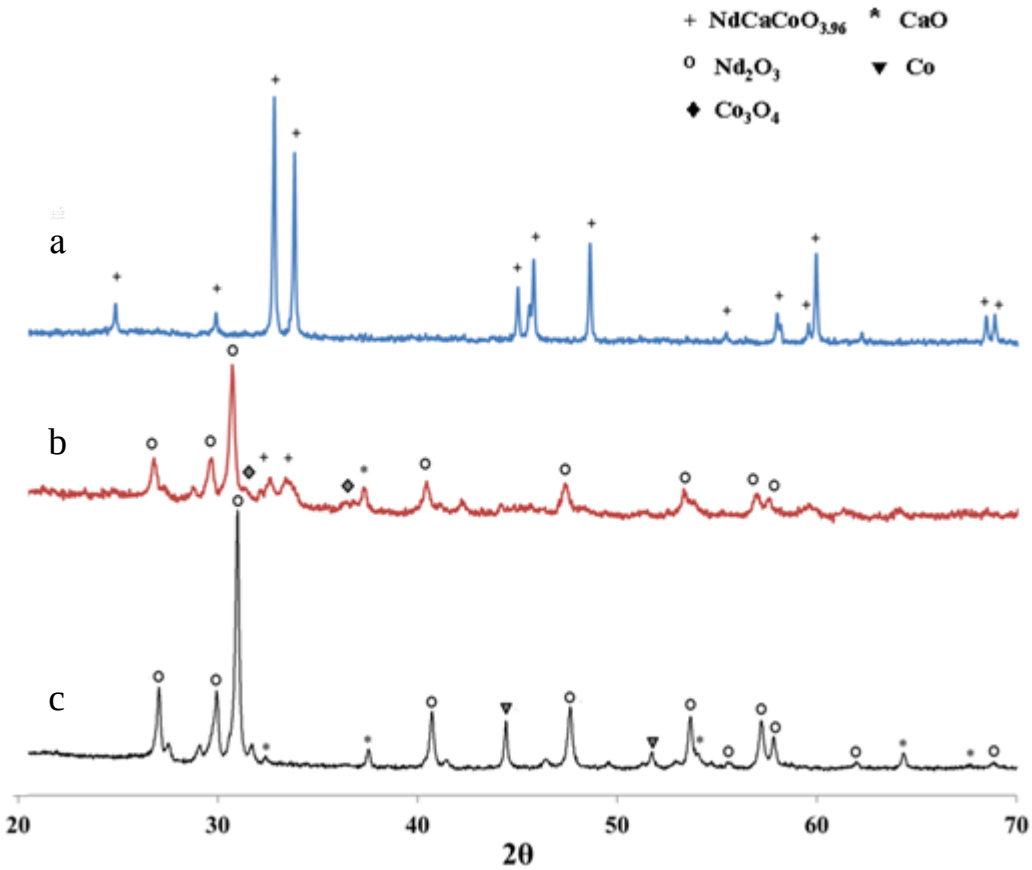


Figure 21 – X-ray diffraction patterns of $NdCaCoO_{3.96}$ :a – before POM; b – after 12 h processing in the POM environmental; c – after140 h processing in the POM environmental.

According to XRD data the fresh-prepared catalyst had single-phase layered peovskite-type structure. No patterns corresponded to initial oxides or other impurities was observed. However, 12 h of processing in POM stream led to the reduction of initial structure and formation of phases assigned to the mixture of $Nd_2O_3$, CaO and $Co_3O_4$. Further contact of the catalyst with reaction environmental $CH_4/O_2$ resulted in complete destruction of initial latered perovskite-type structure and formation of metallic cobalt particles. It should be noted that the catalyst remained its stable activity and selectivity toward CO and $H_2$ close to 100%. Also regeneration of $NdCaCoO_{3.96}$ after 12 h processing in POM environmental allowed complete reconstruction of the initial structure. Regeneration experiment was done at 1000ºC for 6h in air. Obtained information as well as literature data analysis indicated that synthesized $NdCaCoO_{3.96}$ is a precursor, which forms in reaction environmental conditions active metallic cobalt particles, dispersed on the surface of $Nd_2O_3$-CaO oxide matrix. It is known that

materials with perovskite-type structure can create in reductive environment highly dispersed metallic particles and can provide not only high activity but also resistance to sintering and to coke formation processes.

According to SEM analysis, the transformation of initial layered perovskite-type oxide structure and of $NdCaCoO_{3.96}$ was also confirmed (Fig. 22). Reductive decomposition of the complex oxide results in the delamination of the initial micronsize grains to finer particles that primarily contain according to XRD data $Nd_2O_3$, CaO and Co.

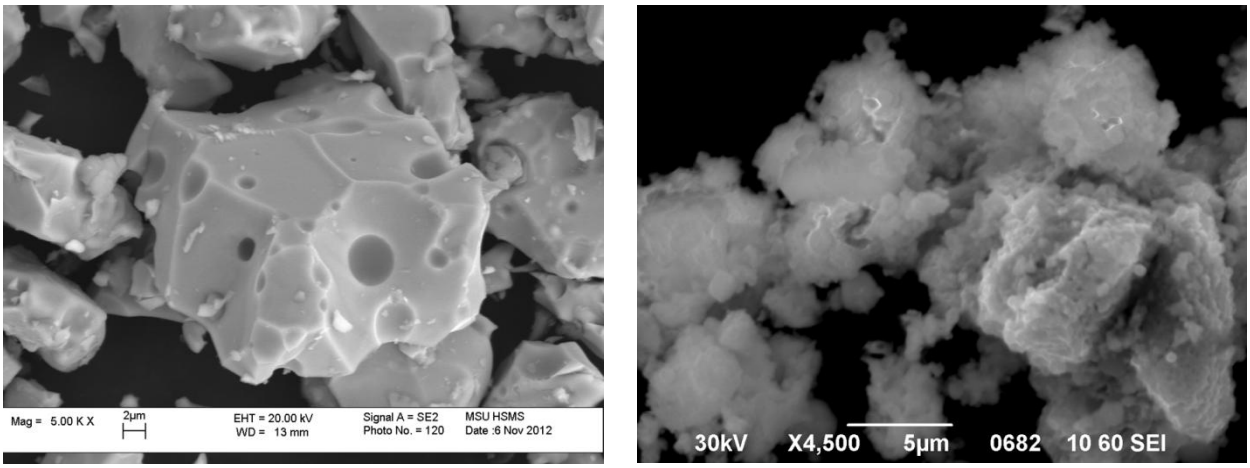


a b

Figure 22 – SEM images of $NdCaCoO_{3.96}$: a - before partial oxidation of methane; b – after 12 h processing

The main features of the TG-MS analysis curves of the 140 h processed catalyst in air (Fig. 23) correlate well with the XRD analysis data. The mass intake at 350–400°C caused by the oxidation of cobalt metal to oxides occurs prior to the two step mass loss at 400–700°C. This temperature range corresponds to the oxidation temperatures of amorphous carbon in air while the mass decrease of the sample corresponds to the amount of carbon deposited on the catalyst. The observed two step mass loss, which is due to the oxidation of amorphous carbon, was confirmed by MS analysis of the evolved gases. The main gaseous product of the reaction that appeared during this process was $CO_2$ with little or no $H_2O$ evolution (MS analysis of CO is complicated by the significant coincidence of the $CO_2$ and CO mass spectra). Burning of

carbon at 430–500°C caused a reduction in the oxygen amount in the air flowing through the TG cell.

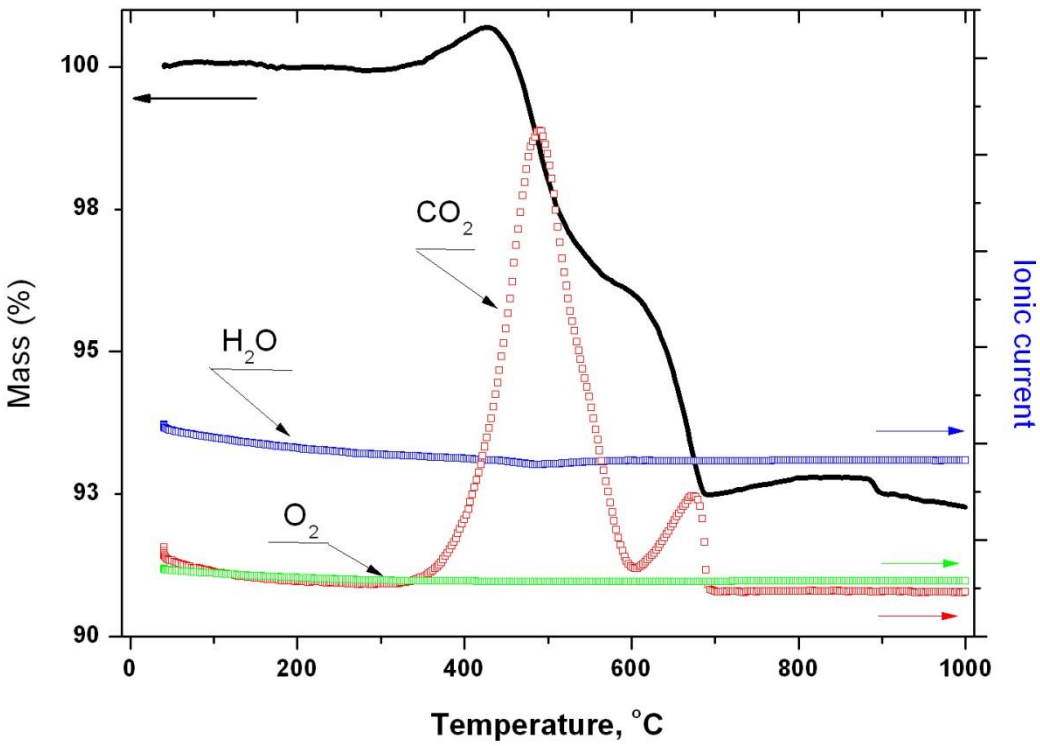


Figure 23 – TGA-MS curves of $NdCaCoO_{3.96}$ after140 h in POM environmental

Carbon deposition during the POM reaction typically results in fast deactivation of the catalysts [12,36]. However, a stability of the corresponding values as a function of time indicates that in the current case the carbon deposition has no effect on the activity and selectivity of the $NdCaCoO_{3.96}$-derived catalyst for at least 140 h. A similar absence in the influence of heavy carbon deposition on the activity and selectivity of the Ni-based POM catalyst has been previously observed [123].

It can be seen form TGA-MS curves that removing of coke deposited on the catalyst completes at 700°C while partial oxidation of methane with selective formation of CO and $H_2$ predominantly proceeded at temperature above 850°C. Perhaps the coke formation process occurs at the cooling down step in $CH_4/O_2$ flow and should not significantly affect the catalytic properties of the composite.

Comparison of the XRD data of $NdCaCoO_{3.96}$ and $LaSrCoO_{4.00}$ after 12 h of time on stream are shown in Fig. 24. Opposite to active and selective in POM Nd-Ca cobaltate its counterpart - $LaSrCoO_{4.00}$ after catalytic test resulted in formation of $La(OH)_3$ and $SrCO_3$.

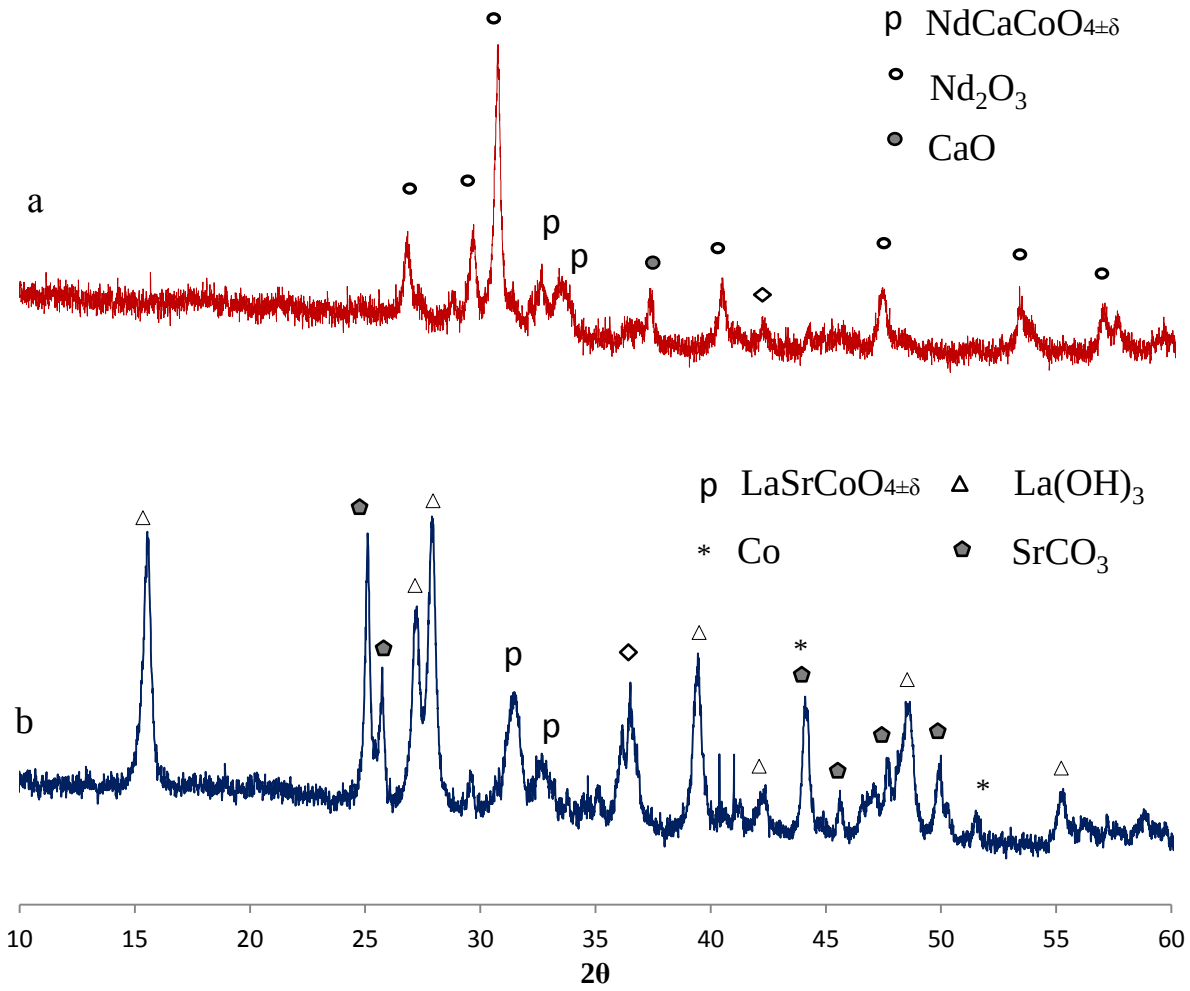


Figure 24 – X-ray diffraction patterns of the catalysts after 12 h processing in POM environmental : a - $NdCaCoO_{3.96}$; b – $LaSrCoO_{4.03}$

The presence of lanthanum hydroxide in the $LaSrCoO_{4.00}$ spent catalyst is in agreement with the XPS data which showed the presence of OH-groups adsorbed on the catalyst surface and which could be intermediates in the formation of $H_2O$ [36, 47]. It should also be noted that the catalyst $LaSrCoO_{4.00}$ was not selective in formation of synthesis gas. Moreover a significant amount of $H_2O$ and $CO_2$ was observed in the outlet gases. Formed during the reaction water can react with the oxides, followed by formation of the lanthanum $La(OH)_3$. In [104], $LaNiO_3$ and $LaNi_{0.55}Co_{0.45}O_3$ perovskite

oxides formed $La(OH)_3$ and $La_2O_2CO_3$ phases during POM. It has been suggested that the formation of such phases can block the access of reactants - $CH_4$ and $O_2$ to the metal sites of the catalyst, active in the POM.

Results of the study of reducibility of synthesized catalytic materials by $H_2$ temperature programmed reduction ($H_2$-TPR) are presented in Fig.25

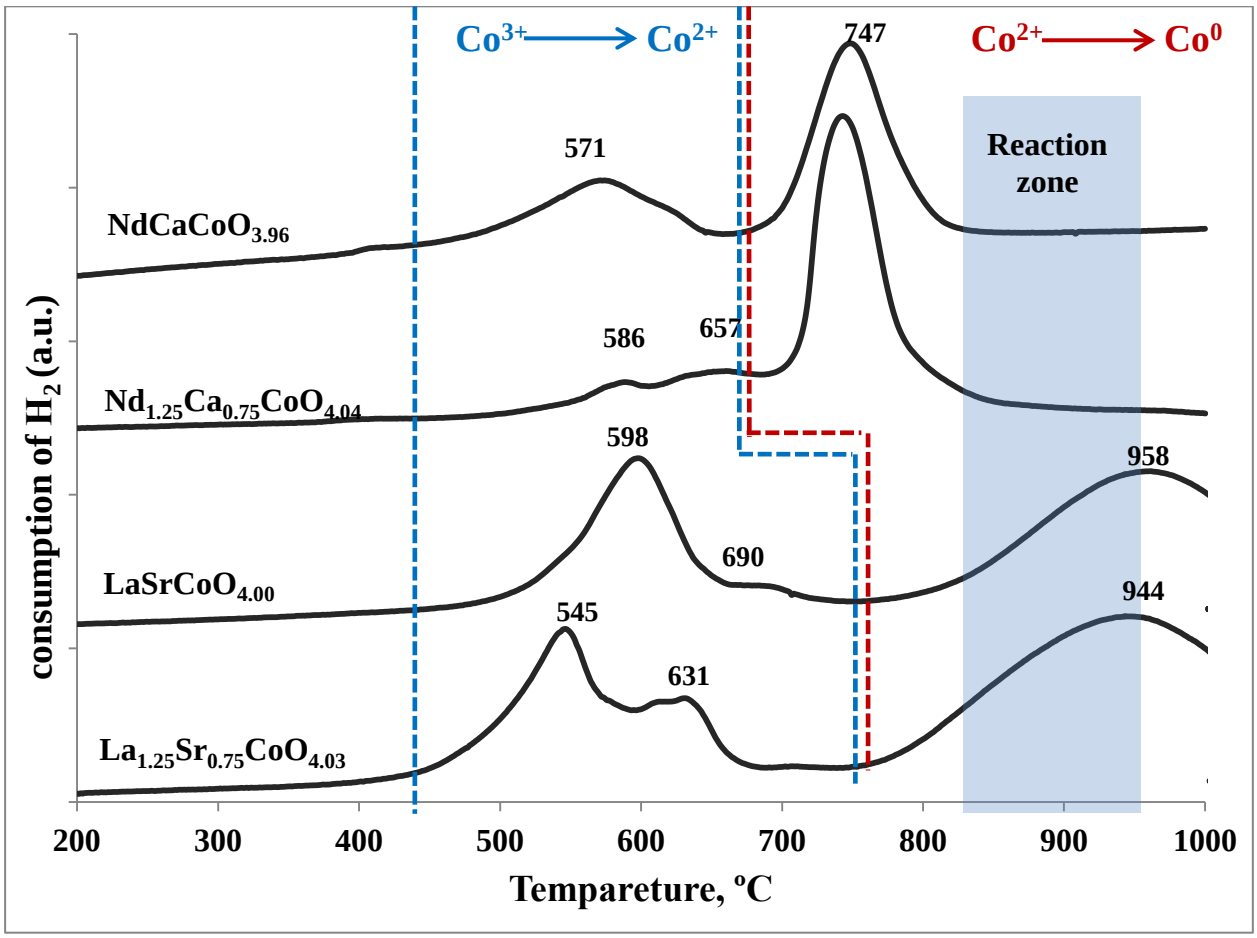


Figure 25 – $H_2$-temperature programmed reduction curves of synthesized catalysts.

It can be seen in Fig. 25 that there were two main consumption peaks of hydrogen for all 4 series of $La_{2-x}Sr_xCoO_4$ and $Nd_{2-x}Ca_xCoO_4$ catalysts. According to the literature [97, 99, 102-104] the low-temperature peak at 550-650°C can be attributed to the reduction of $Co^{3+}$ ions to $Co^{2+}$. Reduction peak at higher temperatures generally corresponds to the reduction of $Co^{3+}$ and $Co^{2+}$ to $Co^0$. The formation of metallic cobalt phase after the $H_2$-TPR of $NdCaCoO_{3.96}$ catalyst proved by XRD (Fig. 26). It is known that complex oxides with perovskite structure can form in a reducing atmosphere fine particles of transition metal elements. Despite the fact that the reducing potential of

methane is lower than that for hydrogen, it has been confirmed by XRD and SEM the transformation of initial structure of $NdCaCoO_{3.96}$ to oxides and metallic cobalt.

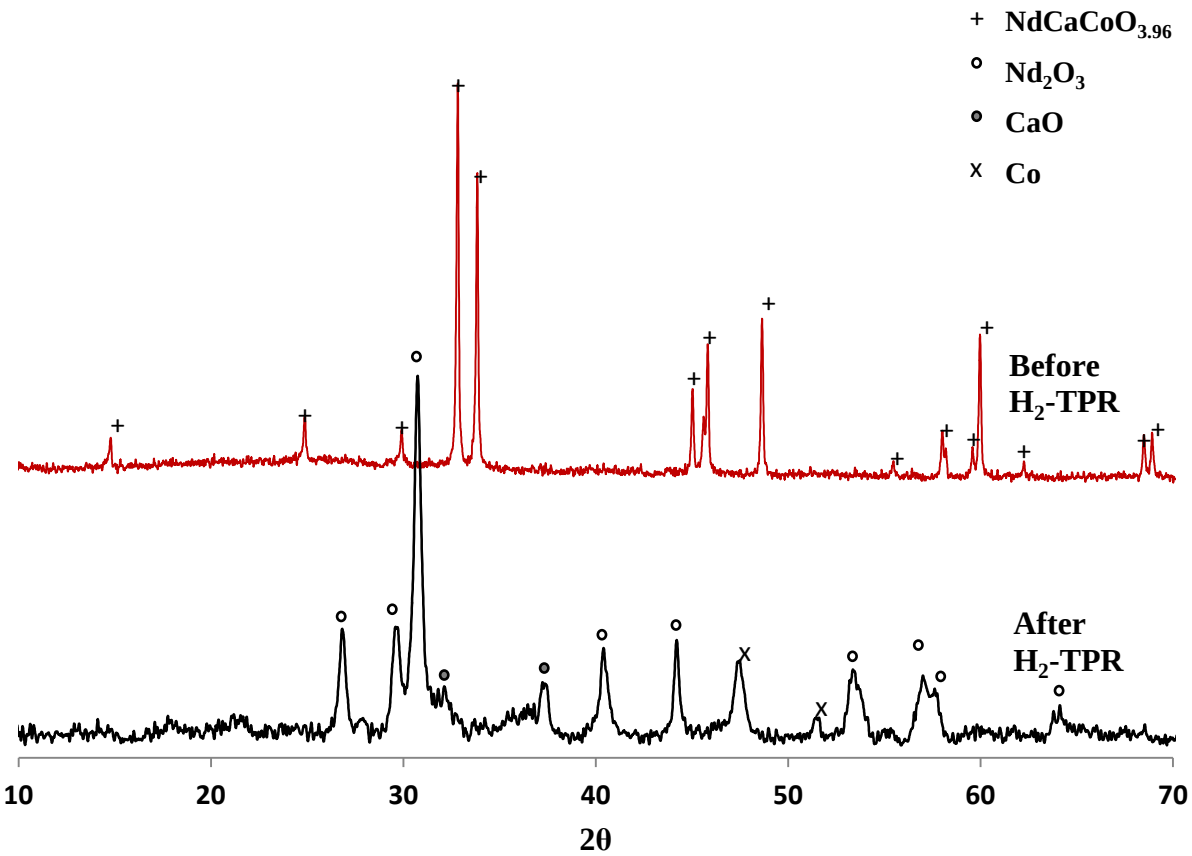


Figure 26 – X-ray diffraction patterns of $NdCaCoO_{3.96}$ before and after $H_2$-TPR

In contrast to $Nd_{2-x}Ca_xCoO_4$ series, for lanthanum cobaltates the second peak of hydrogen consumption, which could be associated with formation of $Co^0$ phase, shifted toward higher temperatures with maximum at 950°C. These temperatures even higher than those in POM. Therefore, the formation of active metallic cobalt particles from these precursors is rather complicated. The initial temperature of the second $H_2$ consumption peak is about 800ºC while the reduction of neodymium cobaltates is already completed at this temperature. It can clarify lower activity and selectivity of $La_{2-x}Sr_xCoO_4$ in comparison with $Nd_{2-x}Ca_xCoO_4$.

For both $Nd_{2-x}Ca_xCoO_4$ series of catalysts $Co^0$ phase formation zone is in the area of comparable temperatures. However, as shown earlier, the $NdCaCoO_{3.96}$ showed highest selectivity in the oxidation of methane to synthesis gas which is closed to 100%, while over $Nd_{1.25}Ca_{0.75}CoO_{4.04}$ the selectivity of synthesis gas formation and $CH_4$

conversion did not exceed 78% and 60%, respectively. A lower concentration of $Nd^{3+}$ in $NdCaCoO_{3.96}$ leads to an increase in the intensity of the low-temperature peak of $H_2$-TPR and lower reduction temperature (Fig. 25), which may be due to the presence of oxygen vacancies as well as with a high content of ions $Co^{3+}$. The presence of oxygen vacancies increases the mobility of the anion sublattice and facilitates the transport of oxygen to the surface, where reduction occurs, leading to the formation of the metal phase [99, 97]. On the other hand, differences in the intensity of the hydrogen consumption peaks for $Nd_{2-x}Ca_xCoO_4$ catalysts may indicate a different mechanism of $Co^0$ formation in these systems. Despite the fact that the low temperature peak of hydrogen consumption is usually associated with a reduction of $Co^{2+}$ to $Co^{3+}$, some studies pointed out that the formation of metallic cobalt is possible even at low temperatures [97]. Perhaps this is what happens during reduction of $NdCaCoO_{3.96}$. Formation $Co^0$ during reduction of $Nd_{1.25}Ca_{0.75}CoO_{4.04}$ is more difficult and takes place at higher temperatures. Formed at a higher temperature active catalyst particles can be sintered.

Thus, based on the $H_2$-TPR results it can be suggested that the catalytic activity of the synthesized cobaltates depends on their ability to be reduced and the temperature at which the active phase of transition element is formed. Hence, it was reasonable to study the catalytic properties of $La_{2-x}Sr_xCoO_4$ and $Nd_{2-x}Ca_xCoO_4$ pre-reduced in a stream of hydrogen, in other words with already formed $Co^0$ phase. For that the catalyst sample with 0.1 g of mass was heated under $H_2$ flow up to a temperature required for forming the metallic cobalt phase. Reduction temperatures of catalysts were selected based on $H_2$-TPR experiment results. After reaching the desired temperature, the gas flow was switched from hydrogen to mixture of $CH_4/O_2$ (2/1). The results are shown in Figures 27, 28.

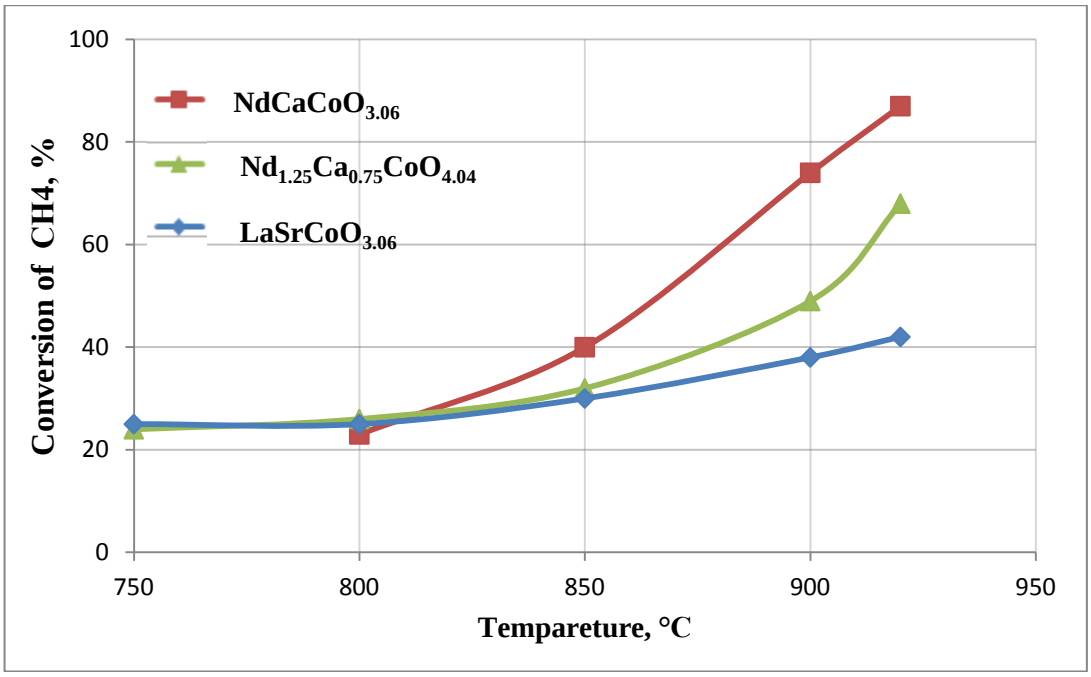


Figure 27 – $CH_4$ conversion as a function of temperature over catalysts pre-reduced in $H_2$ flow ($CH_4/O_2$ = 2; W = 22 L*g$^{-1}$*h$^{-1}$)

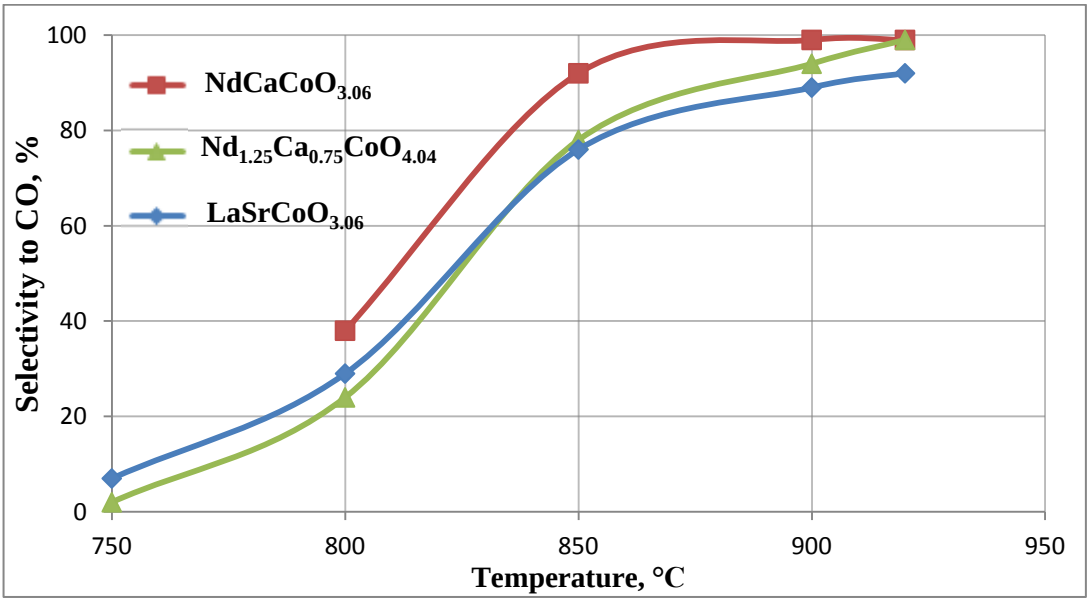


Figure 28 – CO formation selectivity as a function of temperature over catalysts pre-reduced in $H_2$ flow ($CH_4/O_2$ = 2; W = 22 L*g$^{-1}$*h$^{-1}$).

It can be seen that the formation of synthesis gas begins at 800°C (Compare to Fig. 8,9 and 10). The most active catalyst was also $NdCaCoO_{3.96}$ - methane conversion at the catalyst reaches 87%. Activity of preliminary reduced cobaltates is still decreases in a order: $NdCaCoO_{3.96}$ > $Nd_{1.25}Ca_{0.75}CoO_{4.04}$ > $LaSrCoO_{4.00}$. This trend corresponds

quite well to the results of POM obtained over catalysts without pre-reduction step. At the same time pre-reduction allowed to significantly increase the selectivity. Selectivity toward CO is already reaches 80-95% at 850°C whereas over unreduced catalysts at these temperature mostly products of total oxidation of methane and oxidation coupling of methane were detected in outlet gases. Less active $Nd_{1.25}Ca_{0.75}CoO_{4.04}$ and $LaSrCoO_{4.00}$ catalysts without preliminary reduction shows the maximum selectivity of 80 and 70% and being pre-reduced increase it to 99 and 92%, respectively.

The obtained results are also in agreement with the data in [107], where $LnCoO_3$ series of catalysts were tested in the partial oxidation of methane to synthesis gas. Activity of catalysts explored in this paper increased in inverse proportion to the ionic radii of the rare-earth cations: La> Nd> Sm> Gd. The authors noted that the deactivation of the catalysts formed from perovskite oxides precursor often occurs not only due to sintering or coke formation, but also result in reoxidation of the active phase of the transition element into the original perovskite structure. The most active and selective $GdCoO_3$ showed 73% of $CH_4$ conversion, CO selectivity and $H_2$ were 79% and 81%, respectively. XRD data after the catalytic tests revealed the formation of $Co^0$ and $Gd_2O_3$, indicating the absence of metallic phase re-oxidation into perovskite. $NdCoO_3$ was less active and selective and after the POM partially re-oxidation of $Co^0$ phase was observed. On $LaCoO_3$ formed only trace amounts of CO and $H_2$, while XPS and XRD data indicated of complete re-oxidation of components into initial perovskite structure.

XRD data of $NdCaCoO_{3.96}$, $Nd_{1.25}Ca_{0.75}CoO_{4.04}$ and $LaSrCoO_{4.00}$ cobaltates after reduction in $H_2$ flow followed by partial oxidation of methane are shown in Fig. 29.

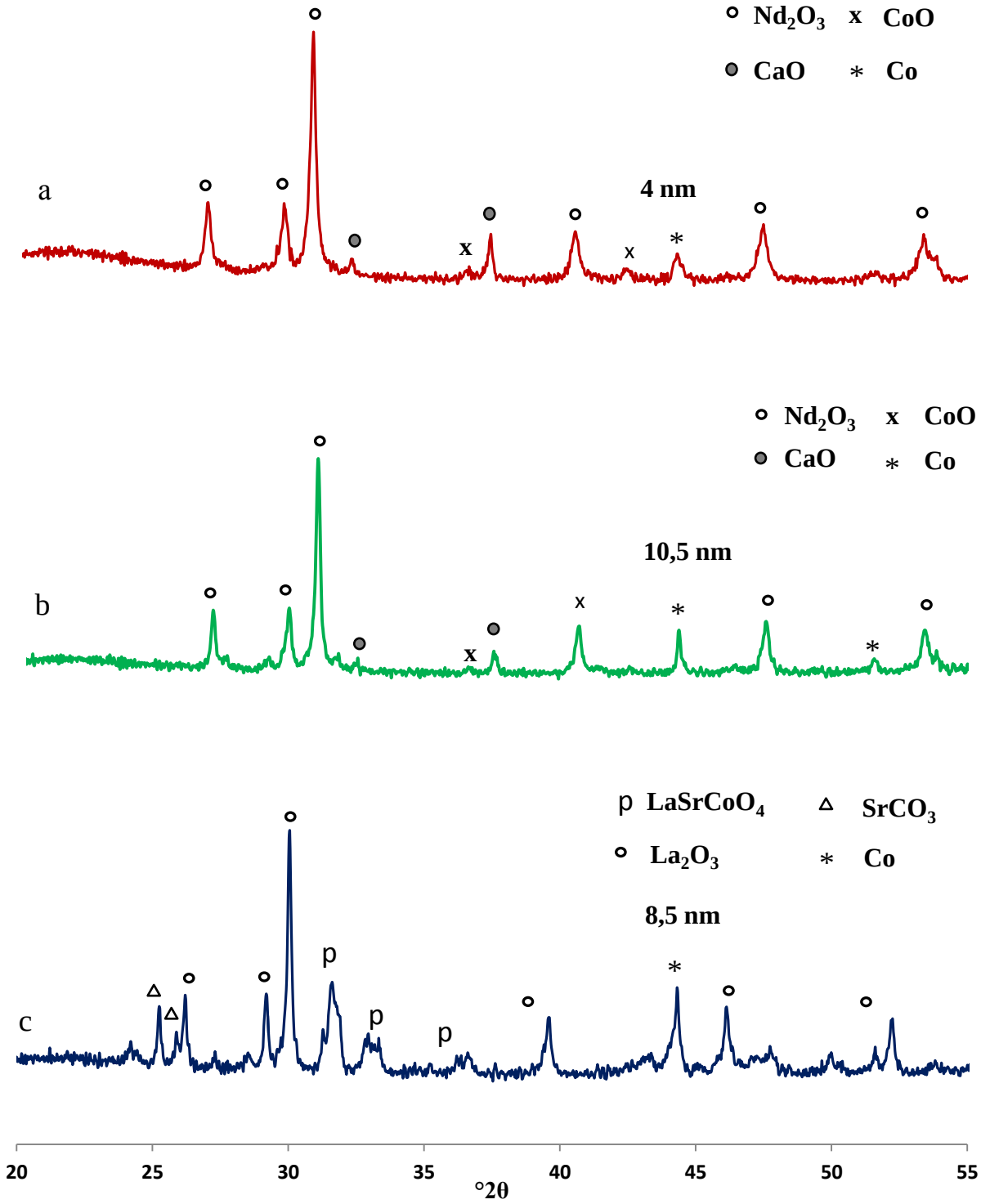
Nd2O3 x CoO
CaO * Co
a
4 nm
Nd2O3 x CoO
CaO * Co
b
10,5 nm
p LaSrCoO4 △ SrCO3
La2O3 * Co
8,5 nm
c
20
25
30
35
40
45
50
55
°2θ

Figure 29 – X-ray diffraction patterns of catalysts after reduction in $H_2$ flow followed by partial oxidation of methane: a - $NdCaCoO_{3.96}$; b - $Nd_{1.25}Ca_{0.75}CoO_{4.04}$;
c – $LaSrCoO_{4.00}$

It can be seen from Fig. 29 that $NdCaCoO_{3.96}$ and $Nd_{1.25}Ca_{0.75}CoO_{4.04}$ catalysts after the pre-reduction treatment and subsequent POM exist in the form of $Co^0$-CoO-$Nd_2O_3$-CaO composite. At the same time in case of $LaSrCoO_{4.00}$ it was also detected $Co^0$-$La_2O_3$-SrO as well as the original layered perovskite-like structure.

In contrast to $LaCoO_3$ in [107], in case of $LaSrCoO_{4.00}$ the only partial re-oxidation of $Co^0$-$La_2O_3$-SrO took place, while $Co^0$-CoO-$Nd_2O_3$-CaO composite was not subjected to re-oxidation. Increased resistance to re-oxidation of composite formed from $NdCaCoO_{3.96}$, $Nd_{1.25}Ca_{0.75}CoO_{4.04}$ and $LaSrCoO_{4.00}$ precursors might be due to the presence of the alkaline-earth elements in the structure. It previously pointed out that the introduction of calcium in $Co/Al_2O_3$ system led to an increase of Co particles dispersion on the $Al_2O_3$ and resistance to the formation of inactive spinel $CoAl_2O_4$ phase [94].

One of the main criteria for determining the possibility of formation of complex oxides with a perovskite structure, as well as their stability is the tolerance factor t (Goldschmidt criterion) $t = \frac{r_A + r_X}{\sqrt{2}(r_B + r_X)} = 1$, where $r_A$, $r_B$ and $r_X$ - radii of the ions [107]. For the most stable ideal cubic perovskite structure $ABO_3$ t = 1. In fact, the system with a perovskite structure may be formed at t <1, however, with to A-O and B-O bonds become effective tensile and compressive stresses, and there is a decrease of symmetry, for example to tetragonal .

Calculation of tolerance factor for synthesized catalysts showed that for $NdCaCoO_{3.96}$ and $Nd_{1.25}Ca_{0.75}CoO_{4.04}$ t = 0.93, whereas for $LaSrCoO_{4.00}$ t = 0.97, indicating the greater stability of lanthanum-strontium cobaltate. The calculations are in agreement with the $H_2$-TPR and XRD data that displayed a greater stability of $La_{2-x}Sr_xCoO_4$ in a reducing atmosphere.

Based on XRD analysis (Fig. 29) crystallite size of $Co^0$ for preliminary reduced and tested catalysts were also calculated. It has previously been proposed different mechanism of forming $Co^0$ from neodymium calcium cobaltates associated with the

supposition that the formation of $Co^0$ from $Nd_{1.25}Ca_{0.75}CoO_{4.04}$ occurs at higher temperatures. The calculation showed that the crystallite size of Co formed from $Nd_{1.25}Ca_{0.75}CoO_{4.04}$ was about 10.5 nm, whereas in case of $NdCaCoO_{3.96}$ precursor cobalt particles crystallite size was significantly smaller - 4 nm. Despite the fact that the tolerance factor for both materials $NdCaCoO_{3.96}$ and $Nd_{1.25}Ca_{0.75}CoO_{4.04}$ was 0.93, and the last one was also resistant to re-oxidation, the difference in catalytic activity may be related to the difference in size of the crystallites of $Co^0$ due to sintering process.

Examination of $NdCaCoO_{3.96}$, $Nd_{1.25}Ca_{0.75}CoO_{4.04}$ and $LaSrCoO_{4.00}$ by TEM showed (Fig. 30-32) that during catalysis over the most active $NdCaCoO_{3.96}$ catalyst nanosized clusters presumably of $Nd_2O_3$, CaO, and Co were found, while these clusters were not found in case of $Nd_{1.25}Ca_{0.75}CoO_{4.04}$ and $LaSrCoO_{4.00}$.

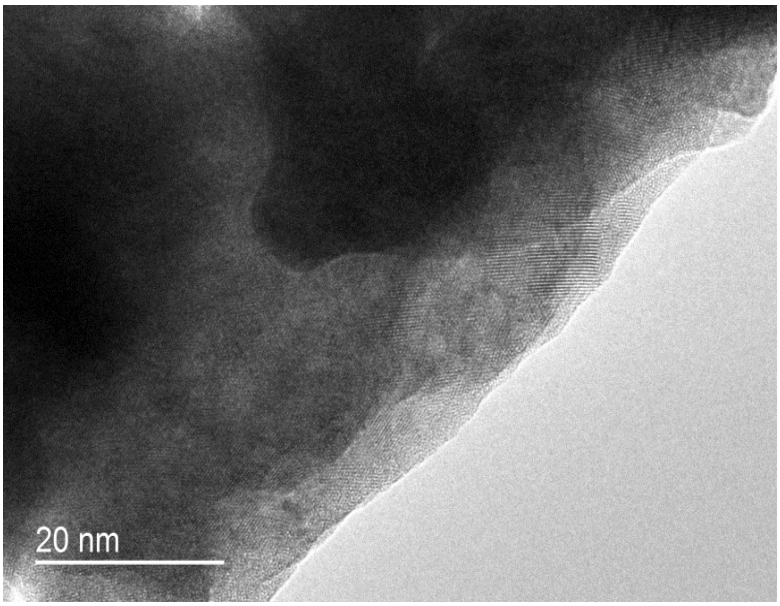


Figure 30 – TEM image of $LaSrCoO_{4.00}$ after treatment in $H_2$ flow followed by methane partial oxidation

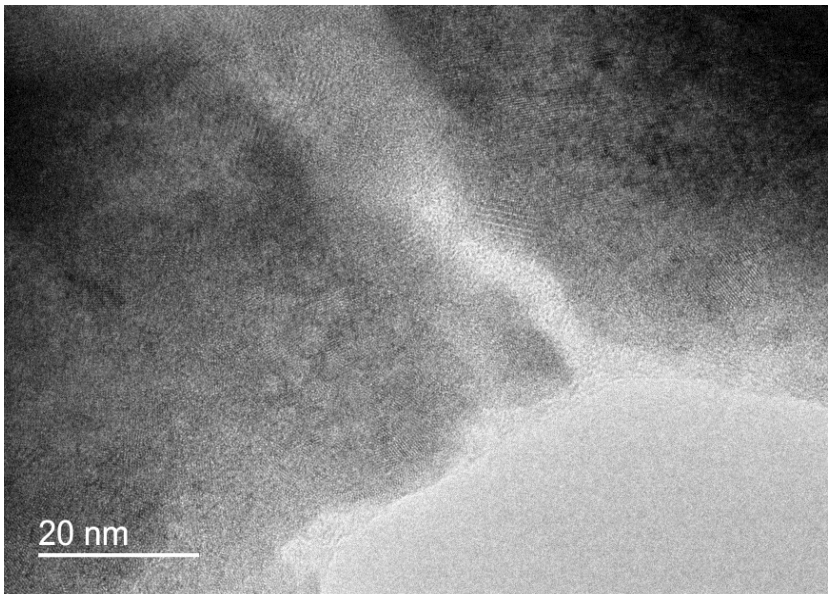


Figure 31 – TEM image of $Nd_{1.25}Ca_{0.75}CoO_{4.04}$ after treatment in $H_2$ flow followed by methane partial oxidation

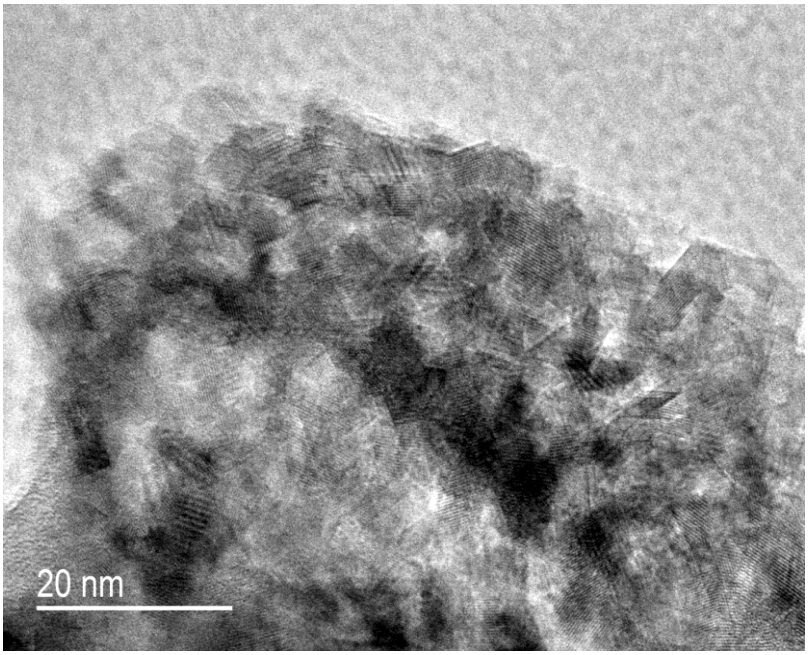


Figure 32 – TEM image of $NdCaCoO_{3.96}$ after treatment in $H_2$ flow followed by methane partial oxidation

## 3.3 Evaluation of catalytic activity of $NdCaCoO_{3.96}$ in dry reforming of methane

As it was noted in Chapter 1, DRM is a perspective way of synthesis gas production from methane which allows to involve in chemical processing such a global waste as $CO_2$. The main problem of DRM is a relatively fast deactivation of catalytic materials mostly due to coke formation and sintering processes.

It was seen form literature review POM can proceed through two different pathways – direct oxidation to final product and indirect through combustion-reforming reactions which involves total oxidation of methane followed by dry and steam reforming processes:

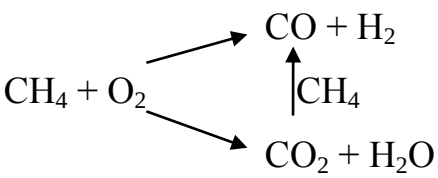


Based on the results presented in chapter 3.1 It can be proposed that over $NdCaCoO_{3.96}$ partial oxidation of methane generally realized through indirect pathway. From this point it is reasonable to propose that $NdCaCoO_{3.96}$ could also be active and selective in dry reforming of methane.

For this purpose catalytic tests in dry reforming of methane over $NdCaCoO_{3.96}$ were carried out. Methods of catalytic experiments described in chapter 2. The results of the experiments DRM (Tab. 7) confirm the assumption of a indirect reaction mechanism POM oxygen on $NdCaCoO_{3.96}$: treatment of methane–carbon dioxide mixtures of different composition in the rector gives synthesis gas with the $CO/H_2$ ratio of ~1. The yields of CO and $H_2$ are as high as 93%. In runs 1–10 (Table 7), the molar ratio $CH_4/CO_2 = 1$ corresponded to the stoichiometry of the DRM reaction:

$$CH_4 + CO_2 = 2CO + 2H_2$$

Table 7 – Results of DRM over $NdCaCoO_{3.96}$

| № | W, $L \cdot g^{-1} \cdot h^{-1}$ | t, °C | Conversion, % | | Yield,% | |
|---|---|---|---|---|---|---|
| | | | $CH_4$ | $CO_2$ | $H_2$ | CO |
| $CH_4/CO_2 = 1$ | | | | | | |
| 1 | 19 | 804 | 1 | 1 | 0 | 1 |
| 2 | 19 | 866 | 54 | 56 | 38 | 55 |
| 3 | 19 | 886 | 75 | 88 | 83 | 81 |
| 4 | 19 | 899 | 90 | 76 | 81 | 83 |
| 5 | 19 | 917 | 93 | 77 | 82 | 85 |
| 6 | 19 | 919 | 87 | 82 | 75 | 85 |
| 7 | 19 | 935 | 90 | 83 | 80 | 87 |
| 8 | 19 | 940 | 96 | 73 | 85 | 84 |
| 9 | 19 | 940 | 94 | 75 | 83 | 84 |
| 10 | 19 | 960 | 96 | 72 | 91 | 84 |
| $CH_4/CO_2 = 1,5$ | | | | | | |
| 11 | 15 | 902 | 83 | 97 | 70 | 89 |
| 12 | 15 | 935 | 82 | 98 | 75 | 88 |
| 13 | 15 | 958 | 83 | 98 | 78 | 89 |
| $CH_4/CO_2 = 1,1$ | | | | | | |
| 14 | 14 | 947 | 91 | 96 | 93 | 93 |

No DRM reaction was observed at 804°C, while at 866°C the methane conversion was 54% and the $CO_2$ conversion, 56%. With increasing temperature from 866 to 960°C, the methane conversion increased to 96%, while the $CO_2$ conversion values were scattered within 72–88%. The results are evidently related to specific features of the DRM reaction mechanism [17-19]:

$CO_2 + (cat) \leftrightarrows CO + O(cat)$

$CH_4$ + (cat) ⇆$CH_x$(cat) + (4-x)H(cat) → C(cat) + $2H_2$

C(cat) + O(cat) → CO(cat) + (cat)

CO(cat) ⇆CO + (cat)

In the course of DRM, the products of dissociative reaction of methane and $CO_2$ with the catalyst seem to accumulate at different rates, which has an effect on both the reagent consumption rate and the reaction product accumulation rates. The results of experiments 1 – 10 (Table 7) demonstrate that, with increasing temperature, the rate of the dissociative reaction of methane with the catalyst noticeably increases, while the dissociation of $CO_2$ and formation of CO from carbon and oxygen bound to the catalyst are hindered

To enhance the conversion of $CO_2$, a methane excess was maintained in the feedstock flow and the feed rate of the gas mixture was decreased (runs 11–13, Table 7). As a result, at the ratio $CH_4/CO_2$ = 1.5, the methane conversion remains constant (82–83%) in the temperature range 902–958°C, and the $CO_2$ conversion increases to 97–98%.

At 947°C, the ratio $CH_4/CO_2$ = 1.1, and the feed rate of the gas mixture 14 $L \cdot g^{-1} \cdot h^{1}$, the methane conversion was 91%, the $CO_2$ conversion was 96%, and the yields of CO and $H_2$ were high (93%) (Table 7). Over a period of 50 h (the total residence time of the catalyst under DRM conditions without the period of its heating in a methane–carbon dioxide mixture to the working temperature) no significant changes in reagent conversion and synthesis gas yield were observed. Thus, the catalyst exhibited stability during DRM and afforded synthesis gas in high yield (80 %) without intermediate regeneration (Fig. 33).

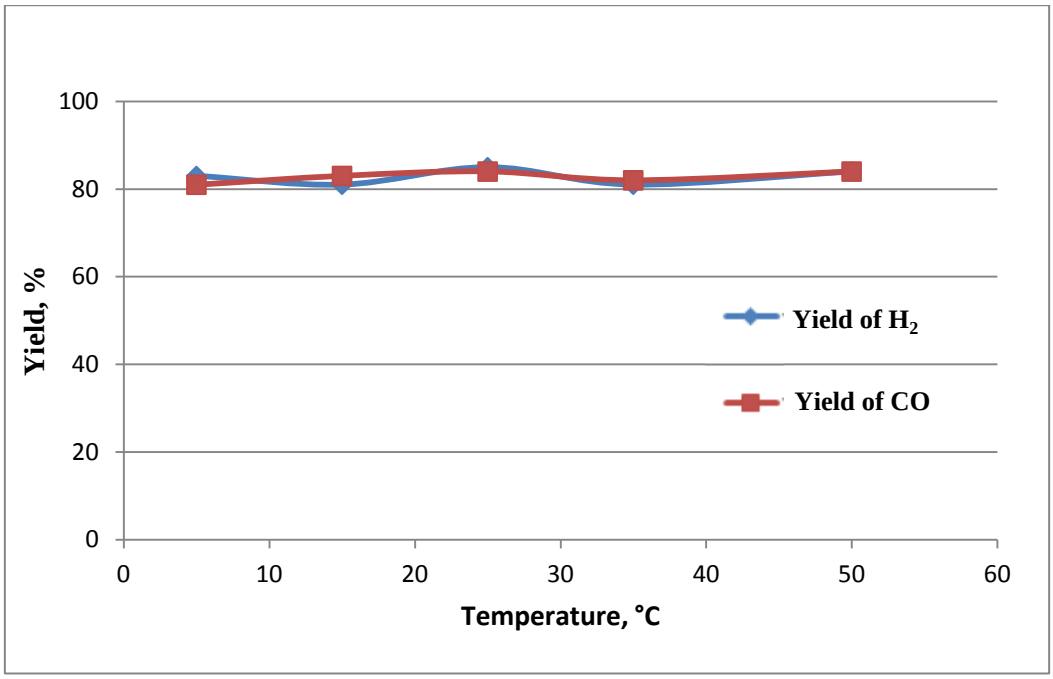


Figure 33 - CO и $H_2$ yields over $NdCaCoO_{3.96}$ in DMR as a function of time on stream (T = 900ºC; $CH_4/CO_2$ = 1; W = 20 $L*g^{-1}*h^{-1}$)

$NdCaCoO_{3.96}$ was active and stable in dry reforming of methane and provided 80% synthesis gas yield. The obtained results indirectly confirmed the combustion-reforming pathway of partial oxidation of methane over $NdCaCoO_{3.96}$.

## Conclusions

1. For the first time partial oxidation of methane to synthesis gas over layered perovskite-type oxides $Nd_{2-x}Ca_xCoO_{4\pm\delta}$ and $La_{2-x}Sr_xCoO_{4\pm\delta}$ (x = 0.75; 1.0) was investigated. The activity of synthesized catalytic materials is determined.
2. New method of synthesis gas production by partial oxidation of methane is developed (Russian №2433950, 21/04/2010).
3. New catalyst of partial oxidation of methane is suggested. $NdCaCoO_{3.96}$ catalyst allows to approach selectivity toward synthesis gas closed to 100% with 90% of $CH_4$ conversion. (T = 900ºC; $CH_4/O_2$ = 2; W = 20 $L*g^{-1}*h^{-1}$). The catalyst was active and stable at least for 140h. No trend to deactivation was observed.
4. Based on XRD, SEM and TEM results it was determined that high activity and selectivity of $NdCaCoO_{3.96}$ as well as stability in POM environmental due to transformation during reaction of initial structure to nano-size particles of cobalt, dispersed in $Nd_2O_3$-CaO matrix.
5. It was observed by $H_2$-TPR and XRD that activity of synthesized layered perovskite-type oxides in POM depends on both size of the formed active metallic particles and stability of initial structure.
6. New efficient catalyst based on neodymium calcium cobaltate for dry reforming of methane is suggested. The catalyst provides yield of CO and $H_2$ closed to 80% (T = 900ºC; $CH_4/CO_2$ = 2; W = 20 $L*g^{-1}*h^{-1}$). The catalyst was active at least for 50h.

## Bibliography


1. URL: http://www.bp.com/en/global/corporate/about-bp/energy-economics/statistical-review-of-world-energy/review-by-energy-type/natural-gas/ дата обращения: 05.06.2015
2. Wood D. Russia speaks global influence by exporting energy geopolitics // Oil & Gas Journal. 2007. Vol. 12. P. 20-24
3. Хазова Т. Газонефтехимия – стратегический рывок // Нефтегаз. – 2013. – №4. – С. 34-35
4. Holman A. Direct conversion of methane to fuels and chemicals // Catalysis today. 2009. Vol. 142. p. 2-8
5. Liu K., Song C., Subramani V. Hydrogen and syngas production and purification technologies // Wiley-Interscience. 2009. 533 p.
6. Арутюнов В.С., Крылов О.В. Окислительные превращения метана // - М.: Наука, 1998. – 361 с.
7. Крылов О.В. Гетерогенный катализ // - М.: ИКЦ «Академ книга» 2004. – 679 с.
8. Арутюнов В.С., Крылов О.В. Окислительная конверсия метана // Успехи химии. – 2005. – Т. 74, №. 3. – С. 1216—1245.
9. Усачев Н.Я, Харламов В.В., Беланова Е.П., Старостина Т.С., Канаев С.А. Окислительная переработка низших алканов: состояние и перспективы // Российских химический журнал. – 2008. – Т. 51, № 2. С. 107–117
10. Усачев Н.Я, Харламов В.В., Беланова Е.П., Казаков А.В., Старостина Т.С., Канаев С.А. Проблемы и перспективы конверсии углеводородов в синтез-газ // Нефтехимия. – 2011. - Т. 51, № 2. С. 107–117
11. Kang J.S., Kim D.H., Lee S.D., Hong S.I., Moon D.J. Nickel-based tri-reforming catalyst for the production of synthesis gas //Appl. Catal. A. 2007. Vol. 332. № 1. P. 153-158
12. Song C.S., Wei P. Tri-reforming of methane a novel concept for catalytic production of industrially useful synthesis gas with desired $H_2$/CO ratios // Catal. Today. 2004. Vol. 98. № 4. P. 463-484

13. Peca M.A., Gymez J.P., Fierro J.L.G. New catalytic routes for syngas and hydrogen production // Appl. Catal. A. 1996. Vol. 144. P. 7-57
14. Kikuchi E. Membrane reactor application to hydrogen production // Catal. Today 2000. Vol. 56. P. 97-101
15. Ismagilov Z.R., Pushkarev V.V., Podyacheva O.Yu, Koryabkina N.A., Veringa H. A Catalytic heat-exchanging tubular reactor for combining of high temperature exothermic and exothermic reactions // Chem. Eng. J. 2001. Vol. 82. P. 355-360
16. Helveg S., Lopez-Cortez C., Selested J., Hansen P.L., Klanser B.S., Rostrup-Nielsen J.R., Norskov J.K. // Nature. 2004. Vol. 427. P. 247
17. Bradford M.C.J., Vannice M.A. Catalytic reforming of methane with carbon dioxide over nickel catalysts 1. Catalysts characterization and activity // 1996. Vol. 142. P. 73-76
18. Bradford M.C.J., Vannice M.A. $CO_2$ reforming of $CH_4$ // Catal. Rev. – Sci.-Eng. 1999. Vol. 41. P.1-42
19. York A.P.E., Xiao T., Creen M.L.H., Claridge J.B. Methane oxyforming for synthesis gas production // Catal. Rev. - Sci. Eng. 2007. Vol. 49. P. 511-560.
20. Бычков В.Ю., Крылов О.В., Корчак В.Н. Морозова О.С., Хоменко Т.И. Исследование механизма углекислотной конверсии метана на Ni/α-$Al_2O_3$ // Кинетика и катализ. – 2002. – Т. 43, №. 1. – С. 94-103.
21. Бычков В.Ю., Тюленин Ю.П., Крылов О.В., Корчак В.Н. Углекислотная конверсия метана на катализаторе Co/α-$Al_2O_3$: образование, состояние и превращения поверхностного углерода // Кинетика и катализ. – 2002. – Т. 43, №. 5. – с. 775-782.
22. Бычков В.Ю., Тюленин Ю.П., Корчак В.Н. Механизм углекислотной конверсии метана: сравнение нанесенных Pt- и Ni(Co)- катализаторов // Кинетика и катализ. – 2003. Т. 44, №. 3. – с. 384-390.
23. Bouarab R., Menad S., Halliche D., Cherifi O., Bettahar M.M. Reforming of methane with carbon dioxide over supported Ni catalysts // Stud. Surf. Sci. Catal. 1998. Vol. 119. p. 717-722.

24. Nagaoka K., Takanabe K., Aika K. Co/$TiO_2$ catalyst for high pressure dry reforming of methane and its modification by other metals // Stud. Surf. Sci. Catal. 2004. Vol. 147. P. 187-192.
25. Provendier H., Petit C., Estoumes C., Kienemann A. Dry reforming of methane. Interest of La-Ni-Fe solid solutions compared to $LaNiO_3$ and $LaFeO_3$ // Stud. Surf. Sci. Catal. 1998. Vol. 119. P. 741-746.
26. Nam J.W., Chae H., Lee S.H., Jung H., Lee K.-Y. Methane dry reforming over well-dispersed Ni catalyst prepared from perovskite-type mixed oxides // Stud. Surf. Sci. Catal. 1998. Vol. 119. P. 843-848.
27. Enger B.C., Rune L., Holmen A. A review of catalytic partial oxidation of methane to synthesis gas with emphasis on reaction mechanism over transition metal catalysts // App. Catal. A., 2008. Vol. 346. P.1 – 27
28. Tsang S.C., Claridge J.B., Green M.L.H. Recent advances in the conversion of methane to synthesis gas // Catal. Today 1995. Vol. 23, P. 3-15
29. Dissanayake D., Rosynek M.P. Kharas K.C.C., Landsford J.H. Partial oxidation of methane to carbon monoxide and hydrogen over a Ni/$Al_2O_3$ catalyst // J. Catal. 1991. Vol. 132. P. 117-127
30. Chang Y.F. Heinemann H. // Partial oxidation of methane to syngas over Co/MgO catalyst // Catal. Lett. 1993. Vol. 21. P. 215-224
31. Jun J.H., Lim T.H., Nam S.-W., Hong S.-A., Yoon K. J., Mechanism of partial oxidation of methane over a nickel-calcium hydroxyapatite catalyst // Appl. Catal. A. 2006. V. 312. P. 27-34
32. Hickman D.A., Schmidt L.D. Production of syngas by direct catalytic oxidation of methane // Science. 1993. Vol. 259. N.5093. P. 343-346
33. Au C.-T., Ng C.-F., Liao M.-S. Methane Dissociation and Syngas Formation on Ru, Os, Rh, Ir, Pd, Pt, Cu, Ag, and Au: A Theoretical Study // J. Catal. 1999. Vol. 185. P. 12-22
34. Au C.T., Liao M.S. Ng S.-F. A detailed theoretical treatment of the partial oxidation of methane to syngas on transition and coinage metal (M) catalysts (M = Nd, Pd, Pt, Cu) // J. Phys. Chem. A. 1998. Vol. 102. P. 3959-3969

35. Zhu J., Ommen J.G., Bouwmeesten H., Leffers L. Activation of $O_2$ and $CH_4$ on yttrium-stabilized zirconia for the partial oxidation of methane to synthesis gas // J. Catal. 2005. Vol. 233. P.434-441
36. Wen C., Liu Y., Guo Y., Wang Y., Lu G. Strategy to eliminate hot-spots in the partial oxidation of methane: enhancing its activity for direct hydrogen production by reducing the reactivity of lattice oxygen // Chem. Commun. 2010. Vol. 46. P. 880-882
37. Salazar-Villalpando M.D., Berry D.A., Cugini A. Role of lattice oxygen in the partial oxidation of methane over Rh/zirconia-deped ceria. Isotopic studies // J. Hydrogen Energy. 2010. Vol. 35. 1998-2003
38. Salazar-Villalpando M.D., Miller A.C. Catalytic partial oxidation of methane and isotopic oxygen exchange reaction over $^{18}O$ labeled Rh/Gadolinium doped ceria // J. Hydrogen Energy. 2011. Vol. 36. P. 3880-3885
39. Hu Y.H., Ruckenstein E. Isotopic GCMS study of the mechanism of methane partial oxidation to synthesis gas // J. Phys. Chem. 1998. V. 102. P. 10568-10571
40. Yan Q. G., Wu T.H., Weng W.Z, Toghiani H., Toghiani R.K., Wan L.H., Pittman C.U. J. Catal., 2004. Vol. 226. P. 247–259.
41. Rabe S., Nachtegaal M., Vogel F. Catalytic partial oxidation of methane to synthesis gas over a ruthenium catalyst: the rose of the oxidation state // Physical Chemistry Chemical Physic. 2007. Vol. 9. P. 1461-1468
42. Buyevskaya O.V., Wolf D., Baerns M. Rhodium catalyzed partial oxidation of methane to CO and $H_2$. Transient studies of its mechanism // Catal. Lett. 1994. Vol. 29, N1/2. P. 249-260
43. Buyevskaya O.V., Walter K., Wolf D., Baerns M. Primary reaction steps and surface sites in the rhodium-catalyzed partial oxidation of methane to CO and $H_2$ // Catal. Lett. 1996 Vol. 38, N1/2. P.81-88
44. Tian Z., Dewaele O., Marin G.B. The state of rhodium during the partial oxidation of methane to synthesis gas // Catal. Lett. 1999. Vol. 57. P. 9-17
45. Au C.T., Hu Y.H., Wan H.L. Pulse studies of $CH_4$ interaction with $NiO/Al_2O_3$ catalyst // Catal. Lett. 1994. Vol. 27. P. 199-206

46. Jin. R., Chen Y., Li W., Cui W., Ji Y., Yu C., Jiang Y. Mechanism for catalytic partial oxidation of methane to syngas over a $Ni/Al_2O_3$ catalyst // Appl. Catal. A. 2000. Vol. 201. P. 71-80
47. Rodrigues L., Silva R.B., Rocha M.G.C., Bargiela P., Noronha F.B., Brandao S.T. Partial oxidation of methane on Ni and Pd catalysts: influence of active phase and $CeO_2$ modification // Catal. Today 2012. Vol. 197. P. 137-143
48. Nguen T.H., Lamacz A., Beaunier P., Czajkowska S., Domanski M., Krzton A., Le T.V., Mariadassou-Djega G. Partial oxidation of methane over bifunctional catalyst I. In situ formation of $Ni^0/La_2O_3$ during temperature programmed POM reaction over $LaNiO_3$ perovskite // Appl. Catal. B. 2014 Vol. 152-153. P. 360-369
49. Zhang Y., Xiong G., Sheng S., Yang W. Deactivation studies over NiO/γ-$Al_2O_3$ catalysts for partial oxidation of methane to syngas // Catal. Today. 2000. Vol. 63. P. 517-522
50. Takenaka S., Umebayashi H., Tanabe E., Matsune H., Kishida M. Specific performance of silica-coated Ni catalysts for the partial oxidation of methane to synthesis gas // J. Catal. 2007. V. 245. P. 392-400
51. Nichio N., Casella M., Ferretti O., Gonza´lez M., Nicot C., Moraweck B., Frety R. Partial oxidation of methane to synthesis gas behavior of different Ni supported catalysts // Catal. Lett. 1996. V.42. P. 65-72
52. Zhang Y., Chu W., Cao W., Luo C., Wen X., Zhou K., A plasma activated Ni/α-$Al_2O_3$ for the conversion of $CH_4$ to syngas // Plasma Chem. Plasma Process. 2000. V.20. P. 137-142
53. Li Z.-H., Tian S.-X., Wang H.-T., Tian H.-B. Plasma treatment of Ni catalyst via a corona discharge // J. Mol. Catal. A: Chem. 2004. V. 211. P. 149-153
54. Wang J.-g., Liu C.-J., Zhang Y.-P., Yu K., Zhu H., He F. Partial oxidation of methane to syngas over glow discharge plasma treated Ni–Fe/$Al_2O_3$ catalyst // Catal. Today 2004. Vol. 89. P. 183-187
55. Zhang Y., Xiong G., Kou Y., Yang W., Sheng S., React. Influence of the sol-gel method on $NiO/Al_2O_3$ for $CH_4/O_2$ to syngas reaction // Kinet. Catal. Lett. 2000. Vol. 69. P. 325-329

56. Zhang Y., Xiong G., Yang W., Sheng S. Partial Oxidation of Methane to Syngas over NiO/γ-$Al_2O_3$ Catalysts Prepared by the Sol-Gel Method // Stud. Surf. Sci. Catal. 2001. Vol. 136. P. 21-26
57. Yan Q. G., Weng W.Z., Wan H.L., Toghiani H., Toghiani R.K., Pittman C.U. Activation of methane to syngas over a Ni/$TiO_2$ catalyst // Appl. Catal. A 2003. Vol. 239. P. 43-58
58. Zhang Y., Li Z., Wen X., Liu Y., Partial oxidation of methane over Ni/Ce-Ti-O catalysts // Chem. Eng. J. 2006. Vol. 121. P. 115-123
59. Wu T., Yan Q., Wan H., Partial oxidation of methane to hydrogen and carbon monoxide over a Ni/$TiO_2$ catalyst // J. Mol. Catal. A: Chem. 2005. Vol. 226. P. 41-48
60. Lee S.J., Jun J.H., Lee S.-H., Yoon K.-J., Lim T.H., Nam S.-W., Hong S.-A. Partial oxidation of methane over nickel-added strontium phosphate // Appl. Catal. A. 2002. Vol. 230. P. 61-71
61. Shamsi A., Spivey J.J., Partial oxidation of methane on Ni-MgO catalysts supported on metal foams // Ind. Eng. Chem. Res. 2005. Vol. 44. P. 7298-7305
62. Sun W.-Z., Jin J.-Q., Guo X.-Y. Partial oxidation of methane over Ni/SiC catalyst // Catal. Commun. 2005. Vol. 6 135-139
63. Sato K., Fujita S., Suzuki K., Mori T. High performance of Ni-substituted calcium aluminosilicate for partial oxidation of methane into syngas // Catal. Commun. 2007. Vol. P. 1735-1738
64. Choudhary V.R., Prabhakar B., Rajput M.A., Beneficial effects of noble metal addition to Ni/$Al_2O_3$ catalyst for oxidative methane-to-syngas conversion // J. Catal. 1995. Vol. 157. P. 752-754
65. Ji Y., Li W., Xu H., Chen Y. A study on the ignition procesess for the catalytic patial oxidation of methane to synthesis gas by MS-TPSR technique // Catal. Lett. 2001. Vol. 71 P. 45-48
66. Gonza´lez M., Nichio N.N., Moraweck B., Martin G. Role of chromium in the stability of Ni/$Al_2O_3$ catalysts for natural gas reforming // Mater. Lett. 2000. Vol. 45. P. 15-18

67. Wang H.-t,, Li Z.-h., Tian S.-x. Effect of promoters on the catalytic performance of $Ni/Al_2O_3$ catalyst for partial oxidation of methane to syngas // React. Kinet. Catal. Lett. 2004. Vol. 83. P. 245-252
68. Chen L., Lu Y., Hong Q., Lin J., Dautzenberg F. Catalytic partial oxidation of methane to syngas over Ca-decorated-$Al_2O_3$-supported Ni and NiB catalysts // Appl. Catal. A 2005. Vol. 292. P. 295-304
69. Choudhary V.R., Rane V.H., Rajput A.M. Beneficial effects of cobalt addition to Ni-catalysts for oxidative conversion of methane to syngas // Appl. Catal. A 1997. Vol. 162 P. 235-238
70. L. Cao, Y. Chen, W. Li Stud Effect of $La_2O_3$ added to $NiO/Al_2O_3$ catalyst on partial oxidation of methane to syngas // Surf. Sci. Catal. 107 (1997) 467-471
71. Miao Q., Xiong G., Li X., Sheng S., Guo X. Acid-base properties and the directions of oxidative transformation of methane over nickel-based catalysts // Catal. Lett. 1996. Vol. P. 165-169
72. Miao Q., Xiong G., Sheng S., Guo X. Controll of the directions oxidative transformation of methane over nickel-based catalysts by acid-base properties // React. Kinet. Catal. Lett. 1997. Vol. 62 P. 363-370
73. Liu S., Xiong G., Yang W., Sheng S. React. The effect of Li and La on $NiO/Al_2O_3$ catalyst for $CH_4/O_2$ to syngas reaction // Kinet. Catal. Lett. 1999. Vol. 68 P. 243-247
74. Miao Q., Xiong G., Sheng S., Cui W., Xu L., Guo X. Partial oxidation of methane to syngas over nickel-based catalysts modified by alkali metal oxide and rare earth metal oxide // Appl. Catal. A. 1997. Vol. 154. P. 17-27
75. Liu S., Xiong G., Sheng S., Miao Q., Yang W. Effects of Alkali and Rare Earth Metal Oxides on the Thermal Stability and the Carbon-deposition over Nickel Based Catalyst // Stud. Surf. Sci. Catal. 1998. Vol.119. P. 119 (1998) 747-752
76. K. Nakagawa, N. Ikenaga, Y. Teng, T. Kobayashi, T. Suzuki Partial oxidation of methane to synthesis gas over iridium–nickel bimetallic catalysts // Appl. Catal A. 1999. Vol. 180. P. 183-193

77. Gonza´les-Corta´s S.L., Orozco J., Moronta D., Fontal B., Imbert F.E. Methane conversion over $Sr^{2+}/La_2O_3$ catalyst modified with nickel and copper // React. Kinet. Catal. Lett. 2000. Vol. 69. P. 145-152
78. Zhu T., Flytzani-Stephanopoulos M., Catalytic partial oxidation of methane to synthesis gas over Ni–$CeO_2$ // Appl. Catal. A. 2001. Vol. 208. P. 403-417
79. Shan W., Fleys M., Lapicque F., Swierczynski D., Kiennemann A., Simon Y., Marquaire P.-M. Syngas production from partial oxidation of methane over $Ce_{1-x}Ni_xO_y$ catalyst prepared by complexation-combustion method // Appl. Catal. A. 2006. Vol. 311. P. 24-33
80. Wang H.Y., Ruckenstein E. Conversion of methane to synthesis gas over $Co/Al_2O_3$ by $CO_2$ and/or $O_2$ // Catal. Lett. 2001. Vol. 75. P. 13-18
81. Slagtern A˚., Swaan H.M., Olsbye U., Dahl M.I., Mirodatos C. Catalytic partial oxidation of methane over Ni-, Co- and Fe-based catalysts // Catal. Today 1998. Vol.46. P. 107-115
82. Sokolovskii V.D., Coville N.J., Parmaliana A., Eskendirov I., Makoa M. Methane partial oxidation. Challenge and perspective // Catal. Today 1998. Vol. 42. P. 191-195
83. Chang Y.-F., Heinemann H. Partial oxidation of methane to syngas over Co/MgO catalysts. Is it low temperature? // Catal. Lett. 1993. Vol. 21. P. 215-224
84. Ruckenstein E., Wang H.Y. Combined catalytic partial oxidation and $CO_2$ reforming of methane over supported cobalt catalyst // Catal. Lett. 2001. Vol. 73. P. 99-105
85. Wang H.Y., Ruckenstein E. Partial Oxidation of Methane to Synthesis Gas over Alkaline Earth Metal Oxide Supported Cobalt Catalysts // J. Catal. 2001. Vol. 199. P. 309-317
86. Choudhary V.R., Rajput A.R., Prabhakar B., Mamman A.S. Partial oxidation of methane to CO and $H_2$ over nickel and/or cobalt containing $ZrO_2$, $ThO_2$, $UO_2$, $TiO_2$ and $SiO_2$ catalysts // Fuel. 1998. Vol. 77 P. 1803-1807

87. Swaan H.M., Rouanet R., Widyananda P., Mirodatos C. Partial oxidation of methane over nickel- and cobalt-based catalysts // Stud. Surf. Sci. Catal. 1997. Vol. 107. P. 447-453

88. Nishimoto H.-a., Nakagawa K., Ikenaga N.-o., Nishitani-Gamo M., Ando T., Suzuki T. Partial oxidation of methane to synthesis gas over oxidized diamond catalysts // Appl. Catal. A. 2004. Vol. 264. P. 65-72

89. Tang S., Lin J., Tan K.L. Partial oxidation of methane to synthesis gas over $\gamma$-$Al_2O_3$-supported rhodium catalyst // Catal. Lett. 1999. Vol. 59. P. 129-135

90. Mo L., Zheng X., Huang C., Fei J. A novel catalyst $Pt/CoAl_2O_4/Al_2O_3$ for combination of $CO_2$ reforming and partial oxidation of $CH_4$ // Catal. Lett. 2002. Vol. 80. P. 165-169

91. Mo L., Fei J., Huang C., Zheng X. Reforming of methane with oxygen and carbon dioxide to produce syngas over a novel $Pt/CoAl_2O_4/Al_2O_3$ catalyst J. Mol. Catal. A: Chem. 2003. Vol. 193. P. 177-184

92. Lødeng R., Bjørgum E., Enger B.C., Eilertsen J.L., Holmen A., Krogh B., Ronekleiv M., Ritter E. Appl. Catal. A. 2007. Vol. 233 P. 11-17

93. Enger B.C., Lødeng R., Holmen A., inpreparation.

94. Gao X.X., Huang C.J., Zhang N.W., Li J.H., Weng W.Z., Wan H.L. Partial oxidation of methane to synthesis gas over $Co/Ca/Al_2O_3$ catalysts // Catal. Today 2008. Vol.131. P. 211–218

95. Патент РФ № 2 333 797, 27.03.2007

96. Mitchell R.H. Perovskites. Modern and ancient // 2002. Almaz Press Inc. 262 P.

97. Pena M.A., Fierro J.L.G. Chemical structures and and performance of perovskite oxides // Chemical Review. 2001. Vol. 101 P. 1981-2017

98. Yin X., Hong L. Partial oxidation of methane to syngas over the catalyst derived from double perovskite $(La_{0.5}Sr_{0.5})_2FeNiO_{6-\delta}$ // Appl. Catal., A. 2009. Vol. 371. P. 153-160

99. Toniolo F.S., Magalhaes R.N., Perez C.A., Schmal M. Structural investigation of $LaCoO_3$ and $LaCoCuO_3$ perovskite-type oxides and the effect of Cu on coke

deposition in the partial oxidation of methane // Appl. Catal., A. 2012. Vol. 117 – 118, P. 156-166

100. Garcia A., Becerra N., Garcia L., Ojeda I., Lopez E., Lopez Provendier H., Petit C., Estournes C., Libs C., Kiennemann A. Stabilisation of active nickel catalysts in partial oxidation of methane to synthesis gas by iron addition // Appl. Catal., A. 1999. Vol. 180. P. 163-183

101. Garcia A., Becerra N., Garcia L., Ojeda I., Lopez E., Lopez C.M. Goldwasser M.R. Structured Perovskite-Based Oxides: Use in the Combined Methane Reforming // Advances in Chemical Engineering and Science 2011. V. 1. P. 169-175

102. Araujo G.C, Lima S., Rangel M.C., Parola V., Pena M.A., FierroJ.L.G. Characterization of precursors and reactivity of $LaNi_{1-x}Co_xO_3$ for the partial oxidation of methane // Catal. Today. 2005. V. 107-108. P. 906-912

103. Silva S., Conceicao L., Ribeiro N., Souza M. Partial oxidation of methane over Ni–Co perovskite catalysts // Catal. Comm. 2011. Vol. 12. P.665-668

104. Vella L.D., Villoria J.A., Specchia S., Mota N., Fierro J.L.G. Specchia V. Catalytic partial oxidation of $CH_4$ with nickel–lanthanum-based catalysts // Catal. Today. 2011. Vol. 171. P. 84-96

105. Hayakawa T., Harihara H., Andersen A.G., Suzuki K., Yasuda H. Tsunoda T., Hamakawa S., York A.P.E., Yoon Y.S., Shimuzi M., Takehira K. Sustainable $Ni/Ca_{1-x}Sr_xTiO_3$ catalyst prepared in situ for the partial oxidation of methane to synthesis gas // Appl. Catal. A. 1997. Vol. 149. P. 391-410

106. Slagtern A., Olsbye U. Partial oxidation of methane to synthesis gas using La-M-O catalysts // Appl. Catal. A. 1994. Vol. 110. P. 99-108

107. Largo L., Bini G., Pena M.A., Fierro J.L.G. Partial Oxidation of Methane to Synthesis Gas Using $LnCoO_3$ Perovskites as Catalyst Precursors // J. Catal. 1997. Vol. 167. P. 198-209

108. Morales M., Espiell F., Segarra M. Performance and stability of $La_{0.5}Sr_{0.5}CoO_{3-y}$ perovskite as catalyst precursor for syngas production b y partial oxidation of methane // International journal of hydrogen energy 2014. Vol. 39. P. 6454-6461

109. Yan E.-h., Noh Y.-s., Ramesh S., Lim S.S., Moon D.J. The effect of promoters in $La_{0.9}M_{0.1}Ni_{0.5}Fe_{0.5}O_3$(M=Sr,Ca) perovskite catalysts on dry reforming of methane // Fuel Processing Technology 2015. In press

110. Borovskikh L., Mazo G., Kemnitz E. Reactivity of oxygen of complex cobaltates $La_{1-x}Sr_xCoO_{3-\delta}$ and $LaSrCoO_4$ // Solid State Sci. 2003. Vol. 5. P. 409–417

111. Deng J., Zhang L., Dai H., He H., Au C.T. Preparation, characterization and catalytic properties of $NdSrCu_{1-x}Co_xO_{4-\delta}$ and $Sm_{1.8}Ce_{0.2}Cu_{1-x}CoxO_{4+\delta}$ (x = 0, 0.2 and 0.4) for methane combustion // Appl. Catal. B. 2009. Vol. 89. P. 87-96

112. Falcon H., Barbero J.A., Araujo G., Casais M.T., Martinez-Lope M.J., Alonso J.A., Fierro J.L.G. Double perovskite oxides $A_2FeMoO_{6-\delta}$ (A = Ca, Sr and Ba) as catalysts for methane combustion // Appl. Catal. A. 2004. Vol. 53. P. 37-45

113. Zhang L., Zhang Y., Dai H., Deng J., Wei L., He H. Hydrothermal synthesis and catalytic performance of single-crystalline $La_{2-x}Sr_xCuO_4$ for methane oxidation // Catal. Today. 2010. Vol. 153. P. 143-149

114. Vereshchagin S.N., Solovyov L.A., Rabchevskii E.V., Dudnikov V.A., Ovchinnikov S.G., Anshits A.G. Methane oxidation over A-site ordered and disordered $Sr_{0.8}Gd_{0.2}CoO_{3-\delta}$ perovskites Chem. Commun. 2014. Vol. 50. P. 6112-6115

115. Bielański A., Haber J. Oxygen in catalysis // Marcel Dekker Inc., New York, 1991. 472 p.

116. Ferri D., Forni L. Methane combustion on some perovskite-like mixed oxides // Appl. Catal. B. 1998. Vol. 16. P. 119-126

117. Borovskikh LV, Putilin SN, Leonova LS, Mazo GN, Synthesis, structure and transport properties of $NdCaCoO_4$. // Inorg. Mater. Appl. Res. 2008. Vol. 5. P.54-59.

118. Shlyakhtin O.A., Mazo G.N., Kaluzhskikh M.S., Komissarenko D.A., Loktev A.S., Dedov A.G. Compositional boundaries of $Nd_{2-x}Ca_xCoO_{4\pm\delta}$ at 900–1200 °C // Mater. Lett. 2012. Vol. 75. P. 20-22

119. Lakshminarayanan N., Choi H., Kuhn J.N., Ozkan U.Z. Effect of additional B-site transition metal doping on oxygen transport and activation characteristics in

$La_{0.6}Sr_{0.4}(Co_{0.18}Fe_{0.72}X_{0.1})O_3$ (where X = Zn, Ni or Cu) perovskite oxides // Appl. Catal. B: Environ. 2011. Vol. 103. P. 318–325.

120. Kuhn J.N., Ozkan U.Z. Surface properties of Sr and Co-doped $LaFeO_3$ // J. Catal. 2008. Vol. 253. P. 200–211

121. Chuang T.J., Brundle C.R., Rices D.W. // Surf. Sci. 1975. Vol. 59. P. 413-517

122. Taguchi H., Kido H., Tabata K. Relationship between crystal structure and electrical property of $K_2NiF_4$-type $(Ca_{1-x}Nd_{1+x})CoO_{4-\delta}$. // Physica B. 2004. Vol. 344. PP. 271-277

123. Choudhary V.R., Rane V.H., Rajput A.M. Selective oxidation of methane to CO and $H_2$ over unreduced NiO-rare earth oxide catalyst // Catal. Lett. 1993. Vol. 22. P. 289-297

# Annex

Table A-1. Results of indexing of X-ray diffraction patterns of $LaSrCoO_{4.00(2)}$

| N | 2*TH | D | I/Io | Qobs | h | k | l | Qcalc | dQ |
|---|---|---|---|---|---|---|---|---|---|
| 1 | 14.176 | 6.24226 | 15 | 256.64 | 0 | 0 | 2 | 256.6 | 0.1 |
| 2 | 24.446 | 3.63819 | 35 | 755.49 | 0 | 1 | 1 | 755.2 | 0.3 |
| 3 | 28.616 | 3.11672 | 25 | 1029.45 | 0 | 0 | 4 | 1026.3 | 3.1 |
| 4 | 31.848 | 2.80740 | 100 | 1268.79 | 0 | 1 | 3 | 1268.3 | 0.4 |
| 5 | 33.294 | 2.68871 | 90 | 1383.28 | 1 | 1 | 0 | 1382.1 | 1.2 |
| 6 | 36.354 | 2.46911 | 10 | 1640.28 | 1 | 1 | 2 | 1638.7 | 1.6 |
| 7 | 43.319 | 2.08692 | 40 | 2296.08 | 0 | 1 | 5 | 2294.6 | 1.4 |
| 8 | 43.446 | 2.08111 | 30 | 2308.92 | 0 | 0 | 6 | 2309.2 | -0.3 |
| 9 | 44.422 | 2.03762 | 70 | 2408.53 | 1 | 1 | 4 | 2408.4 | 0.1 |
| 10 | 47.773 | 1.90222 | 80 | 2763.63 | 0 | 2 | 0 | 2764.2 | -0.6 |
| 11 | 50.062 | 1.82045 | 5 | 3017.46 | 0 | 2 | 2 | 3020.8 | -3.3 |
| 12 | 54.342 | 1.68676 | 15 | 3514.74 | 1 | 2 | 1 | 3519.4 | -4.7 |
| 13 | 55.782 | 1.64657 | 30 | 3688.42 | 1 | 1 | 6 | 3691.3 | -2.9 |
| 14 | 56.587 | 1.62506 | 25 | 3786.72 | 0 | 2 | 4 | 3790.5 | -3.8 |
| 15 | 56.968 | 1.61509 | 25 | 3833.60 | 0 | 1 | 7 | 3834.1 | -0.5 |
| 16 | 58.534 | 1.57554 | 80 | 4028.47 | 1 | 2 | 3 | 4032.5 | -4.1 |
| 17 | 59.127 | 1.56115 | 20 | 4103.06 | 0 | 0 | 8 | 4105.2 | -2.2 |
| 18 | 66.487 | 1.40507 | 50 | 5065.32 | 1 | 2 | 5 | 5058.8 | 6.5 |
| 19 | 69.572 | 1.35011 | 25 | 5486.07 | 1 | 1 | 8 | 5487.3 | -1.2 |
| 20 | 69.868 | 1.34512 | 35 | 5526.88 | 2 | 2 | 0 | 5528.4 | -1.5 |
| 21 | 75.273 | 1.26137 | 5 | 6285.13 | 0 | 3 | 1 | 6283.6 | 1.5 |
| 22 | 77.172 | 1.23500 | 10 | 6556.43 | 2 | 2 | 4 | 6554.7 | 1.7 |
| 23 | 77.468 | 1.23102 | 20 | 6598.83 | 1 | 2 | 7 | 6598.3 | 0.5 |
| 24 | 78.818 | 1.21329 | 20 | 6793.15 | 0 | 3 | 3 | 6796.7 | -3.6 |
| 25 | 79.366 | 1.20628 | 15 | 6872.31 | 0 | 2 | 8 | 6869.4 | 2.9 |
| 26 | 79.661 | 1.20255 | 20 | 6915.02 | 1 | 3 | 0 | 6910.5 | 4.5 |

TAble A-2 - Results of indexing of X-ray diffraction patterns of $La_{1.25}Sr_{0.75}CoO_{4.03}$

| N | 2*TH | D | I/Io | Qobs | h | k | l | Qcalc | dQ |
|---|---|---|---|---|---|---|---|---|---|
| 1 | 14.119 | 6.26749 | 10 | 254.57 | 0 | 0 | 2 | 254.9 | -0.3 |
| 2 | 24.456 | 3.63665 | 30 | 756.13 | 0 | 1 | 1 | 756.2 | -0.0 |
| 3 | 28.491 | 3.13013 | 20 | 1020.65 | 0 | 0 | 4 | 1019.5 | 1.1 |
| 4 | 31.844 | 2.80779 | 90 | 1268.44 | 0 | 1 | 3 | 1265.9 | 2.5 |
| 5 | 33.328 | 2.68605 | 100 | 1386.03 | 1 | 1 | 0 | 1384.9 | 1.1 |
| 6 | 36.352 | 2.46928 | 10 | 1640.06 | 1 | 1 | 2 | 1639.8 | 0.3 |
| 7 | 43.199 | 2.09241 | 30 | 2284.05 | 0 | 1 | 5 | 2285.5 | -1.4 |
| 8 | 43.326 | 2.08658 | 30 | 2296.84 | 0 | 0 | 6 | 2293.9 | 2.9 |
| 9 | 44.384 | 2.03927 | 45 | 2404.65 | 1 | 1 | 4 | 2404.4 | 0.2 |
| 10 | 47.810 | 1.90084 | 70 | 2767.63 | 0 | 2 | 0 | 2769.8 | -2.2 |
| 11 | 50.134 | 1.81802 | 5 | 3025.53 | 0 | 2 | 2 | 3024.7 | 0.8 |
| 12 | 54.400 | 1.68511 | 20 | 3521.62 | 1 | 2 | 1 | 3526.0 | -4.4 |
| 13 | 55.708 | 1.64859 | 25 | 3679.36 | 1 | 1 | 6 | 3678.8 | 0.5 |
| 14 | 56.820 | 1.61894 | 25 | 3815.38 | 0 | 1 | 7 | 3814.7 | 0.6 |
| 15 | 58.577 | 1.57451 | 60 | 4033.77 | 1 | 2 | 3 | 4035.7 | -2.0 |
| 16 | 58.914 | 1.56629 | 10 | 4076.20 | 0 | 0 | 8 | 4078.1 | -1.9 |
| 17 | 66.414 | 1.40643 | 40 | 5055.48 | 1 | 2 | 5 | 5055.3 | 0.2 |
| 18 | 69.402 | 1.35300 | 30 | 5462.68 | 1 | 1 | 8 | 5463.0 | -0.3 |
| 19 | 75.372 | 1.25995 | 10 | 6299.28 | 0 | 3 | 1 | 6295.8 | 3.5 |
| 20 | 77.369 | 1.23235 | 20 | 6584.69 | 1 | 2 | 7 | 6584.5 | 0.1 |
| 21 | 79.194 | 1.20846 | 15 | 6847.54 | 0 | 2 | 8 | 6847.9 | -0.4 |

Table A-3 - Results of indexing of X-ray diffraction patterns of $NdCaCoO_{3.96}$

| N | 2*TH | D | I/Io | Qobs | h | k | l | Qcalc | dQ |
|---|---|---|---|---|---|---|---|---|---|
| 1 | 14.109 | 6.27168 | 10 | 254.23 | 0 | 0 | 2 | 254.6 | -0.3 |
| 2 | 24.196 | 3.67514 | 30 | 740.38 | 0 | 1 | 1 | 740.9 | -0.5 |
| 3 | 28.449 | 3.13471 | 20 | 1017.66 | 0 | 0 | 4 | 1018.2 | -0.6 |
| 4 | 31.593 | 2.82948 | 100 | 1249.07 | 0 | 1 | 3 | 1250.0 | -1.0 |
| 5 | 32.953 | 2.71575 | 90 | 1355.88 | 1 | 1 | 0 | 1354.6 | 1.3 |
| 6 | 36.012 | 2.49183 | 5 | 1610.52 | 1 | 1 | 2 | 1609.1 | 1.4 |
| 7 | 43.059 | 2.09892 | 30 | 2269.91 | 0 | 1 | 5 | 2268.3 | 1.6 |
| 8 | 43.271 | 2.08913 | 20 | 2291.24 | 0 | 0 | 6 | 2291.0 | 0.2 |
| 9 | 44.076 | 2.05278 | 45 | 2373.09 | 1 | 1 | 4 | 2372.8 | 0.3 |
| 10 | 47.258 | 1.92173 | 60 | 2707.78 | 0 | 2 | 0 | 2709.1 | -1.4 |
| 11 | 53.786 | 1.70287 | 10 | 3448.57 | 1 | 2 | 1 | 3450.1 | -1.5 |
| 12 | 55.439 | 1.65596 | 20 | 3646.71 | 1 | 1 | 6 | 3645.6 | 1.1 |
| 13 | 56.074 | 1.63869 | 20 | 3723.97 | 0 | 2 | 4 | 3727.4 | -3.4 |
| 14 | 56.667 | 1.62294 | 20 | 3796.59 | 0 | 1 | 7 | 3795.6 | 1.0 |
| 15 | 57.980 | 1.58928 | 50 | 3959.13 | 1 | 2 | 3 | 3959.2 | -0.1 |
| 16 | 58.870 | 1.56737 | 10 | 4070.60 | 0 | 0 | 8 | 4072.9 | -2.3 |
| 17 | 65.853 | 1.41704 | 10 | 4980.04 | 1 | 2 | 5 | 4977.4 | 2.6 |
| 18 | 69.110 | 1.35800 | 20 | 5422.54 | 2 | 2 | 0 | 5418.3 | 4.3 |
| 19 | 76.846 | 1.23943 | 10 | 6509.66 | 1 | 1 | 9 | 6509.4 | 0.3 |
| 20 | 77.944 | 1.22468 | 10 | 6667.33 | 0 | 3 | 3 | 6668.3 | -1.0 |
| 21 | 78.662 | 1.21530 | 10 | 6770.73 | 1 | 3 | 0 | 6772.9 | -2.1 |

Table A-4 - Results of indexing of X-ray diffraction patterns of $Nd_{1.25}Ca_{0.75}CoO_{4.03}$

| N | 2*TH | D | I/Io | Qobs | h | k | l | Qcalc | dQ |
|---|---|---|---|---|---|---|---|---|---|
| 1 | 14.807 | 5.98250 | 10 | 279.41 | 0 | 0 | 2 | 279.4 | -0.0 |
| 2 | 24.812 | 3.58830 | 15 | 776.64 | 0 | 1 | 1 | 777.4 | -0.7 |
| 3 | 29.861 | 2.99200 | 10 | 1117.06 | 0 | 0 | 4 | 1117.7 | -0.7 |
| 4 | 32.746 | 2.73470 | 100 | 1337.15 | 0 | 1 | 3 | 1336.3 | 0.9 |
| 5 | 33.705 | 2.65910 | 90 | 1414.26 | 1 | 1 | 0 | 1415.0 | -0.8 |
| 6 | 36.997 | 2.42970 | 5 | 1693.93 | 1 | 1 | 2 | 1694.5 | -0.6 |
| 7 | 44.918 | 2.01790 | 30 | 2455.84 | 0 | 1 | 5 | 2454.0 | 1.8 |
| 8 | 45.496 | 1.99360 | 5 | 2516.08 | 0 | 0 | 6 | 2514.9 | 1.2 |
| 9 | 45.654 | 1.98710 | 50 | 2532.56 | 1 | 1 | 4 | 2532.8 | -0.2 |
| 10 | 48.438 | 1.87920 | 60 | 2831.74 | 0 | 2 | 0 | 2830.1 | 1.6 |
| 11 | 55.147 | 1.66540 | 10 | 3605.48 | 1 | 2 | 1 | 3607.5 | -2.0 |
| 12 | 57.804 | 1.59500 | 20 | 3930.78 | 1 | 1 | 6 | 3930.0 | 0.8 |
| 13 | 57.936 | 1.59170 | 10 | 3947.09 | 0 | 2 | 4 | 3947.8 | -0.7 |
| 14 | 59.422 | 1.55540 | 10 | 4133.48 | 0 | 1 | 7 | 4130.6 | 2.9 |
| 15 | 59.709 | 1.54860 | 60 | 4169.86 | 1 | 2 | 3 | 4166.4 | 3.5 |
| 16 | 62.035 | 1.49600 | 10 | 4468.24 | 0 | 0 | 8 | 4471.0 | -2.7 |
| 17 | 68.145 | 1.37600 | 10 | 5281.57 | 1 | 2 | 5 | 5284.1 | -2.5 |
| 18 | 68.604 | 1.36790 | 15 | 5344.31 | 0 | 2 | 6 | 5345.0 | -0.7 |
| 19 | 70.902 | 1.32910 | 15 | 5660.89 | 2 | 2 | 0 | 5660.2 | 0.7 |
| 20 | 72.895 | 1.29760 | 15 | 5939.07 | 2 | 2 | 2 | 5939.6 | -0.6 |

UNIVERSITÉ DE STRASBOURG

# Dmitry KOMISSARENKO

## Oxydation catalytique sélective du méthane en gaz de synthèse avec des oxydes mixtes de cobalt et des éléments des terres rares


## Résumé

Nouveau catalyseur efficace basée sur cobaltate de calcium et néodyme pour reformage à sec du méthane a été suggéré. Le catalyseur fournit le rendement en CO et $H_2$ près de 80% (T = 900 °C; $CH_4/CO_2$ = 2; W = 20 $L \cdot g^{-1} \cdot h^{-1}$). Le catalyseur a été actif et stable pendant 50 h. Pour la première fois l'oxydation partielle du méthane en gaz de synthèse a été effectué en présence de pérovskites lamellaires $Nd_{2-x}Ca_xCoO_{4\pm\delta}$ et $La_{2-x}Sr_xCoO_{4\pm\delta}$ (x = 0.75; 1.0). Nouvelle méthode de production de gaz de synthèse par oxydation partielle du méthane a été développé et breveté (brevet russe № 2433950, 21/04/2010). Nouveau catalyseur d'oxydation partielle $NdCaCoO_{3.96}$ de méthane a été suggéré qui permet d'obtenir la sélectivité en gaz de synthèse proche de 100% avec 90% de la conversion de $CH_4$ (T = 900ºC; $CH_4/O_2$ = 2; W = 20 $L \cdot g^{-1} \cdot h^{-1}$). Le catalyseur a été active et stable au moins 140 h, aucune tendance à la désactivation n'a été observée. Sur la base des analyses DRX, MEB et MET, il a été déterminé que l'activité et la sélectivité élevées de $NdCaCoO_{3.96}$ ainsi que la stabilité dans l'oxydation partielle du méthane sont dues à sa transformation au cours de la réaction de la structure initiale en des nanoparticules de cobalt métallique dispersées dans $Nd_2O_3$-CaO matrice. Il a été observé que l'activité des pérovskites lamellaires dans l'oxydation partielle du méthane dépend à la fois de la taille des particules métalliques actives formées et à la stabilité de la structure initiale.



## Résumé en anglais

New efficient catalyst based on neodymium calcium cobaltate for dry reforming of methane was suggested. The catalyst provides the yield of CO and $H_2$ close to 80% (T = 900ºC; $CH_4/CO_2$ = 2; W = 20 $L \cdot g^{-1} \cdot h^{-1}$). The catalyst was active for 50 h. For the first time partial oxidation of methane to synthesis gas over layered perovskite-type oxides $Nd_{2-x}Ca_xCoO_{4\pm\delta}$ and $La_{2-x}Sr_xCoO_{4\pm\delta}$ (x = 0.75; 1.0) was investigated. New method of synthesis gas production by partial oxidation of methane was developed and patented (Russian patent № 2433950, 21/04/2010). New catalyst $NdCaCoO_{3.96}$ for partial oxidation of methane was suggested allowing the selectivity toward synthesis gas close to 100% with 90% of $CH_4$ conversion (T = 900ºC; $CH_4/O_2$ = 2; W = 20 $L \cdot g^{-1} \cdot h^{-1}$). The catalyst was active and stable at least for 140 h, no trend to deactivation was observed. Based on XRD, SEM and TEM results it was determined that high activity and selectivity of $NdCaCoO_{3.96}$ as well as stability in partial oxidation of methane are due to its transformation during reaction of initial structure to nanosized particles of metallic cobalt dispersed in $Nd_2O_3$-CaO matrix. It was observed that the activity of synthesized layered perovskite-type oxides in partial oxidation of methane depends both on the size of the formed active metallic particles and on the stability of initial structure.